LATE EOCENE PALAEOENVIRONMENTS AND PALAEOCLIMATE OF THE US GULF COAST

By

Nursufiah Sulaiman

A thesis submitted to the University of Birmingham for the degree of DOCTOR OF PHILOSOPHY

School of Geography, Environment and Earth Sciences
College of Life and Environmental Sciences
University of Birmingham
January 2017

UNIVERSITY OF
BIRMINGHAM

University of Birmingham Research Archive

e-theses repository

This unpublished thesis/dissertation is copyright of the author and/or third parties. The intellectual property rights of the author or third parties in respect of this work are as defined by The Copyright Designs and Patents Act 1988 or as modified by any successor legislation.

Any use made of information contained in this thesis/dissertation must be in accordance with that legislation and must be properly acknowledged. Further distribution or reproduction in any format is prohibited without the permission of the copyright holder.

ABSTRACT

This thesis presents new micropalaeontological and geochemical palaenvironmental proxy data through the late Eocene into the earliest Oligocene from a clay-rich succession from the US Gulf Coast. It is based on samples from the Yazoo Clay Formation, recovered in the Mossy Grove Core near Jackson, Mississippi. This represents an apparently continuous section of relatively uniform lithology, clay-rich deposits, that host very well preserved assemblages of calcareous nannofossil, foraminifera and organic biomarkers. This thesis makes use of these to generate a detailed calcareous nannofossil taxonomy, high-resolution calcareous nannofossil assemblage data and coccolith-fraction bulk isotope data, as well as pilot planktonic foraminifera abundance and isotope records. It also develops pilot data for organic biomarkers that demonstrate the presence and utility of biomarker proxies for ancient sea surface temperatures within the Yazoo Clay. The results of this project characterize the late Eocene US Gulf Coast as a sub-tropical shelf sea environment that experiences several stages of sea surface cooling and increasing nutrient contents – potentially linked to sea level fall – in the late Eocene and earliest Oligocene. The most important finding of this project is evidence for cooling and major perturbations to the climate-carbon cycle significantly before the onset of the major phases of Antarctic glaciation.

ACKNOWLEDGEMENTS

Praise to be to the Almighty, for all the countless gifts you have offered me.

First of all I would like to express my sincere gratitude to my main supervisor, Dr Tom Dunkley Jones for his supervision, encouragement, support, understanding, patience and assistance through my whole PhD journey, especially during my ups and downs. Then, I would like to thank to my co-supervisor, Dr Ian Boomer who always assisted me with technical support, and to Dr Kristy Edgar for her help and advice with the study of planktonic foraminifera.

To my colleagues, Azrin and Ulrike for always give me constructive suggestions, Marcelo and Federike for helping me in the lab, I am extremely grateful. I would like to acknowledge Hidayah, Syazwana, Mashitah, Naaemah, Anisa, Faiqa, Hajar and Rohazaini for helping me survive all the stress and not letting me down.

My deepest appreciation goes to my parents and family for all cooperation, encouragement, and contributions, from the beginning till the end of this journey. I would also like to acknowledge all staffs and PhD students in Earth Sciences Department for your direct or indirect contributions to this study. Last but not least to my funding, Ministry of Higher Education Malaysia, and University Malaysia Kelantan for sponsoring me to pursue this study.

LIST OF CONTENTS

		Page
ABSTRACT		i
ACKNOWLEDGEMENTS		ii
LIST OF CONTENTS		iii
LIST OF FIGURES		vi
LIST OF TABLES		viii
LIST OF PLATES		ix
APPENDICES		x
CHAPTER 1: INTRODUCTION		
1.1	Introduction	1
1.2	Calcareous nannofossils and coccolithophores	3
1.3	The Greenhouse- Icehouse Transition	8
1.4	Biotic response to late Eocene cooling and EOT	12
1.5	Location and stratigraphy of study area	13
1.6	Objectives and overview of the thesis	18
CHAPTER 2: NANNOFOSSILS FROM THE MOSSY GROVE CORE		
2.1	Introduction	20
2.2	Depositional environments of Mossy Grove core	23
2.3	Methodology	24
2.4	Systematic taxonomy	24
2.4.1	Placolith coccoliths	24
2.4.2	Murolith coccoliths	33
2.4.3	Holococcoliths	38
2.4.4	Nannoliths	40

CHAPTER 3: CALCAREOUS NANNOFOSSIL ASSEMBLAGES THROUGH EOCENE/OLIGOCENE TRANSITION IN THE MOSSY GROVE CORE

3.1	Introduction	56
3.2	Methods and materials	58
3.3	Results	60
3.3.1	Biostratigraphy	60
3.3.2	Nannofossil assemblages	64
3.3.3	Multivariate assemblage analysis	65
3.4	Discussion	83
3.4.1	Late Eocene cooling phase	84
3.4.2	Eocene/Oligocene Transition	87
3.4.3	Palaeoecological preferences of calcareous nannofossil	88

CHAPTER 4: GEOCHEMICAL PROXIES FOR PALAEOENVIRONMENTAL CHANGE AND PLANKTONIC FORAMINIFERA FROM MOSSY GROVE CORE

4.1	Introduction	91
4.2	Methodology	93
4.2.1	Fine-fraction (<20μm) bulk isotope analyses	92
4.2.2	Planktonic foraminfera assemblages and isotope analyses	94
4.2.3	TEX_{86} analyses	94
4.2.4	Benthic foraminifera isotope and trace metal analyses; bulk XRF analyses	96
4.3	Results	96
4.3.1	Fine-fraction (<20μm) bulk isotope analyses	96
4.3.2	Planktonic foraminfera assemblages and isotope analyses	97
4.3.3	Planktonic foraminifera isotope	111
4.3.4	TEX_{86} analyses	112
4.3.5	Benthic foraminifera isotope and trace metal analyses;bulk XRF analyses	116

4.4	Discussion	117
4.4.1	Coccolith-fraction stable isotope stratigraphy and environmental interpretation	117
4.4.2	Palaeotemperature estimation through the layte Eocene and EOT	120

CHAPTER 5: THE EOCENE/OLIGOCENE TRANSITION ON THE US GULF COASTAL PLAIN

5.1	Introduction	121
5.2	The late Eocene-Oligocene Transition (E/OT) boundary at Mossy Grove core	122
5.3	Phytoplankton changes during the EOT	126
5.4	Comparison of ostracode and palynology analysis with calcareous nannofossil assemblages at Mossy Grove core	128

CHAPTER 6: CONCLUSION

6.1	Conclusion	131
6.2	Recommendation	133

REFERENCES 135

LIST OF FIGURES

(short version of figure captions)

No. of Figure		Page
1.1	The global climate over the past 65 Ma	2
1.2	Inside the coccolithophores cell	4
1.3	The overview of late Eocene lead up to EOT	10
1.4	The location of Mossy Grove core	14
1.5	The stratigraphy of Mossy Grove core	17
2.1	Location of Mossy Grove core	22
2.2	Sketched diagram of *R.daviesii* and *R.callida*	55
3.1	The age model of Mossy Grove	62
3.2	Plotted graph of *Reticulofenestra* spp.	67
3.3	Plotted graph of *Reticulofenestra* spp. (continued).	68
3.4	Plotted graph of *Coccolithus* spp.	69
3.5	Plotted graph of *Coccolithus* spp. (continued).	70
3.6	Plotted graph of *Blackites* spp.	71
3.7	Plotted graph of *Helicosphaera* spp.	72
3.8	Plotted graph of *Umbilicosphaera* spp.	73
3.9	Plotted graph of *Pontosphaera* spp.	74
3.10	Plotted graph of *Holococcolithus* spp.	75
3.11	Plotted graph of *Discoaster* spp.	76
3.12	Plotted graph of *Braarudosphaera* spp.	77
3.13	Plotted graph of *Sphenolithus* spp.	78
3.14	PC1 loadings on selected species for PCA analysis	81
3.15	PC2 loadings on selected species for PCA analysis	81
3.16	The PC1 and PC2 loadings of multivariate analysis PCA	83
4.1	The carbon isotope data from the bulks sediments	98
4.2	The oxygen isotope data from the bulks sediments	99
4.3	Relative abundance of planktonic foraminifera	110
4.4	The cross plotting multispecies of planktonic foraminifera	113
4.5	Planktonic foraminifera isotope data of Mossy Grove core	114

4.6 The oxygen, carbon isotope and TEX86 temperature data 115
5.1 The compilation data of Mossy Grove core 130

LIST OF TABLES

(short version of table captions)

No. of Table		Page
3.1	Species and group of species used in PCA analysis	79
3.2	The values of PCA analysis for all species	80
3.3	Ecological preferences of different species based on PCA analysis	86
4.1	The counting of planktonic foraminifera	100

LIST OF PLATES

No. of Plate		Page
2.1	Noelaerhabdaceae	44
2.2	Noelaerhabdaceae	45
2.3	Coccolithaceae, calcidiscacease, incertea sedis, mesozoic survivor	46
2.4	Helicosphaeraceae	47
2.5	Rhabdosphaeraceae, holococcoliths	48
2.6	Nannoliths	49
2.7	Nannoliths	50
2.8	Noelaerhabdaceae (SEM)	51
2.9	Noelarhabdaceae, coccolithaceae (SEM)	52
2.10	Pontosphaeraceae (SEM)	53
2.11	Rhabdosphaeraceae, holococcoliths, nannoliths (SEM)	54
4.1	*Globoturborotalita* spp.	107
4.2	*Turborotalia* spp.	108
4.3	*Hantkenina* spp. and *Globigerinatheka index*	109

Chapter 1

Introduction of late Eocene Palaeoenvironments and Palaeoclimate of the US Gulf Coast

1.1 Introduction

In recent years, there has been an increasing interest in Cenozoic climate change. The Cenozoic Era, divided into the Paleogene, Neogene and Quaternary periods, began 66.00 ±0.05 million years ago and continues to the present. During the Cenozoic, there were several long-term, gradual warming and cooling trends which were most likely driven by the interplay of global tectonic processes and transfers of carbon between the principal planetary reservoirs (Zachos et al., 2001; Zachos et al., 2008). The most significant among these long-term changes was the major global cooling from the warm, greenhouse-climates of the early Palaeogene, with minimal continental polar ice caps, to the glaciated, "one-cold pole" climate of the Oligocene icehouse (Zachos et al., 2008) (Figure 1.1). Although this cooling trend started immediately following the Early Eocene Climatic Optimum (EECO) at ~50 Ma, and progressed through the middle and late Eocene, the most rapid and dramatic climatic transition occurred within ~500 ka during the Eocene-Oligocene Transition (EOT) (~34 Ma) (Lear et al., 2008; Coxall et al., 2005).

The Eocene-Oligocene transition, even though not as large as the 'big five' mass extinctions, is still globally recognised as a major turning point in the structuring and diversity of both marine (Ezard et al., 2011; Falkowski et al., 2004; Rabosky and Sorhannus, 2009) and terrestrial ecosystem (Prothero 1994). These major biotic changes were associated with a similar fundamental shift in the climate system, from a condition of limited or no Antarctic ice caps in Paleocene-Eocene times to a persistently glaciated Antarctica from the earliest

Oligocene to modern times (Cramer et al., 2011; Lear et al., 2000). The tectonic and climatic causes and preconditions for this geologically rapid transition are still widely debated,

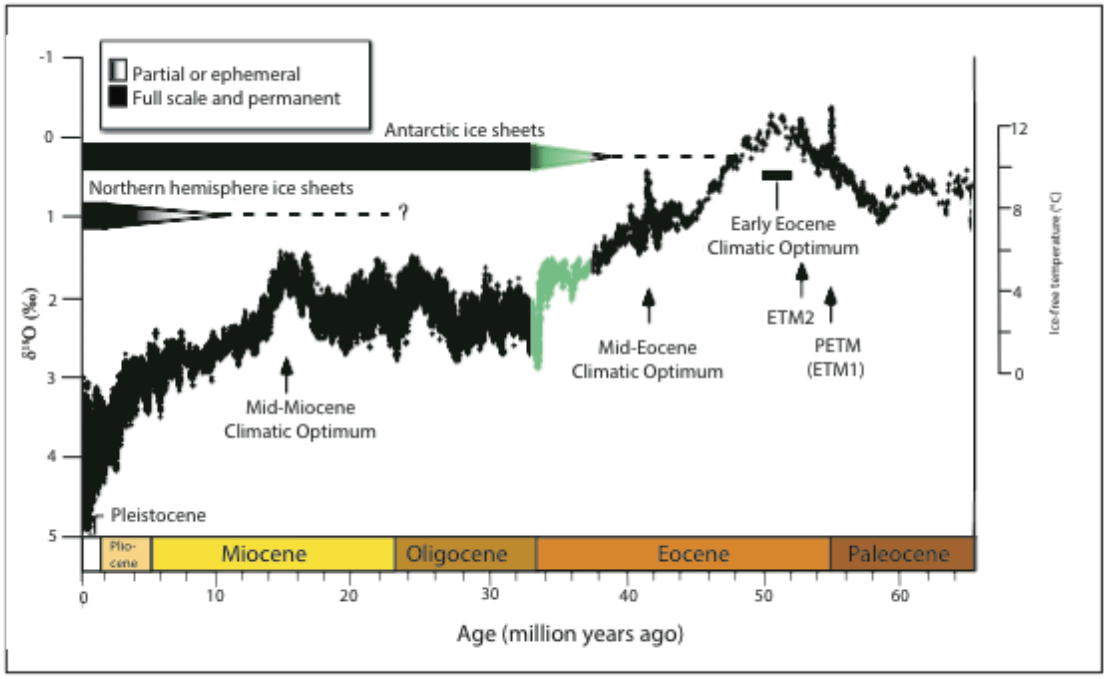


Figure 1.1: The global climate over the past 65 Ma (Zachos et al., 2008). The graph shows several warming and cooling events during Cenozoic. Note: green area marked the study section of Mossy Grove core.

including the tectonic evolution of Antarctic gateways - the Drake Passage (Persico & Villa 2004; Scher and Martin, 2004; Scher and Martin, 2006) and Tasman gateway (Stickley et al., 2004) and a long-term decline in the level of atmospheric CO_2 (DeConto & Pollard 2003; Pagani et al., 2005; Pearson et al., 2009; Anagnostou et al., 2016). My interest in the study of this climatic boundary is to understand the links between a major climate regime change and the functioning and composition of marine primary producers, in the form of the calcifying phytoplankton. To do this, the Mossy Grove section was chosen because of the apparently complete sequence through the late Eocene, up to, and potentially including the Eocene-Oligocene boundary. One of the aims of this research was to refine and constrain the

stratigraphy of the section using calcareous nannofossil biostratigraphy and isotope stratigraphy. The uniform, clay-rich sediments throughout this section also host well-preserved assemblages of calcareous nannofossil suitable for detailed assemblages and biodiversity studies. Although planktonic foraminifera are less abundant in this section, additional studies were made for the purposes of oxygen isotopic temperature estimation.

1.2 Calcareous nannofossils and coccolithophores

Coccolithophores are calcifying unicellular marine phytoplankton within the Prymnesiophyceae, Phylum Haptophyta (De Vargas et al., 2007). Typically in the size range of ~1-10 microns (Young & Henriksen 2003), the living cells of coccolithophores are surrounded by coccoliths that form an extracellular covering, or coccosphere (Figure 1.2). As with other prymnesiophyte algae, the cell wall (periplast) of coccolithophores consists of various layers of organic scales held in place by fibrillar or columnar material with adhesive properties (Billard & Inouye 2004). The coccolithophores are distinctive in possessing distal scales of the periplast that are generally calcified (coccoliths) and visible under the light microscope (Billard & Inouye 2004). Many coccolithophore species possess two different biomineralization modes, within the hapoid and diploid life cycle phases of a single species producing different types of coccoliths (Figure 1.2). In the diploid phase of most coccolithophore species, coccoliths are formed within intra-cellular vesicles (Young and Henriksen, 2003). These “heterococcoliths” have a complex construction of radial arrays of, typically <100, crystal-units with diverse morphology (Young & Henriksen 2003). In species where the haploid phase also produces calcified scales, these are typified by more simply constructed holoccoliths, formed of numerous - usually several hundreds to few thousands -

minute equant or euhedral calcite crystallites (Young & Henriksen 2003). There is growing evidence that these holococcoliths are produced outside of, or very close, to the external cell membrane (Young and Henriksen, 2003). The final common coccolith-type are the nannoliths. This group consists of coccoliths and calcareous nannofossil whose morphology

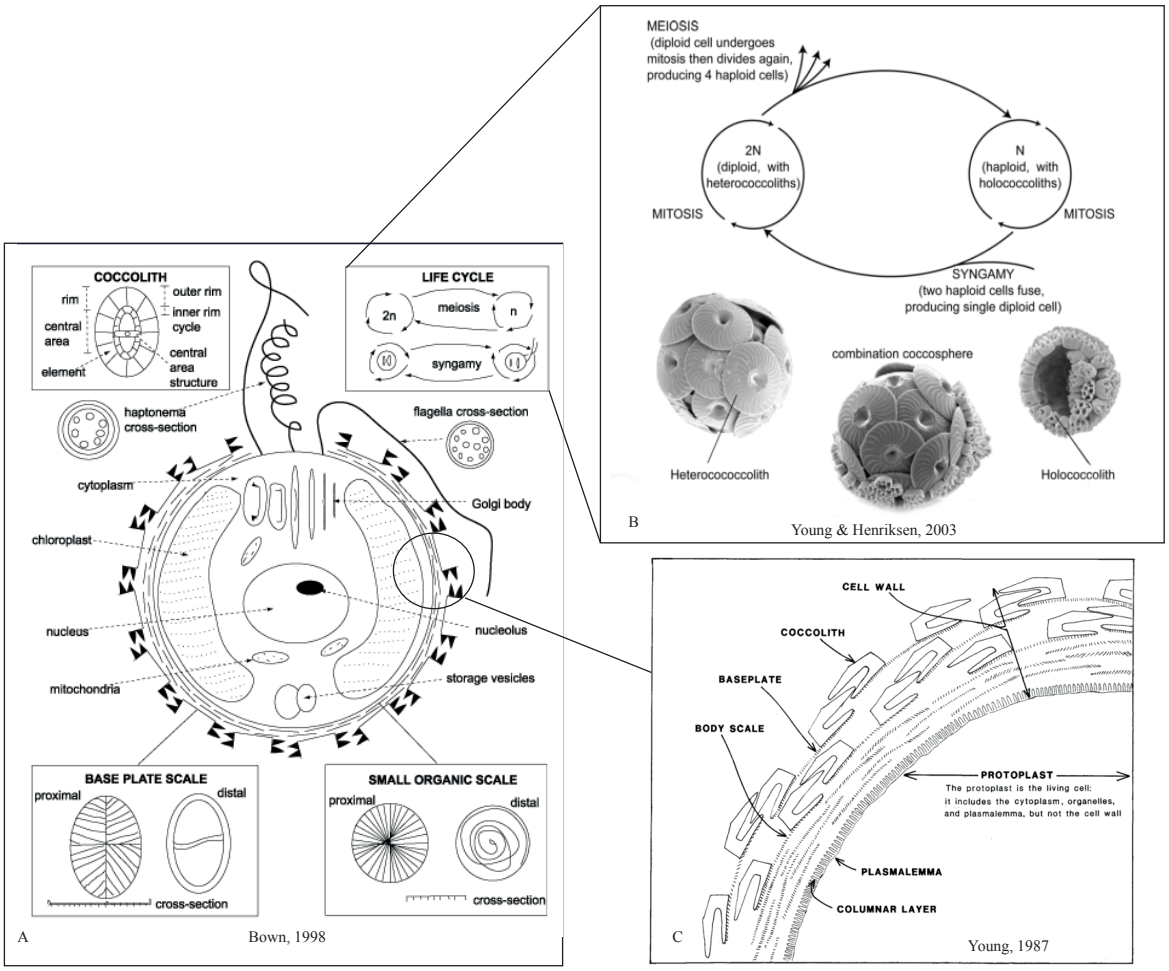


Figure 1.2: Inside the coccolithophores cell; A: The cross section overview of coccolithophores cell, and the life cycle of the coccolithophores, B: The life cycle of coccolithophores, C: The coccolithophores wall cell and coccoliths (combined from Bown, 1998; Young & Henriksen, 2003 and Young, 1987).

cannot be included in either hetero- or holococcoliths. In the fossil record, where there are no living ancestors, these cannot be confidently associated with production by haptophyte algae, but this seems their most likely origin, based on their size and pervasive co-occurrence with

other coccoliths (Young et al., 1999). This is supported by observations of one group of living coccolithophores that produce nannoliths (ceratoliths), that are postulated to be equivalent to holococcoliths and represent the haploid life cycle stage (Billard & Inouye 2004).

Although it is difficult to constrain the biological function of coccoliths, the principal evolutionary advantage of coccolith-production is most likely for cellular protection against damage, predation and pathogen attack by increasing the diameter external strength of the cell (Young 1994). Some have suggested that, as a marine phythoplankton, the buoyancy effect of coccoliths of different mass may also play a role in regulating coccolith production and morphology. For example, the large and heavy coccoliths promote sinking, whilst elongate-shaped coccospheres may provide additional buoyancy (Young 1994). The particular shape of coccoliths may also play a role in light regulation in two ways: 1) by reflecting harmful ultraviolet light, enabling coccolithophore cells to live higher in the water column, especially in clear-water tropical conditions (Young 1987); and, 2) by refracting light into the cell, for the purpose of enhancing photosynthesis, since the refractive index for calcite is higher than surrounding waters (Young 1987). This would appear to be the case for the distinctive coccolith morphologies produced by many deep-photic zone taxa (Bown et al., 2009). Finally, the calcification in coccolithophores has been linked to the production of carbon dioxide which required within the cell for photosynthesis (Young 1987). However, recent work suggests more complex competing relationships between the allocation of carbon for photosynthesis and calcification (Bolton and Stoll, 2013).

The first recorded observations of calcareous nannofossil - of elliptical, flattened disc shapes, with one or several concentric rings on their surface - were made by C.G. Ehrenberg in 1836 while examining the fine structures of Cretaceous chalks from the island of Rugen in the Baltic Sea (in Siesser, 1994). Then, in 1858 T.H. Huxley, working on North Atlantic

deep-sea sediments discovered tiny calcareous objects and named them ‘coccoliths’ (in Siesser, 1994). In 1857, G.C. Wallich observed that coccoliths live as constituents of a larger body which he called a coccosphere, first noted within a sample from a salp gut, collected on his return to Europe from India (in Siesser, 1994). Later, in 1861, H.C. Sorby also observed coccoliths in the Upper Cretaceous chalk in England and understood that the small discs were concave / convex and were sometimes united in small, hollow spheres within the chalk sediments. This observation connected this ancient fossil material with Huxley’s observation of coccoliths in recent deep-sea sediments. Wallich and Sorby both believed that these coccospheres had an organic origin unlike Ehrenberg and Huxley, who in their early discoveries, considered those platelets to have an inorganic origin. The study of calcareous nannofossil then rapidly evolved, with T. Braarud and E. Nordli, in 1952, initiating the modern, detailed investigation of nannofossil using transmission electron microscopy (in Siesser, 1994).

In the modern Earth System, coccolithophores are significant for total marine primary production and carbon fixation, playing a key function within modern marine environments (Field et al., 1998). The sensitivity of coccolithophore assemblages, in the range of species present and their biological diversity, to the surface ocean environmental conditions, such as temperature and nutrient availability (Ziveri et al., 2004), make them useful indicators of both physical and ecological conditions within the surface ocean. The abundance and widespread distribution of coccoliths, as fossil remains in marine sediments, can be used to reconstruct past marine conditions. These studies typically focus on large scale shifts in assemblage compositions (e.g. Dunkley Jones et al., 2008), rates of extinction or speciation (Gibbs et al., 2006) or long-term patterns of diversity (Bown et al., 2004). More recently alkenones, organic biomarkers produced by coccolithophore alage, have been used to reconstruct ancient marine

temperatures (Haywood et al., 2005) and atmospheric carbon dioxide concentrations (Zhang et al., 2013).

This PhD study focuses on the taxonomy, assemblages and preservation of calcareous nannofossil as tools to identify marine palaeoenvironmental change, from the late Eocene to early Oligocene, at a sub-tropical site on the Gulf Coast of North America. The studied section is from the Mossy Grove core, which recovered a near-complete succession of the Yazoo Clay near Jackson, Mississippi. In this location the Yazoo Clay hosts very well-preserved calcareous nannofossil assemblages, which justifies the detailed taxonomic investigation presented in Chapter 2. Coccolith assemblages are diverse, and seemingly preserve communities similar to the primary living assemblages. These include a diverse reticulofenestrid assemblage, including species useful as indicators of tropical, temperature and cool-water conditions during the late Eocene and through EOT boundary (Chapter 3). The quality of preservation of the reticulofenestrid group in this site is demonstrated by the *Reticulofenestra lockeri* group, where the morphological variation within and between different species were determined by observing the central area plug and net, as well as pores. Detailed illustration of the differences of these morphologies is important to illustrate the variability and inter-gradations between species that cannot be seen in more poorly preserved material (Chapter 2). The distinctive shelf / opportunist taxa, *Braarudosphaera bigelowii*, is also preserved throughout the core, with distinct patterns of abundance variations downcore indicative of palaeoenvironment conditions at this site (Chapter 3).

1.3 The Greenhouse – Icehouse Transition

The long-term climate history of the Earth can be divided into two broad climatic states; a world free of major polar ice-caps, known as "greenhouse" conditions, and one with significant land-based polar ice-sheets, known as "icehouse" conditions. Coupled with the absence of polar ice-sheets, greenhouse conditions are characterized by high concentrations of atmospheric carbon dioxide, estimated to be in excess of ~750 ppm (Pagani et al., 2011) and a mean planetary surface temperature >10ºC warmer than modern (Lunt et al., 2012). The modern icehouse conditions, on the other hand, which have persisted for the last ~34 million years, are characterized by the presence of, at minimum, the East Antarctic Ice Sheet (EAIS), and atmospheric carbon dioxide concentrations, for the most-part, below 500 ppm (Zhang et al., 2013). Although the exact timing of the first development of the EAIS is still uncertain, and may have been within the later part of the middle Eocene or late Eocene (Cramer et al., 2011), the most prominent and rapid expansion of Antarctic ice-sheets occurs within the 500 ka on either side of the Eocene/Oligocene boundary (Coxall et al., 2005). This study focuses on both the significant cooling trend during the latest Eocene, and potential for sea level variation associated with ice sheet expansion, as well as the major and more rapid change associated with the Eocene/Oligocene Boundary. This interval marks the most recent of the Earth's fundamental climate mode switches from a warm, ice free greenhouse world into a cold icehouse world (Zachos et al., 2001; Villa et al., 2008).

The climatic regime of the early Cenozoic (Palaeocene and Eocene) greenhouse climate state was not only different in the absence of polar ice sheets and warmer planetary surface temperatures (Figure 1.1) (Zachos et al., 2008), but the nature of climate variability also seems to have been fundamentally different. Within this interval, short-term orbital-scale

variations were dominated by carbon-cycle rather than ice-sheet dynamics, including the occurrence of transient warming events, or hyperthermals, such as the Palaeocene–Eocene Thermal Maximum (PETM) (Kennett & Stott 1991) and the Eocene Thermal Maximum 2 (ETM2) (Lourens et al., 2005; Sluijs et al., 2009). These are characterized by an increase in global temperatures, negative carbon isotope excursions in the global carbon cycle and dissolution of deep-sea carbonate. On longer, secular timescales, peak Cenozoic warmth was reached during the Early Eocene Climatic Optimum (EECO) 53-51 Ma (Figure 1.1) (Zachos et al., 2001). After the EECO, the Earth started to gradually cool through the middle to late Eocene, with ~7°C deep sea cooling (Zachos et al., 2001). This was briefly interrupted by ~2-3ºC warming during the Middle Eocene Climatic Optimum (MECO) around 40 million years ago (Figure. 1.1) (Bohaty & Zachos 2003), but this warming only persisted for ~500 ka.

In this study, my attention focuses on the late Eocene and the Eocene-Oligocene transition (EOT) boundary at the end of this long-term cooling trajectory. The detailed climate dynamics of the late Eocene are still poorly constrained, although they are clearly a critical interval with the potential for multiple intervals of growth and decay of the Antarctic Ice sheet prior to the final switch into the icehouse conditions across the Eocene/Oligocene boundary (Peters et al., 2010). Evidence for this variation in continental ice volume is derived from the geological observations of sea-level fluctuations during the late Eocene, such as valley incision and delta progradation (Peters et al., 2010). Distinct the late Eocene positive shifts in benthic foraminiferal $\delta^{18}O$, reflecting similar positive shifts in the isotopic composition of global seawater as well as local cooling, have also been noted, such as the Priabonian oxygen isotope maximum (PrOM) event (Figure 1.3) (Scher et al., 2014). This oxygen maximum isotope together with the contemporaneous marked increase in the flux of terrigenous material with a pronounced negative Nd isotope signal (εNd) into circum-Antarctic seawater, is

evidence that late Eocene ice-sheet expansion is concentrated within a growing EAIS (Figure 1.3) (Scher et al., 2014).

The Eocene/Oligocene Transition (EOT) itself, is the most marked and rapid phase of the climate transition from the warm greenhouse worlds of the Cretaceous to early Cenozoic into the cold icehouse world of today (Prothero, 1994). When first documented, the EOT was

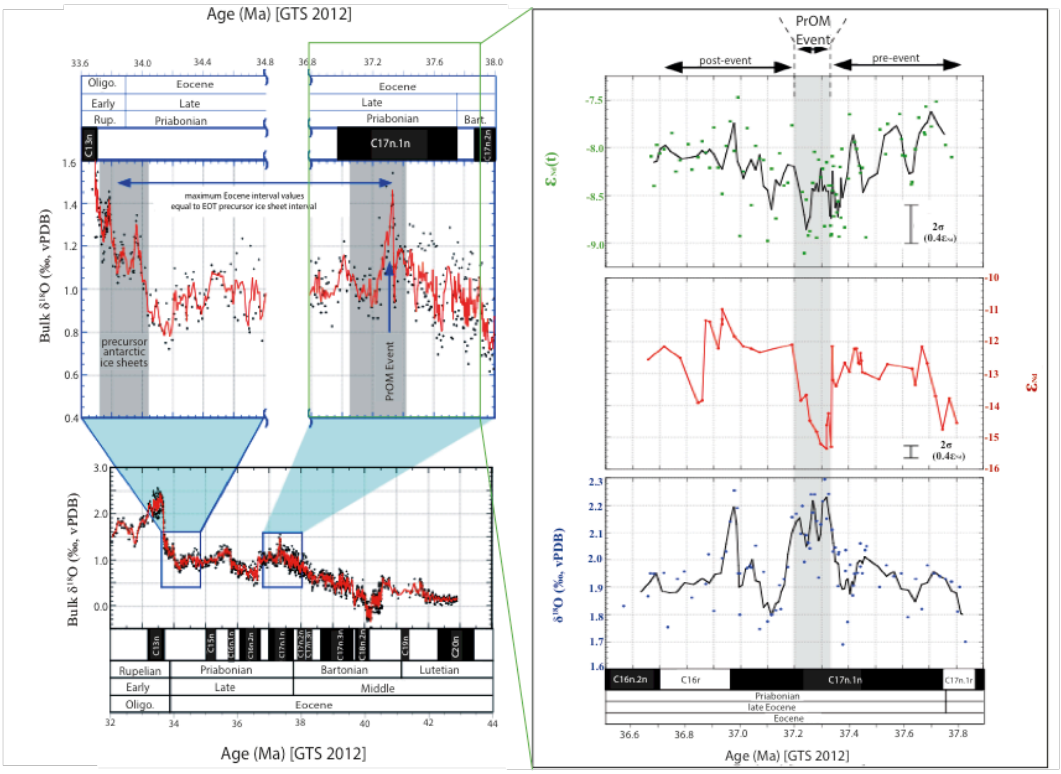


Figure 1.3: (Left) The overview of late Eocene lead up to EOT and (Right) the results of benthic foraminiferal $\delta^{18}O$, terrigenous sediment εNd, and fossil fish teeth εNd from ODP site 738 during the late Eocene cooling event (Priabonian Oxygen Maximum-PrOM) (Scher et al., 2014).

found to be associated with a major unconformity surface that spanned the latest late Eocene to middle Oligocene (Kennett et al., 1975). This sea-level related unconformity of global significance, was then found to be consistent with oxygen isotope records that coupled this to

the primary greenhouse-icehouse transition and the appearance of permanent ice sheets on Antarctica during late Eocene and early Oligocene (Miller et al., 1998; Coxall et al., 2005). Many mechanisms have been proposed to explain the cause of long-term cooling, as well as the timing and rate of the EOT, including the opening of the major Southern Ocean getaways, the Tasman Gateway and Drake Passage (Kennett 1977), a long-term decrease in atmosphere CO_2 concentrations (DeConto & Pollard 2003; Pagani et al., 2005; Pearson et al., 2009), and orbital-paced variations in high-latitude solar insolation (Coxall et al., 2005). Finally, the association of late Eocene cooling with an increase in meteorite impact rates, and a number of large scale impact events (Ravizza and Peucker-Ehrenbrink, 2003) has led to the suggestion that global cooling, and shifts in biotic communities, during late Eocene is, at least in part, driven by the atmospheric effects of these events (Vonhof et al., 2000).

The effects of the rapid rate of Antarctic ice-sheet growth at the EOT itself were widespread on both the climate system, ocean and atmospheric circulation and the biosphere. These effects include global cooling (Liu et al., 2009; Zanazzi et al., 2007), a major eustatic sea level fall of 60-70m (Lear et al., 2008), dramatic changes to oceanic carbonate chemistry (Coxall et al., 2005), and marine planktonic communities (Pearson et al., 2008; Dunkley Jones et al., 2008). In terrestrial vertebrate communities, there is evidence for cooling-related range-shifts and extinctions in North America and Central Asia (Zanazzi et al., 2007). These include the extinction of a range of cold-blooded animals in North America, a community that are very sensitive to temperature decrease (Zanazzi et al., 2007). In Central Asia, terrestrial lake and playa deposits, indicate marked aridification of the Tibetan Plateau region synchronous with Antarctic glaciation (Dupont-Nivet et al., 2007).

1.4 Biotic response to late Eocene cooling and EOT

The EOT represents a major floral and faunal turnover. Most of the major groups of marine microfossils show changes in assemblage characteristics through this interval, such as radiolarians (Funakawa et al., 2006; Lazarus & Caulet 1993), diatoms (Suto 2007), planktonic foraminifera (Wade & Pearson 2008), benthic foraminifera (Alegret et al., 2008; Wade & Pearson 2008) and calcareous nannoplankton (Bown et al., 2008; Dunkley Jones et al., 2008; Persico & Villa 2004; Villa et al., 2008; Wei & Wise 1990).

The calcareous nannofossil assemblage data from the late Eocene of the Southern Ocean indicate several minor decreases in sea-surface temperature (SST) from 36-34 Ma, before the EO boundary and a sharp cooling event during the earliest Oligocene (~33.54 Ma) (Perciso & Villa 2004). Across the EOT in the Southern Ocean there is a rapid shift in calcareous nannofossil assemblages from temperate-water to cool-water taxa (Perciso & Villa 2004). In the tropics there are also indications of significant nannofossil turnover directly associated with the EOT (Wei and Wise 1990; Dunkley Jones et al., 2008). However these are hypothesized to be related to changes in productivity regimes rather than the direct effect of sea surface cooling at the EOT (Dunkley Jones et al., 2008).

The earliest study of planktonic foraminifera in the stratotype section, Massignano, Italy shows a less marked change through the EOT boundary (Coccioni et al., 2000). More recently, Molina et al., (2006) studied the effect of meteorite impacts on patterns of foraminifera extinction and observed increased extinction at the EO boundary. This close coupling between extinction and abrupt turnover in planktonic foraminifera assemblages at the EOT was demonstrated by the observation of extinction of all five remaining species of

the family Hantkeninidae, and a reduction size of *Pseudohastigerina* across the EOT succession in Tanzania (Wade & Pearson 2008).

1.5 Location and stratigraphy of study area

The Mossy Grove Core was named after the adjacent lake, Mossy Grove, which is located on the east side of Clinton-Tinnin Road opposite Camp Kickapoo, in north-western Hinds County, Mississippi (Figure 1.4). The Mossy Grove core, along with the Society Ridge and Miss-Lite boreholes, was one of three drilled in Hinds County Mississippi by the Mississippi Department of Environmental Quality (DEQ). The majority of the recovered succession consisted of the late Eocene Yazoo Clay of the Jackson Formation, which is a relatively uniform claystone and undifferentiated in Western Mississippi. The Yazoo Clay in eastern Mississippi and southwestern Alabama is more heterogeneous, and has been divided into the North Twistwood Creek Clay Member, the Cocoa Sand Member, the Pachuta Marl Member and the Shabuta Clay Member.

The main objectives of drilling the Mossy Grove core was to obtain a fresh, complete and unweathered section of the Yazoo Clay, and then to use this to reveal the geologic history of the late Eocene of western Mississippi (Dockery III et al., 1991). Additional targets were two distinct bentonite layers that had been identified by John Obradovich, US Geological Survey, Denver, Colorado and Carl Swisher of Institute of Human Origins in Berkeley, California, with the aim of obtaining radioisotope data in Upper Yazoo Clay in Western and Central Mississippi (Dockery III et al., 1991).

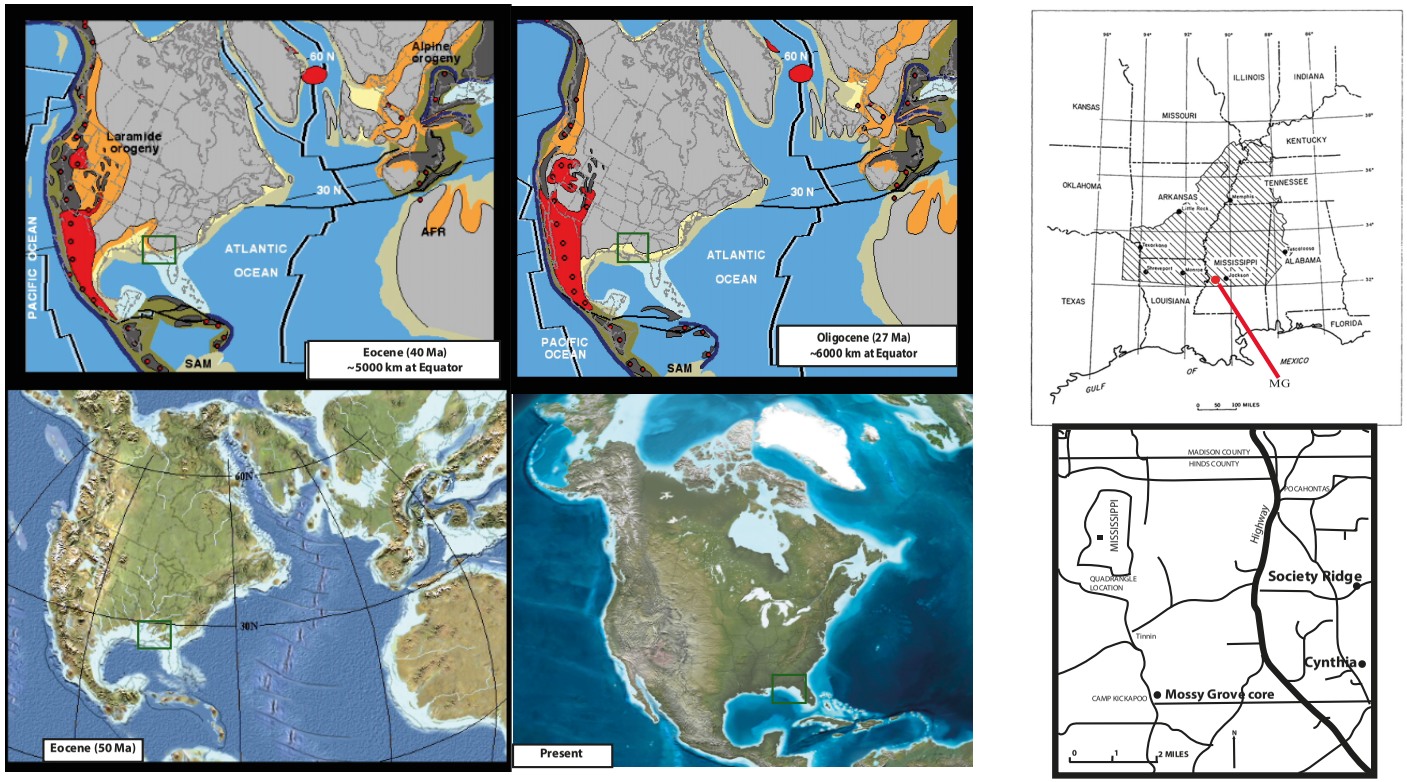


Figure 1.4: The location of Mossy Grove core during the Eocene, Oligocene and present (left), the shaded area (right above) is Mississippi Embayment area edited from Cushing et al, 1964, and (right below) the location of Mossy Grove core. Noted that during the Eocene, Mossy Grove core was offshore, sea level fall at the end of Eocene brought rivers and swamps across central Mississippi (Dockery, 1997), that interpreted as a source of freshwater environment. (Green box on left shows the possible location of Mossy Grove core, whilst Red dot on right is the location of Mossy Grove core).

To obtain the most detailed geological records, the location of the Mossy Grove core was selected where the thickest, most complete and unweathered Yazoo Clay was mapped to be present in the sub-surface. This was based on available geophysical logs from nearby commercial wells. The thick Yazoo Clay section recovered during drilling provides the most continuous record of late Eocene history on the US Gulf Coastal plain. At the top of the Mossy Grove core, there is a thin sequence of the lignitic Forest Hill Formation above Yazoo Clay, which was also a prime target for drilling, as this was identified as potentially representing the major regional sequence boundary in the lowest Oligocene (Dockery III et al., 1991).

The core recovered a continuous section through the Jackson Group of western Mississippi, including the Forest Hill, Yazoo Clay and Moodys Branch Formations as well as Creola Member of Cockfield Formation at the base of the borehole. Stratigraphically, the core encountered 28 feet (~8.5 m) of Pleistocene loess, 10 feet (~3 m) of lignites, sands and shales of the early Oligocene Forest Hill Formation (Vicksburg Group), 462 feet (~140 m) of the late Eocene Yazoo clay (Jackson Group), 12 feet (~3.7 m) of glauconitic sand of the late Eocene Moodys Branch Formation (Jackson Group) and 18 feet (~5.5 m) of clays and sands of Middle Eocene Cockfield Formation (Claiborne Group) (Figure 1.5). Core recovery started below 30 feet (~9.1 m) depth and reached to 530 feet (~161.5 m), with a total length of the recovered core of 462 feet (~140.8 m) (Dockery III et al., 1991).

From the fresh core itself, the following lithostratigraphy of Mossy Grove had been observed. The contact between the Forest Hill Formation and Yazoo Clay was determined by the present of lignite unconformably overlying the marine clay. The Yazoo Clay is grayish green in color, and contain montmorillonitic clay that varies in darkness and lightness of hue. In the upper part, down to 150 feet depth, this is rich in mollusk shells and contain of thin

layers of shell hash. At 10 feet below the top, there is a 3-inch thick horizon of glauconitic sands. At 50 feet below the clay's top, there is a 4-inch thick bentonite. The dusky green, fossiliferous Moodys Branch Formation consists of glauconitic sand. The contact between Moodys Branch Formation and Cockfield Formation was sharp, and marked by the presence of burrows and clasts. The upper 8 feet of the Cockfield Formation is dusky yellowish brown in color, and consists of a silty clay formation with crushed oyster shells.

Within the Yazoo Clay Formation, benthic foraminiferal distribution is reported to be controlled by organic carbon flux to sediments and bottom water dissolved oxygen concentrations (Loubere et al., 1993). More recent studies indicate a significant role for sea level fluctuations on benthic communities, within a relatively shallow shelf setting (Yamaguchi et al., 2014). To date there has been no study of the biostratigraphy, taxonomy or assemblage variability of calcareous nannofossil from the Mossy Grove core, even though this group are consistently present throughout the Yazoo Formation and generally very well preserved. It is the aim of the research thesis to fill this gap. This thesis will focus on the stratigraphy of the late Eocene and EOT boundary within the Mossy Grove core based on calcareous nannofossil biostratigraphy, together with planktonic foraminifera occurrences, and detailed high-resolution coccolith-fraction (<20 μm) isotope records.

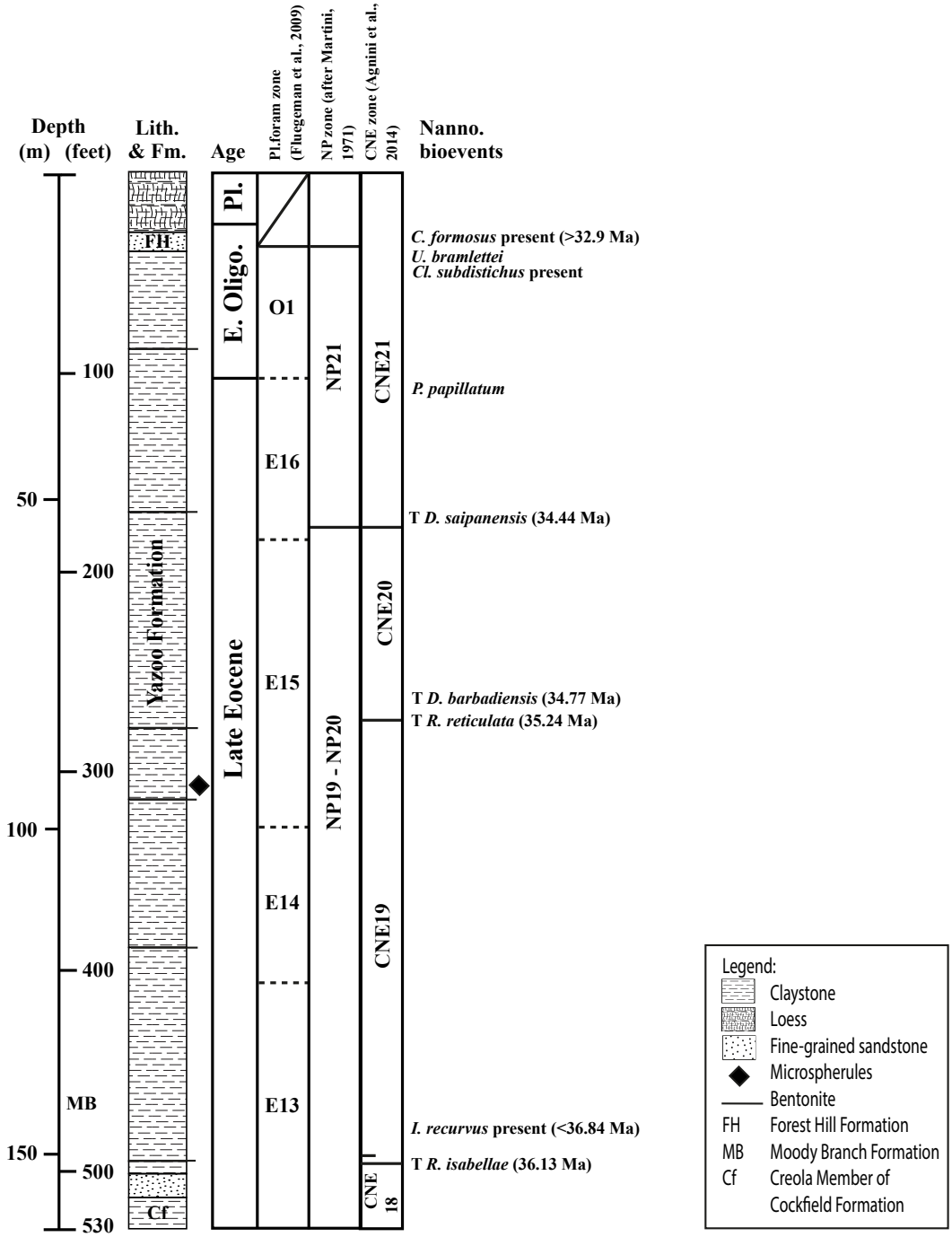


Figure 1.5: The stratigraphy of Mossy Grove core and the overview of the age based on the planktonic foraminifera (from Fluegeman et al., 2009) and nannofossil zone (Martini, 1971 and Agnini et al., 2014).

1.6 Objectives and overview of the thesis

A number of studies have been conducted to examine the relationship of microfauna with late Eocene cooling and the Eocene-Oligocene boundary in the Mossy Grove core. Fluegemen conducted studies of planktonic foraminifera assemblages and biostratigraphy (Fluegeman, 1996, 2009). The first aimed to identify planktonic foraminifera biozones in the Mossy Grove succession within the global biozonation scheme of Berggren & Miller (1988) and Miller (1988), generating an age model based on the geochronological scale of Berggren et al., (1995). This was updated with an extended study of biostratigraphy and taxonomy (Fluegeman, 2009), to follow the new Berggren and Pearson (2005) global biozonation. This concluded that planktonic foraminifera assemblages within the Mossy Grove succession are equivalent to biozones E13 to O1, but this was largely based on the use of secondary markers and general assemblage composition in the absence of most of the zonal marker taxa. The most recent study of microfauna in Mossy Grove was conducted by Yamaguchi et al., (2014), who studied the changes of ostracod assemblages during the EOT. The ostracod assemblages show distinct patterns of assemblage change and extinction through the Yazoo Clay succession, which are primarily associated with sea level changes.

This thesis will focus on characterizing the assemblages, taxonomy and preservation of calcareous nannofossil in the late Eocene and across the EOT of the Mossy Grove core. Together with inorganic geochemistry proxies and the planktonic foraminifera assemblages, this study will lead to the updated version of the Mossy Grove core age model and provide further details on the response of sub-tropical phytoplankton communities to global cooling through the EOT. In recent years, there has been an increasing interest in the coupling of marine ecosystem functioning and climate change, including the major climate events of the

Palaeogene greenhouse world. The EOT boundary is perhaps the most profound of these Paleogene events, representing the rapid and long-term shift into the modern icehouse climate state.

This thesis consists of six chapters, including this first introductory chapter. Chapter 1 provides a review of late Eocene and EOT climate change and the associated biotic responses. It also introduces the main study group, the coccolithophore algae and their fossil representatives, the calcareous nannoplankton. This chapter will also include the research objectives, plan of study, and the overview of the study area's location and stratigraphy. Chapter 2 provides a detailed taxonomy of calcareous nannofossil recovered from the Mossy Grove core, including both light microscope (LM) and scanning electron microscope (SEM) observations and descriptions. Chapter 3 presents detailed calcareous nannofossil assemblage data and discusses assemblage variations in detail through the Yazoo Clay succession of the Mossy Grove core. Chapter 4 presents the results of geochemical proxy analyses, including stable isotope and organic biomarker temperature estimates, as well as presenting new planktonic foraminifera occurrence data for the Mossy Grove core. Chapter 5 will provide an overall integrated discussion of the thesis, including both calcareous nannofossil assemblages data and geochemical proxy data. The final chapter, Chapter 6 will provide a brief summary and conclusion of the main findings of this research.

Chapter 2

Nannofossils from the Mossy Grove core

2.1 Introduction

Thirty years ago, William Seisser published a comprehensive survey of the taxonomy and biostratigraphy of calcareous nannofossil from Paleogene strata of the US Gulf Coast states of Mississippi, Alabama and Tennessee (Seisser, 1983). This included images of very well preserved nannofossil specimens, especially from the late Eocene Yazoo Formation of Alabama and Mississippi. Most of this work, however, was undertaken from surface outcrop samples that are more susceptible to weathering and dissolution than cored material (Siesser, 1983). In 1991 the entire late Eocene Yazoo Formation of central Mississippi was recovered in a continuous core at Mossy Grove, Hinds County, MS (Dockery et al., 1991). A collaborative undertaking of the Mississippi Office of Geology and the Geology Department of the University of Mississippi, this core was stored for research purposes at the Office of Geology, Jackson, MS. Here we present a detailed taxonomic assessment of the calcareous nannofossil assemblages of the late Eocene Yazoo Formation from the Mossy Grove Core.

This taxonomic study of Mossy Grove core will be of broad interest to the calcareous nannofossil research community in the following ways:

Firstly, the late Eocene and the early Oligocene sequences of the US Gulf Coast have been extensively studied to provide palaeoclimate and sequence stratigraphic constraints on the magnitude of temperature and sea level fall across the Eocene/Oligocene transition (Katz et al., 2008; Miller et al., 2008; Wade et al., 2012). All of these studies are based on core material through the St Stephen's Quarry (SSQ) succession in Alabama. Although this section

has good calcareous microfossil preservation in the immediate vicinity of the Eocene/Oligocene boundary, sedimentation is not continuous through the late Eocene and the quality of microfossil preservation is patchy where carbonate content is higher in the lower Yazoo Formation (Miller et al., 2008). In contrast, at the resolution of nannofossil biostratigraphy, the Mossy Grove core appears to represent a continuous section through the late Eocene Yazoo Formation (Figure 2.1). This is consistent with the regional geology, where the Pachuta Marl and Shubuta Clay of southwest Alabama grade into the thick, undifferentiated Yazoo Clay in central Mississippi (Dockery et al., 1991). Here we present a taxonomic analysis of consistently well-preserved calcareous nannofossil from this thick late Eocene clay-rich facies.

Secondly, patterns of late Paleogene temperature-controlled provincialism have been used to develop semi-quantitative palaeotemperature indicators. These have been successfully applied to high-latitude sites in the Southern Hemisphere to demonstrate the temporal dynamics of progressive late Eocene to Oligocene cooling (Persico and Villa, 2004; Villa et al., 2008). One of the key species in these reconstructions, *Reticulofenestra daviesii*, is however, not well imaged within the literature and, on the basis of the existing diagnosis, difficult to reliably distinguish from related grill-bearing reticulofenestrids, such as *Reticulofenestra lockeri* and *Reticulofenestra callida*. In the subtropical setting of the US Gulf Coast a range of grill-bearing reticulofenestra morphologies are present, with systematic changes in morphology occurring through the late Eocene global cooling phase. The quality of preservation of these forms allows for detailed LM imaging of grills that would often be broken or overgrown in other settings. With this new imaging we attempt to clarify the relationship between *R. lockeri, R. daviesii* and *R. callida*.

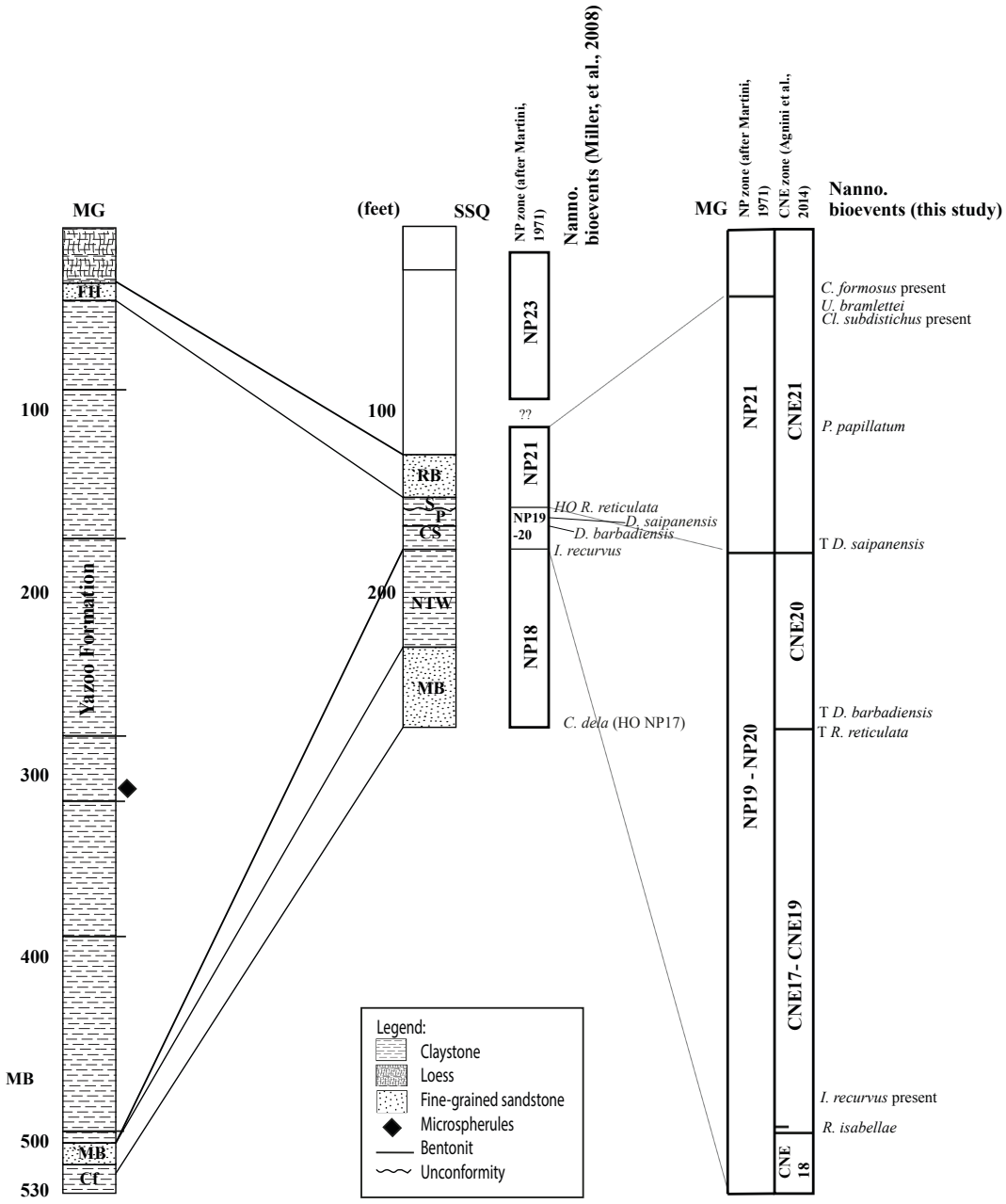


Figure 2.1: The comparison of lithology and biozonation between Mossy Grove core (MG) and St Stephen Quarry (SSQ)(Miller, et al., 2008). Abbreviation: T = Top, B = Base, HO =highest occurrence, Cf = Creola Member of Cockfield Formation, MB = Moody Branch Formation, FH = Forest Hill Formation, NTW = North Twistwood Creek Clay, CS = Cocoa Sand, P = Pachuta Marl, S = Shubuta Marl, RB = Red Bluff Bumpnose Formation.

Thirdly, the generation and publication of combined LM and SEM images, with taxonomic summaries, from well-preserved material provides key reference data for both industrial biostratigraphers and those undertaking nannofossil-based palaeoenvironmental reconstructions.

2.2 Depositional environments of Mossy Grove core

GPlates software for plate reconstructions (Müller et al., 2008) indicate a palaeolatitude for the Mossy Grove of ~31.5 N, which is close to the modern latitude. Based on the benthic foraminiferal and ostracod assemblages, the Yazoo Clay from the Mossy Grove core is estimated to have been deposited in middle neritic to upper bathyal water depths (~150 to 1000 m water depth based on benthic foraminifera assemblages) (Fluegeman et al., 1996; Yamaguchi et al., 2014). Ostracod assemblages suggest a three-step decrease in water depth through the late Eocene (Yamaguchi et al., 2014), consistent with global patterns of cooling and ice sheet growth. The continuous presence of relatively abundant and diverse calcareous nannofossil assemblages throughout the Yazoo Clay interval sampled in this study, support the persistence of fully marine conditions throughout the late Eocene. Typical shelf-dwelling taxa, especially members of the Braarudosphaeraceae are present through the sequence, with discrete intervals of high abundance in the latest Eocene (~44.8 m (147 feet)) shows a shallow mixed layer depth.

2.3 Methodology

Seventy-five samples from Mossy Grove core were prepared as smear slides and observed under the light microscope (x1000). A smear slide was prepared by scraped sample onto the slide and applied with a couple of drops of distilled water (to prevent contamination). Then smear the slide with tooth pick to get a thinner smear, by scraped off sand grains. The slide was dried on a hot plate to remove excess water and the cover slip was placed over the glass slide and placed in a UV light box to dry. The smear slide was then observed under the light microscope and the quantitative counts of calcareous nannofossil assemblages were recorded to get the relative abundance of nannofossils.

2.4 Systematic Taxonomy

Descriptive terminology is based on the guidelines of Young et al., (1997). The higher taxonomic classifications follow those of Young & Bown (1997) and Young et al., (2003); the application of these to late Eocene and early Oligocene aged taxa is discussed in more detail in Dunkley Jones et al., (2009).

2.4.1 Placolith coccoliths

Order Isochrysidales Pascher, 1910

Family NOELAERHABDACEAE Jerkovic, 1970 emend Young & Bown, 1997

Coccoliths with *Reticulofenestra*-type structure:

Cyclicargolithus floridanus (Roth & Hay in Hay et al., 1967) Bukry, 1971

Pl. 2.1, figs 1-7; Pl.2.8, figs 1-7. **Remarks:** Small to large coccoliths with sub-circular shape and a narrow, vacant central area. Distinguished from *R.westerholdii* by its slightly narrower central area and sub circular outline.

***Reticulofenestra umbilicus* group**

Reticulofenestrids with open central area, elliptical and Palaeogene range.

Reticulofenestra hillae Bukry & Percival, 1971

Pl.2.1, figs 9-12; Pl.2.8, figs 25, 26. **Remarks**: Broadly elliptical reticulofenestrids with narrow central area and broad tube, which can be quadrate or lens-shaped. Large to very large-sized (~>9 μm).

Reticulofenestra dictyoda (Deflandre in Deflandre & Fert, 1954) Stradner in Stradner & Edwards, 1968

Pl.2.1, figs 13-15; Pl.2.8, figs 21-24. **Remarks:** Elliptical reticulofenestrid coccoliths with what appears to be an open central area in LM. SEM imaging clearly shows the presence of fragile reticulate grills (Pl. 8, figs 21-23).

Reticulofenestra circus de Kaenel & Villa, 1996

Pl.2.1, fig 16. **Remarks**: Medium to large subcircular reticulofenestrid with a medium-sized, distinctly quadrate central opening.

Reticulofenestra umbilicus (Levin, 1965) Martini & Ritzkowski, 1968

Pl.2.1, figs 21-24. **Remarks**: Very large elliptical reticulofenestrids, with long axis in excess of 14µm. In LM appears to have a very wide and vacant central area, but as with *R. dictyoda*, this is spanned by a fine reticulate grill that is only visible in SEM.

Reticulonestra macmillani Dunkley Jones, Bown & Pearson, 2009

Pl.2.1, fig 20. **Remarks:** A small reticulofenestrid identified by a narrow rim and very wide central area. It has an elliptical shape with weak birefringence net at the outer edge.

***Reticulofenestra pseudoumbilicus* group**

Neogene range reticulofenestrids with open central area and elliptical shape.

Reticulofenestra minuta Roth, 1970

Pl.2.1, figs 17, 18; Pl.2.8, figs 7, 9, 10. **Remarks**: Very small (<3µm) elliptical reticulofenestrids with an apparently open central area in LM. As with other members of the *R. umbilicus* group, a fine grill structure is visible in SEM (Pl.8, figs 7, 9, 10).

Reticulofenestra haqii Backman, 1978

Pl.2.1, figs 19; Pl.2.8, fig 8. **Remarks:** Same morphology as *R. minuta* but small in size (3-5µm) rather than very small.

***Reticulofenestra reticulata* group**

Reticulofenestrids with narrow central opening, and typically circular

Reticulofenestra reticulata (Gartner & Smith, 1967) Roth & Thierstein, 1972

Pl.2.1, figs 25-27, 29; Pl.2.8, figs 17, 18. **Remarks**: A medium to large (6-10 μm) circular to sub-circular coccolith, with a narrow central area cross in XPL. In SEM a distinctly elevated collar is seen on the distal surface, corresponding to the bright tube cycle characteristically seen in XPL.

Reticulofenestra westerholdii Bown & Dunkley Jones, 2012

Pl.2.1, fig 8. **Remarks**: Circular reticulofenestrids with open central area, without perceptible net. Differentiated from *R. reticulata* by the absence of visible net, and from *C.floridanus* by the circular outline, wider central area and low tube cycle.

Reticulofenestra isabellae Catanzariti et al. in Fornaciari et al. 2010

Pl.2.1, fig 28. **Remarks**: Circular reticulofenestrids with narrow central area, and broad tube cycle. Similar to R. reticulate but relatively longer >12μm.

***Reticulofenestra lockeri* group**

Elliptical reticulofenestrids, open central area with robust grill.

Reticulofenestra lockeri Muller, 1970

Pl.2.2, figs 1-4. **Remarks**: Elliptical reticulofenestrid coccoliths with a medium to wide central area spanned by a weak birefringent net which is not visibly perforated in LM observations.

Reticulofenestra daviesii (Haq, 1968) Haq, 1971

Pl.2.2, figs 5-17, 21-25; Pl.2.8, figs 19,20. **Remarks**: Medium reticulofenestrid coccoliths with wide central area net, which is surrounded by a faint but distinct ring of pores around its outer margin. Differentiating *R. lockeri*, *R. daviesii* and *R. callida* is not easy, even in samples with excellent preservation. In LM we distinguish *R. daviesii* from *R. lockeri* by the presence of perforations at the outer margin of the central area net, and from *R. callida* by its wider central area, the slightly lower birefringence of the central area net compared to the plug in *R. callida* and occasional faint perforations visible in the central area net. These observations are supported by SEM imaging, which shows the central area net in *R. daviesii* (Pl.2.8; fig. 19) versus plug in *R. callida* (Pl. 2.8; fig. 11, 13-14).

Reticulofenestra callida (Perch-Nielsen, 1971) Bybell, 1975

Pl.2.2, figs 18- 20; Pl.2.8, figs 11-15; Pl.9, figs 1-8. **Remarks**: An elliptical coccoliths with narrow and solid central area plug and surrounded by distinct perforations. For differentiation from *R. daviesii*, see Remarks above (Figure 2.2).

***Reticulofenestra bisecta* group**

Closed central area, and elliptical in shape.

Reticulofenestra bisecta (Hay et al., 1966) Roth 1970

Pl.2.2, figs 31, 32; Pl.2.8, fig 16. **Remarks**: Medium-sized (<10μm) elliptical reticulofenestrid coccolith with solid central plug.

Reticulofenestra stavensis Levin & Joerger, 1967

Pl.2.2, fig 33. **Remarks:** Reticulofenestrid coccolith, with *R. bisecta* morphology but distinguished by its larger size of >10µm.

Reticulofenestra filewiczii (Wise & Wiegand in Wise, 1983) Dunkley Jones et al., 2009

Pl.2.2, figs 26-30, 34,35. **Remarks**: Broad elliptical reticulofenestrid coccoliths with a narrow central area. Larger specimens (~>10µm in length) can show faint pores surrounding the narrow central area.

Order Coccolithales Schwarz, 1932

Family COCCOLITHACEAE Poche, 1913 emend. Young & Bown, 1997

Genus COCCOLITHUS Schwarz, 1894

Coccolithus pelagicus (Wallich 1877) Schiller 1930

Pl.2.3, figs 1-4, 6-8; Pl.2.9, figs 9,10.

Coccolithus cf. pelagicus

Pl.2.3, figs 5. **Remarks:** A *C. pelagicus* type with smaller extant (5-10 µm).

Coccolithus formosus (Kamptner, 1963) Wise 1973

Pl.2.3, fig 9,10; Pl.2.9, figs 11-13.

Coccolithus scheri Bown & Dunkley Jones, 2012

Pl.2.3, figs 10,11; Pl.2.9, figs14,15. **Remarks**: *Coccolithus*-type shields but with central area spanned by a bar. Differentiated from *C. biparteoperculatus* by its smaller size (2-3 μm), and single-part bar.

Genus CHIASMOLITHUS Hay et al., 1966

Chiasmolithus nitidus Perch-Nielsen, 1971

Pl.2.3, fig 13-14. **Remarks**: Medium-sized *Coccolithus*-type shields with diagonal central area cross, typically with two slightly curved and two straight arms.

Chiasmolithus oamaruensis (Deflandre, 1954) Hay et al., 1966

Pl.2.3, fig 17. **Remarks:** A large to very large elliptical *Chiasmolithus* with wide central area, distinguished by symmetrical, narrow and straight diagonal bars.

Genus CLAUSICOCCUS Prins, 1979

Clausicoccus subdistichus (Roth & Hay in Hay et al., 1967) Prins, 1979

Pl.2.3, figs 15,16; Pl.2.9, figs 16-18.

Genus BRAMLETTEIUS Gartner, 1969

Bramletteius serraculoides Gartner, 1969

Pl.2.3, figs 19,20; Pl.2.9, figs 19,20. **Remarks**: A small coccolith, *Cruciplacolithus* like, with

thin, tall and paddle-like processes.

Family CALCIDISCACAEAE Young & Bown, 1997

Genus UMBILICOSPHAERA Lohmann, 1902

Umbilicosphaera jordanii Bown, 2005

Pl.2.3, fig 21. **Remarks**: A circular ring-shaped placolith, medium in size, non-birefringent distal shield, and vacant central area which is typically wider than the shields.

Umbilicosphaera bramlettei (Hay & Towe, 1962) Bown et al., 2007

Pl.2.3, figs 22-25.

Umbilicosphaera protoannulus (Gartner, 1971) emend. Young & Bown, 2014

Pl.2.3, figs 26,27.

Synonym: *Calcidiscus protoannulus* (Gartner, 1971) Loeblich & Tappan, 1978

Genus CORONOCYCLUS Hay Mohler & Wade 1966

Coronocyclus nitescens (Kamptner, 1963) Bramlette and Wilcoxon, 1967

Pl.2.3, figs 28,29.

Genus HAYELLA Gartner, 1969

Hayella situliformis.

Pl.2.3, fig 30.

Incertea sedis: Tetralithoides

Tetralithoides sp

Pl.2.3, figs 31,32; Pl.2.9, fig 21.

Ilselithina iris Stradner in Stradner and Adamiker, 1966

Pl. 2.9, figs 22, 23. **Remarks**: Heterococcolith that smaller than *I.fusa* (~2-3 μm). Conical proximal shield with slits between the elements and robust elevated distal shield.

Ilselithina fusa

Pl. 2.9, figs 24, 25 **Remarks**: Proximal shield without slits between elements, and delicate distal shield with well separated tips.

Mesozoic survivor: watznaueriaceae

Low abundance in the early Palaeogene.

Cyclagelosphaera margereli Noel, 1965

Pl.2.3, fig 35. **Remarks:** *C. margerelli* was found very low in this section. The first occurrence of *C. margereli* was within NJ11 zone, in Mesozoic period (Bown & Cooper 1998). This suggested as a reworked nannofossil.

Genus HELIOLITHACEAE

Bomolithus? sp.

Pl.2.3; figs 33,34. **Remarks:** *Bomolithus* sp. occur during middle Palaeocene to early Eocene. This, as well suggested as a reworked nannofossil.

2.4.2 Murolith coccoliths

Order Zygodiscales Young & Bown, 1997

Family HELICOSPHAERACEAE Black, 1971

Genus HELICOSPHAERA Kamptner, 1954

Helicosphaera compacta Bramlette & Wilcoxon, 1967

Pl.2.4, figs 1,2.

Helicosphaera reticulata Bramlette & Wilcoxon, 1967

Pl.2.4, figs 3,4.

Helicosphaera gartneri Theodoridis, 1984

Pl.2.4, figs 5,6.

Helicosphaera bramletti (Müller, 1970) Jafar & Martini, 1975

Pl.2.4, figs 7-14.

Family PONTOSPHAERACEAE Lemmermann, 1908

Genus Pontosphaera Lohmann, 1902 (= "Crassapontosphaera" Boudreaux & Hay, 1969; Discolithina Loeblich & Tappan, 1963; Discolithus Huxley, 1868; KoczyiaBoudreaux & Hay, 1969.

Pontosphaera plana (Bramlette & Sullivan, 1961) Haq, 1971

Pl.2.4, figs 15. **Remarks**: Simple unadorned plate without a distinct margin; sometimes with two narrow longitudinal slits.

Pontosphaera multipora (Kamptner, 1948) Roth, 1970 [Discolithus]

Pl.2.4, figs 16-18; Pl.2.10, figs 1-7. **Remarks**: Simple plate with narrow rim, central area perforated by several cycles of pores.

Pontosphaera punctosa (Bramlette & Sullivan, 1961) Perch-Nielson, 1984

Pl.2.4, figs 19-21. **Remarks**: Pontosphaera that has central area plate with larger pores towards the centre, marginal furrows with small pores.

Pontosphaera alta Roth, 1970

Pl.2.4, figs 22-24; Pl.2.10, figs 8-10. **Remarks:** Pontosphaera with numbers of small perforations on the low birefringent central area plate, and thin, birefringent rim.

Pontosphaera distincta (Bramlette & Sullivan, 1961) Roth & Thierstein, 1972

Pl.2.4, fig 25. **Remarks:** *P. distincta* is a large thick coccolith, have a thick narrow perforate

central plate, with broad and thick rim/margin.

Pontosphaera pulchra (Deflandre in Deflandre & Fert, 1954) Romein, 1979

Pl.2.4, fig 26; Pl.2.10, figs 14,15. **Remarks:** Central area plate perforated by two large holes forming a distinct transverse bar. The plate is scalloped towards its outer edge, where there are narrow radial ridges and furrows just inside the margin of the plate.

Pontosphaera pulcheroides (Sullivan, 1964) Romein, 1979

Pl.2.4, figs 27-34; Pl.2.10, fig 11-13, 17-19. **Remarks**: Central area plate with row of small pores towards its outer edge and two holes forming an oblique transverse bar.

Pontosphaera versa (Bramlette & Sullivan, 1961) Sherwood, 1974

Pl. 2.4, fig 35. **Remarks**: Pontosphaera with a distinctly raised margin and birefriengent central area plate.

Family ZYGODISCACEAE Hay and Mohler, 1967

Genus ISTHMOLITHUS Deflandre in Deflandre and Fert, 1954

Isthmolithus recurvus Deflandre in Deflandre and Fert, 1954

Pl. 2.5, figs, 10-13; Pl.2.10, fig 23. **Remarks**: A narrow elliptical to oblong murolith, which relatively high walls and central area spanned by two parallel transverse bars.

Order Syracosphaerales Hay, 1977 emend. Young et al., 2003

Family RHABDOSPHAERACEAE Haeckel, 1894

Genus BLACKITES Hay & Towe, 1962

Blackites tenuis **(**Bramlette & Sullivan 1961) Sherwood 1974

Pl.2.5, figs 1,2. **Remarks**: A tall, narrow, styliform central area spine with narrow base and a narrow axial canal that slightly broadens initially before gentle tapering. The rim is relatively dark with a bright inner cycle.

Blackites spp. bases

Pl.2.5, figs 3,4; Pl.2.11, fig 1-3.

Blackites spinosus (Deflandre & Fert, 1954) Hay & Towe, 1962

Pl.2.5, fig 5. **Remarks**: Spine-bearing coccolith similar to *B. tenuis* but with a spine that tapers outwards at its base.

Blackites shafikii Shafik, 1989

Pl. 2.11, figs 4. **Remarks**: Sub-circular to elliptical rhabdoliths, with a low domed process formed of a continuous lamellar cycle. Possesses a distinct collar at the base of the process.

Blackites sp.

Pl.2.11, figs 5,6. **Remarks**: Similar to *B. shafikii*, but with more broadly spaced crystallites in a series of lamellar cycles at the top of the process, producing a set of distinct radial slots towards the top of the process. Similar to *Blackites* sp. 1 of Dunkley Jones et al., (2009).

Blackites perfecta **(**Shafik, 1989) comb. nov.

Pl. 2.11, figs 7-11. **Basionym.** *Amitha perfecta* Shafik, 1989.

Description: Sub-circular to elliptical rhabdoliths, with low domed process surrounded by a distinct collar at its base. Similar to *B. shafikii* but with more broadly spaced crystallites in the first lamellar cycle above the collar, producing a set of distinct radially oriented slots at the base of the process. **Remarks**: Recombined into the genus *Blackites* based on the characteristic components of the coccolith base – a bicyclic rim, radial lath cycle and process formed of multiple lamellar cycles (Dunkey Jones et al., 2009).

Genus RHABDOSPHAERA Haeckel, 1894

Rhabdosphaera vitrea (Deflandre in Deflandre & Fert, 1954) Bramlette & Sullivan, 1961

Pl.2.5, fig 6; Pl.2.11, fig 12, 13. **Remarks:** As shown for specimens from Tanzanian (Dunkley Jones et al., 2009), these specimens lack the radial lath cycle characteristic of *Blackites*, supporting the placement of this species in *Rhabdosphaera*.

Family Syracospharaceae Lohmann, 1902

Genus SYRACOSPHAERA Lohmann, 1902

Syracosphaeraceae tanzanensis Bown, 2005

Pl.2.5, figs 7-9.

Calciosolenia fossilis (Deflandre in Deflandre & Fert, 1954) Bown in Kennedy et al., 2000

Pl. 2.10, fig 20. **Remarks:** Similar to scapholiths found in Tanzanian sediments around the

Paleocene/Eocene (Bown 2010) and Eocene/Oligocene boundaries (Dunkley Jones et al., 2009). Extant species show significant variomorphism and this is likely to be the cause of the variable morphology observed here, between narrow and tall (Pl. 2.10, fig. 20), and broader morphologies (Pl. 2.10, fig. 21).

Calciosolenia aperta (Hay & Mohler, 1967*)* Bown, 2005

Pl. 2.10, figs 21-22.

2.4.3 HOLOCOCCOLITHS Young et al., 2003

Genus LANTERNITHUS Stradner, 1962

Lanternithus minutus Stradner, 1962

Pl. 2.5, figs 14-17.

Genus ZYGRHABLITHUS Deflandre, 1959

Zygrhablithus bijagatus bijagatus (Deflandre in Deflandre & Fert, 1954) Deflandre, 1959

Pl.2.5, figs 18-21, 23-25.

Zygrhablithus bijagatus cornatus Bown, 2005

Pl. 2.5, figs 22; Pl. 2.11, fig 25.

Genus HOLODISCOLITHUS Roth, 1970

Holodiscolithus minolettii Bown, 2005

Pl.2.5, figs 26-28.

Holodiscolithus macroporus (Deflandre in Deflandre & Fert, 1954) Roth, 1970

Pl. 2.5, figs. 30-32; Pl.2.11, figs 14-16. **Remarks**: A elliptical holococcolith with non-birefringent (appears as dark plate), and comprised of numbers of pores (10-16).

Genus Orthozygus Bramlette & Wilcoxon, 1967

Orthozygus aureus (Stradner, 1962) Bramlette & Wilcoxon, 1967

Pl.2.5, figs 29; Pl.2.11, figs 17,18. **Remarks**: Elliptical non-birefringent holococcolith consisting of a narrow rim spanned by an arched and perforate bridge. In SEM the structure of *O. aureus* is shown to be close to that of *H. macroporus*, but with a more upwardly domed central-area structure, and two larger pores at each end of the coccolith.

Genus CLATHROLITHUS Deflandre in Deflandre & Fert, 1954

Clathrolithus ellipticus Deflandre in Deflandre & Fert, 1954

Pl.2.5, figs 33, 34***;*** Pl.2.11, fig 26.

2.4.4 NANNOLITHS

Family BRAARUDOSPHEARACEAE Deflandre, 1947

Genus BRAARUDOSPHAERA Deflandre, 1947

Braarudosphaera bigelowii (Gran & Braarud 1935) Deflandre 1947

Pl.2.6, figs 1-5; Pl.2.11, figs 23,24.

Genus PEMMA Klumpp, 1953

Pemma basquense (Martini, 1959) Baldi-Beiki, 1971

Pl.2.6, fig 6.

Pemma papillatum Martini, 1959

Pl.2.6, figs 7,8.

Genus MICRANTHOLITHUS Deflandre in Deflandre and Fert, 1954

Micrantholithus triquetra (Bown & Dunkley Jones, 2006) Dunkley Jones et al., 2009 Pl.2.6, fig. 9. **Remarks:** First noted in late Eocene sediments from Tanzania (Bown & Dunkley Jones, 2006), this species is also found in low abundances from the same interval in the Mossy Grove core.

Micrantholithus attenuatus Bramlette & Sullivan, 1961

Pl.2.6, fig. 10.

Family DISCOASTERACEAE Tan, 1927

Genus Discoaster Tan, 1927

Discoaster spinescens Bown & Dunkley Jones, 2006

Pl.2.6, figs 11-13, 16-17. **Remarks**: Similar to *Discoaster barbadiensis* but with a prominent tall, thin stem on one side. Most clearly seen in side view (Pl. 2.6, fig. 11) but prominent stem also observed in plan view (Pl. 2.6, fig. 12-13, 16-17). Specimens of both *D. spinescens* and *D. barbadiensis* span a large size range in this material, from medium to very large specimens. *D. spinescens* occur in early Eocene thus it suggested that *D. spinescens* suggested is a reworked nannofossil in this section.

Discoaster barbadiensis Tan, 1927

Pl.2.6, figs 14-15, 18-22, 25-26; Pl.2.11, fig 27.

Discoaster saipanensis Bramlette & Riedel, 1954

Pl.2.6, figs 23, 24.

Discoaster tanii Bramlette & Riedel, 1954

Pl.2.7, figs 1, 6, 8. **Remarks**: Typical specimens have long free rays of uniform width terminating in a flat or slightly notched ray-end, although some specimens (Pl. 2.7, fig. 1) show some terminal thickening of ray tips.

Discoaster williamsii Bown & Dunkley Jones, 2012

Pl.2.7, figs 2, 3. **Remarks:** Six rayed discoaster with broad central area. In this section, ray-ends typically end with paired lateral nodes just before the ray tips.

Discoaster deflandrei Bramlette & Riedel, 1954

Pl.2.7, figs 4, 5.

Discoaster nodifer (Bramlette & Riedel, 1954) Bukry, 1973

Pl.2.7, figs 7.

Discoaster distinctus Martini, 1958

Pl.2.7, figs 9,10.

Family SPHENOLITHACEAE Deflandre 1952

Genus Sphenolithus Deflandre in Grassé, 1952

Sphenolithus moriformis (Bronnimann and Stradner, 1960) Bramlette and Wilcoxon, 1967

Pl.2.7, figs 13-15.

Sphenolithus predistentus Bramlette & Wilcoxon, 1967

Pl.2.7, figs 11,12.

Sphenolithus grandis Haq & Berggren, 1978

Pl.2.7, fig 16.

Ascidian spicule

Pl.2.7, fig 17.

Family LITHOSTROMATIONACEAE Deflandre, 1959

Genus LITHOSTROMATION Deflandre, 1942

Lithostromation sp.

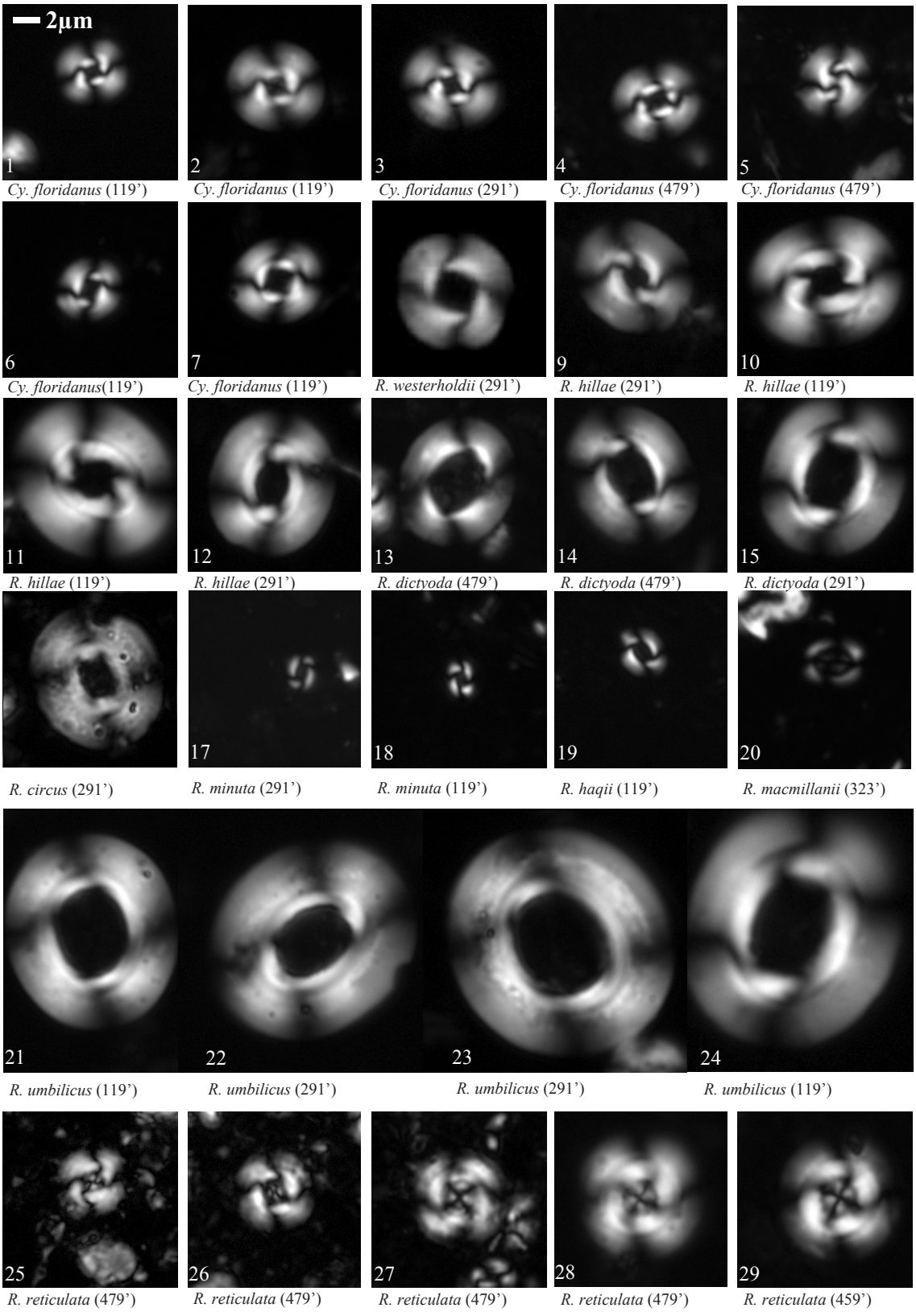
Pl.2.7, fig 18; Pl.2.11, figs 28.29.

Lithostromation simplex (Klumpp, 1953) Bybell, 1975

Pl.2.7, fig 19. **Remarks**: Low birefringence hexagonal nannoliths with 6 thin rays extending beyond the margin of the disc. Secondary shorter rays are present between each of the longer rays, which terminate at the disc edge.

Plate 2.1

Noelaerhabdaceae: *Cyclicargolithus floridanus* Group, *Reticulofenestra umbilicus* Group, *Reticulofenestra pseudoumbilicus* Group, *Reticulofenestra reticulata* Group



1 *Cy. floridanus* (119')
2 *Cy. floridanus* (119')
3 *Cy. floridanus* (291')
4 *Cy. floridanus* (479')
5 *Cy. floridanus* (479')
6 *Cy. floridanus*(119')
7 *Cy. floridanus* (119')
9 *R. westerholdii* (291')
10 *R. hillae* (291')
11 *R. hillae* (119')
12 *R. hillae* (291')
13 *R. dictyoda* (479')
14 *R. dictyoda* (479')
15 *R. dictyoda* (291')
17 *R. circus* (291')
18 *R. minuta* (291')
19 *R. minuta* (119')
20 *R. haqii* (119')
21 *R. macmillanii* (323')
22 *R. umbilicus* (119')
23 *R. umbilicus* (291')
24 *R. umbilicus* (291')
25 *R. umbilicus* (119')
26 *R. reticulata* (479')
27 *R. reticulata* (479')
28 *R. reticulata* (479')
29 *R. reticulata* (479')
R. reticulata (459')

Plate 2.2

Noelaerhabdaceae: *Reticulofenestra lockeri* Group, *Reticulofenestra bisecta* Group

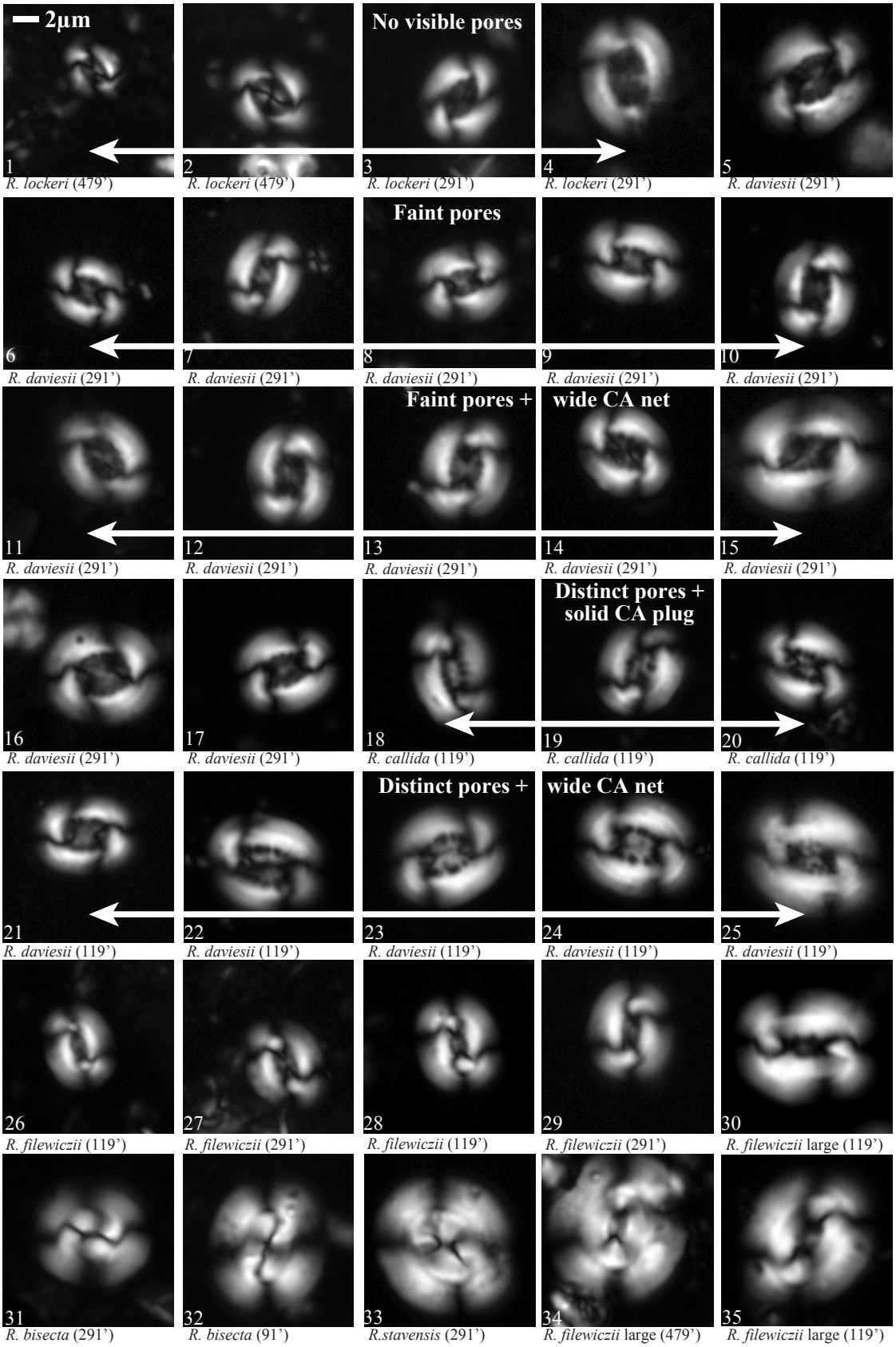


Plate 2.3

Coccolithaceae: ***Coccolithus, Cruciplacolithus, Chiasmolithus, Clausicoccus, Bramletteius,***
Calcidiscaceae: ***Umbilicosphaera, Calcidiscus, Coronocyclus, Hayella***
Incertae sedis: ***Tetralithoides;***
Mesozoic survivor: Watznaueriaceae: ***Cyclagelosphaera***

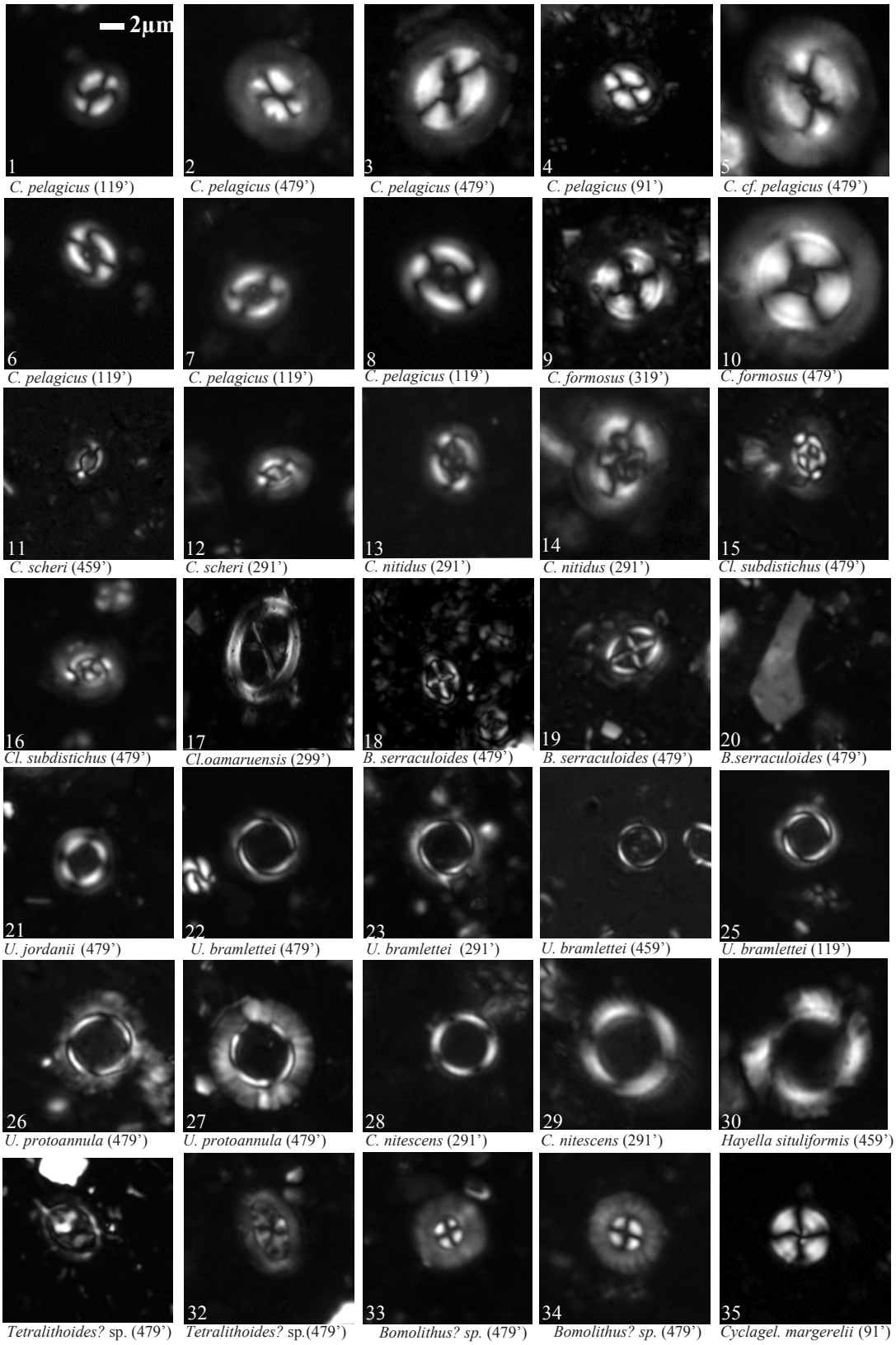


Plate 2.4

Helicosphaeraceae: *Helicosphaera*, Pontosphaeraceae: *Pontosphaera*

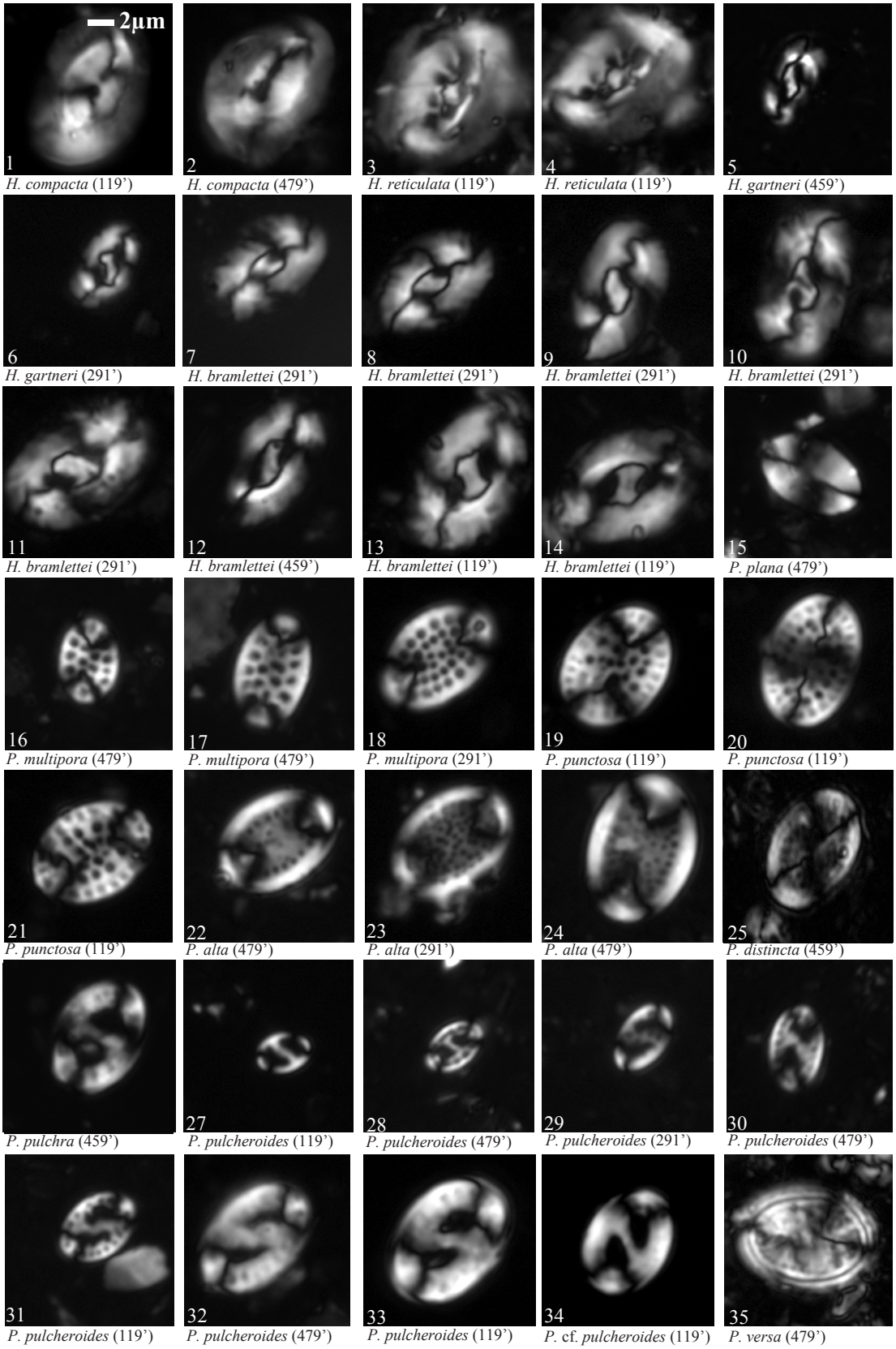


Plate 2.5

Rhabdosphaeraceae: ***Blackites, Rhabdosphaera;*** **Zygodiscacaeae:** ***Syracosphaera, Isthmolith***
Holococcoliths: ***Lanternithus, Zygrhablithus, Holodiscolithus, Ortozygus, Clathrolithus***

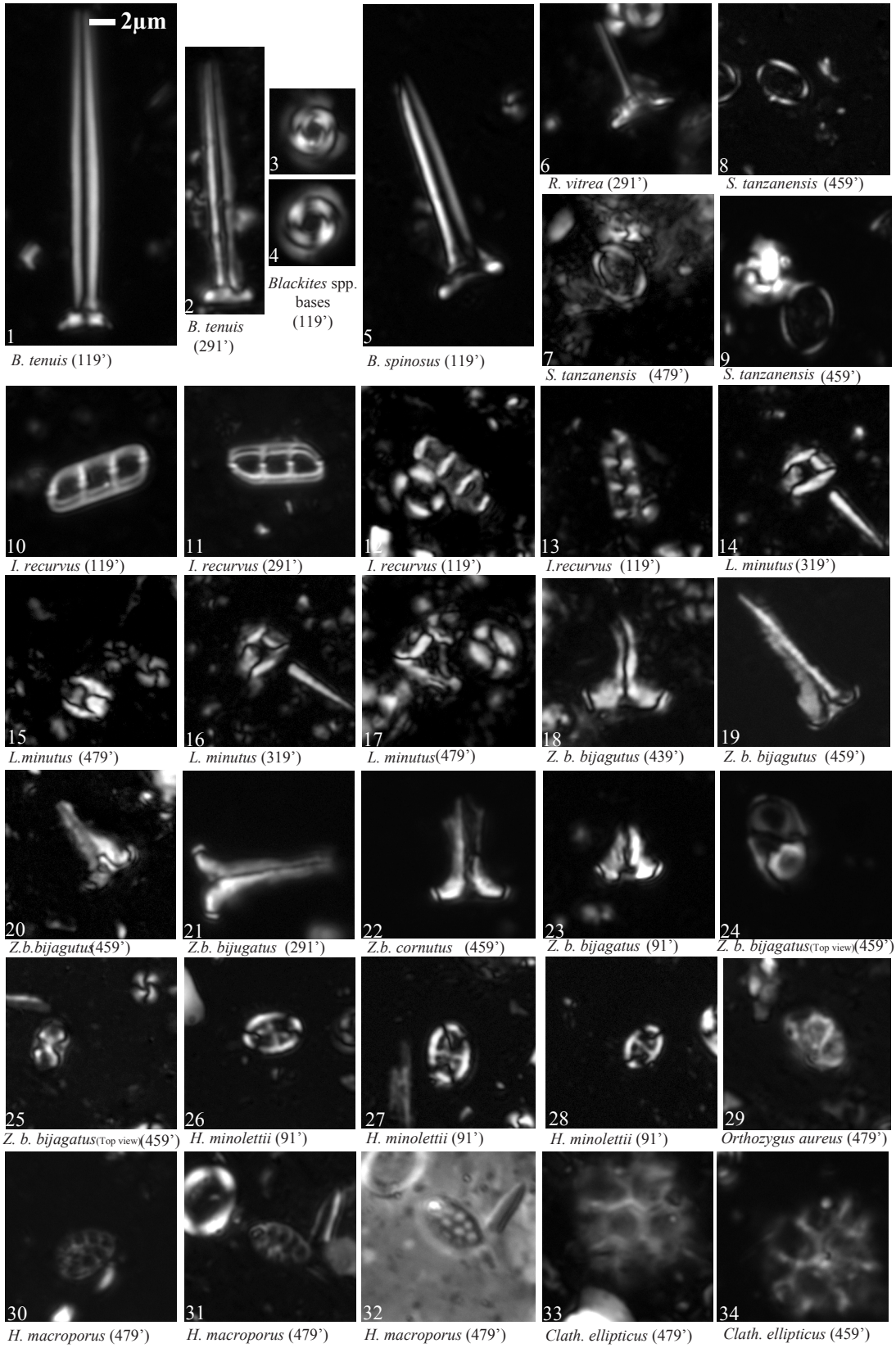


Plate 2.6

Nannoliths: *Braarudosphearaceae, Discoasteraceae*

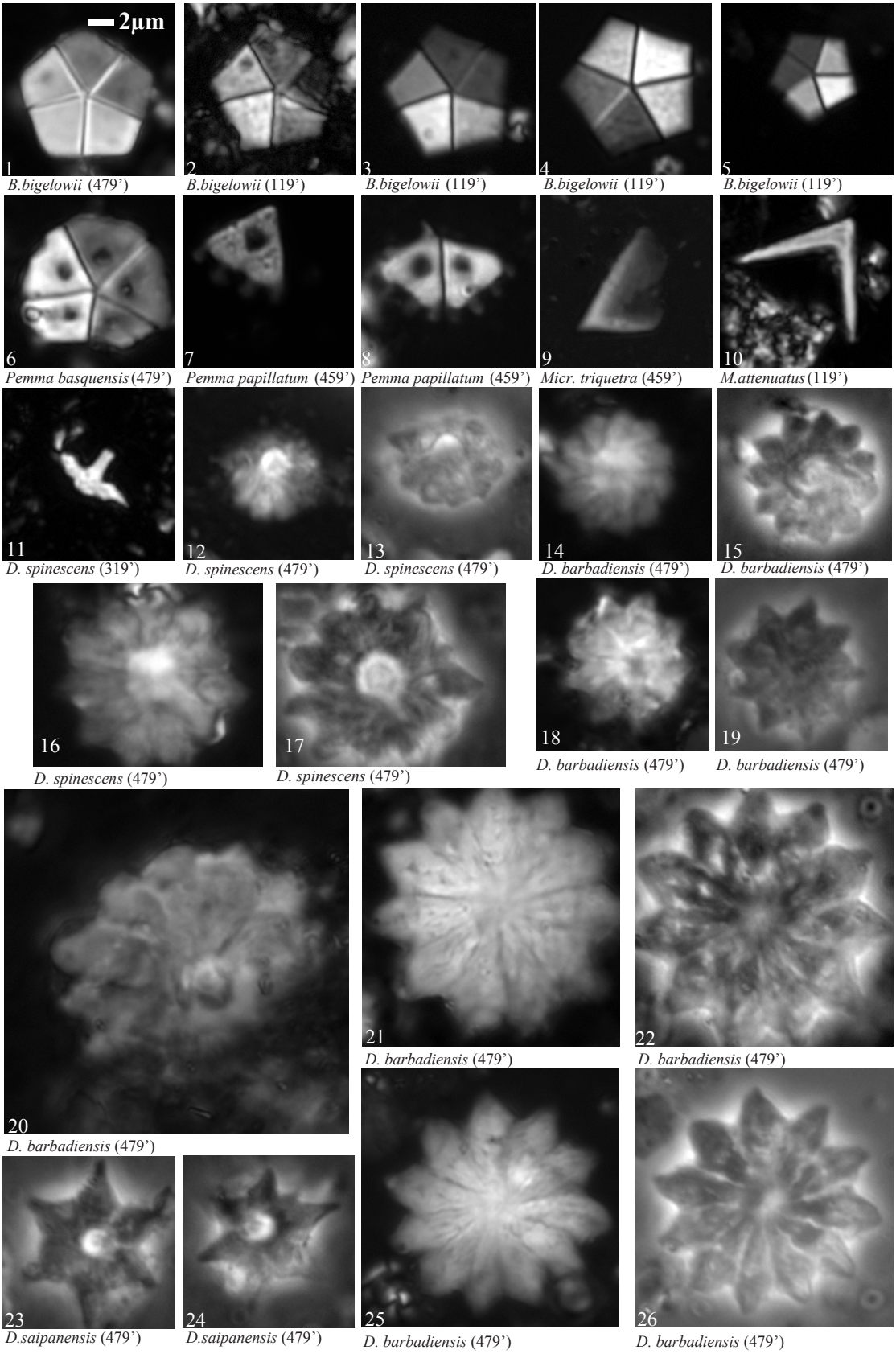
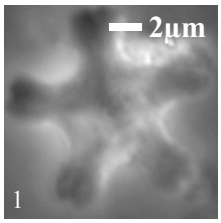
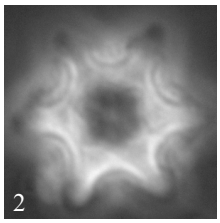


Plate 2.7

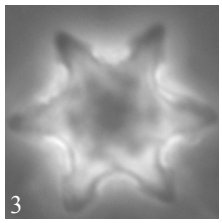
Nannoliths: *Discoasteraceae, Sphenolithaceae, Lithostromationaceae*



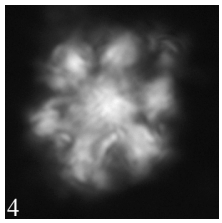
Discoaster tanii (291')



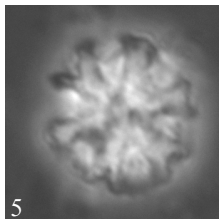
D. cf. *williamsii* (119')



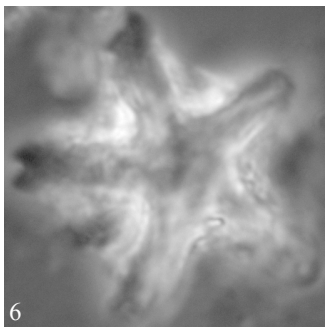
D. cf. *williamsii* (119')



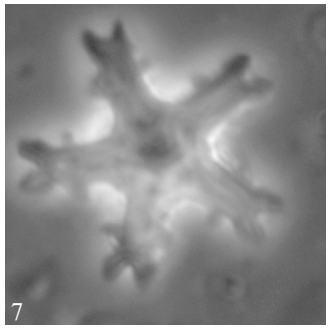
Disc. deflandrei (291')



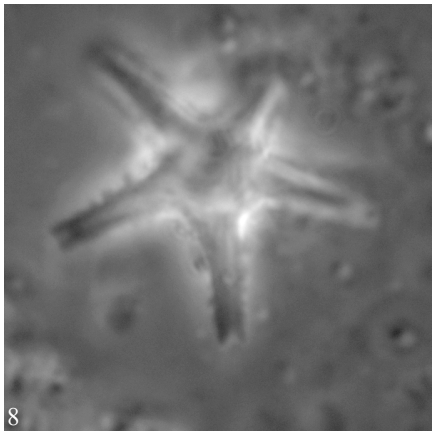
Disc. deflandrei (291')



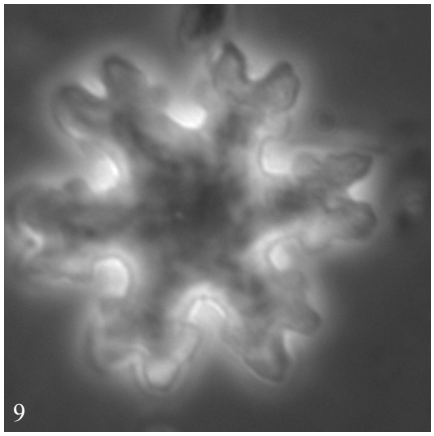
D. tanii (291')



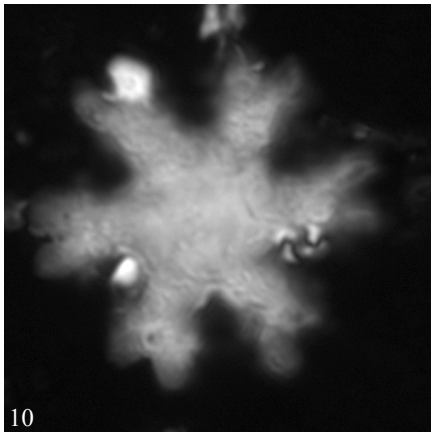
D. nodifer (291')



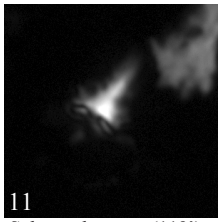
D. tanii (291')



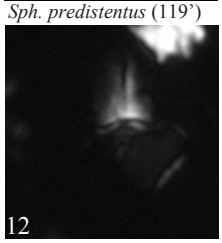
Discoaster distinctus (119')



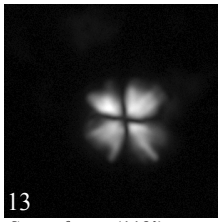
Discoaster distinctus (119')



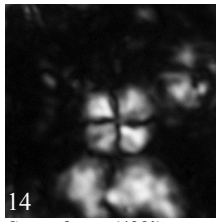
Sph. predistentus (119')



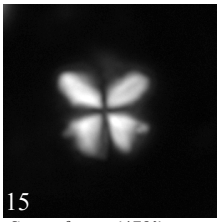
Sph. predistentus (119')



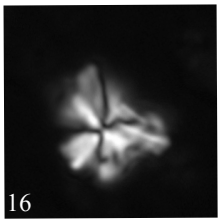
S.moriformis (119')



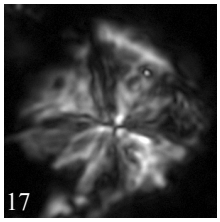
S.moriformis (439')



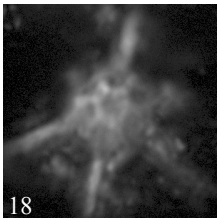
S.moriformis (479')



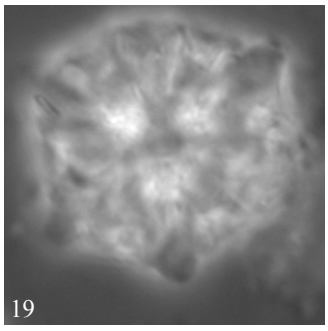
S. moriformis (479')



Ascidian spicule (119')



Lithostromation sp. (91')



Lithostromation simplex (291')

Plate 2.8

Noelaerhabdaceae (SEM taken from Tamsin)

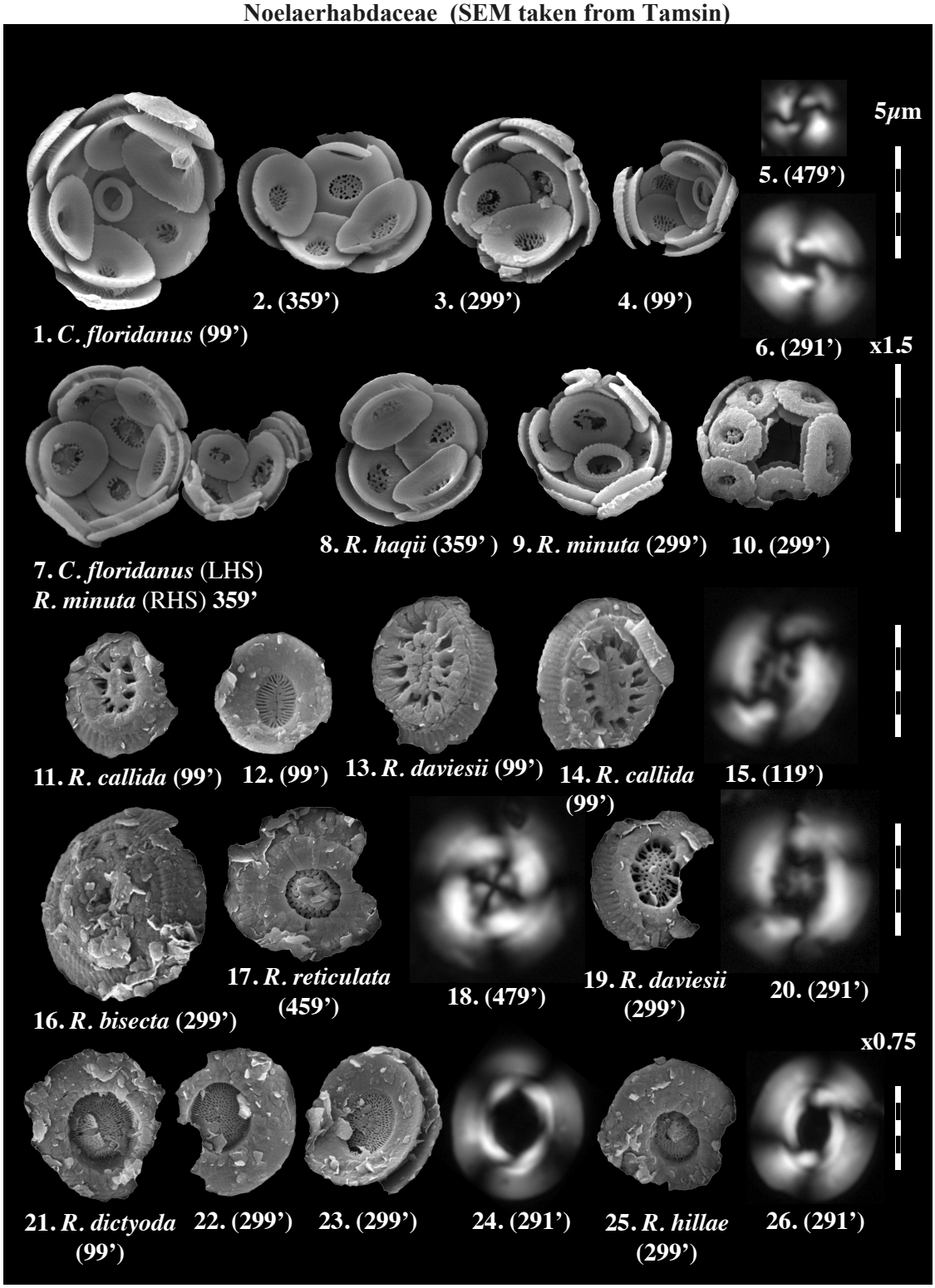


Plate 2.10

Pontosphaeraceae (SEM taken from Tamsin)

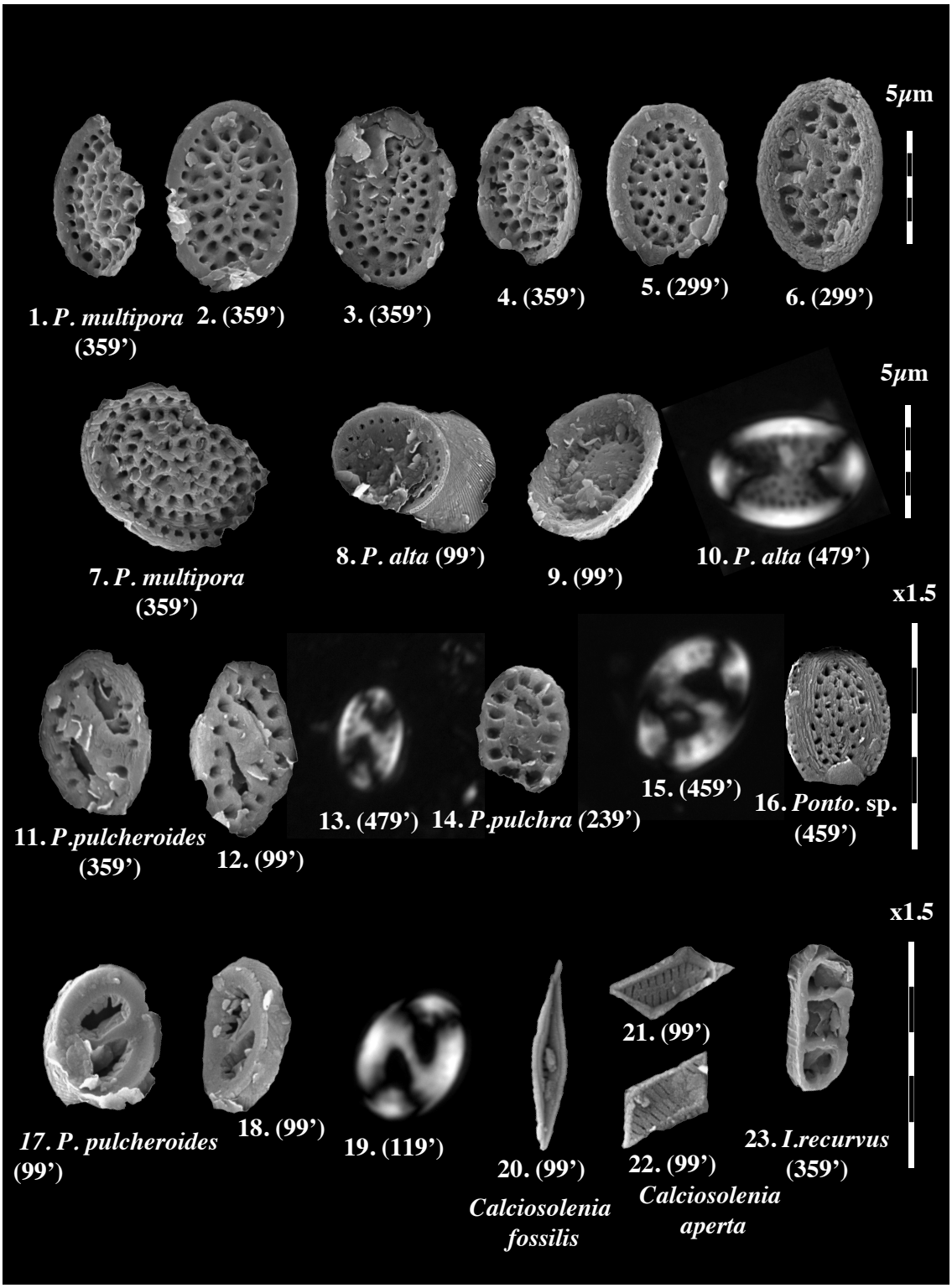


Plate 2.9

Noelaerhabdaceae, Coccolithaceae (SEM taken from Tamsin)

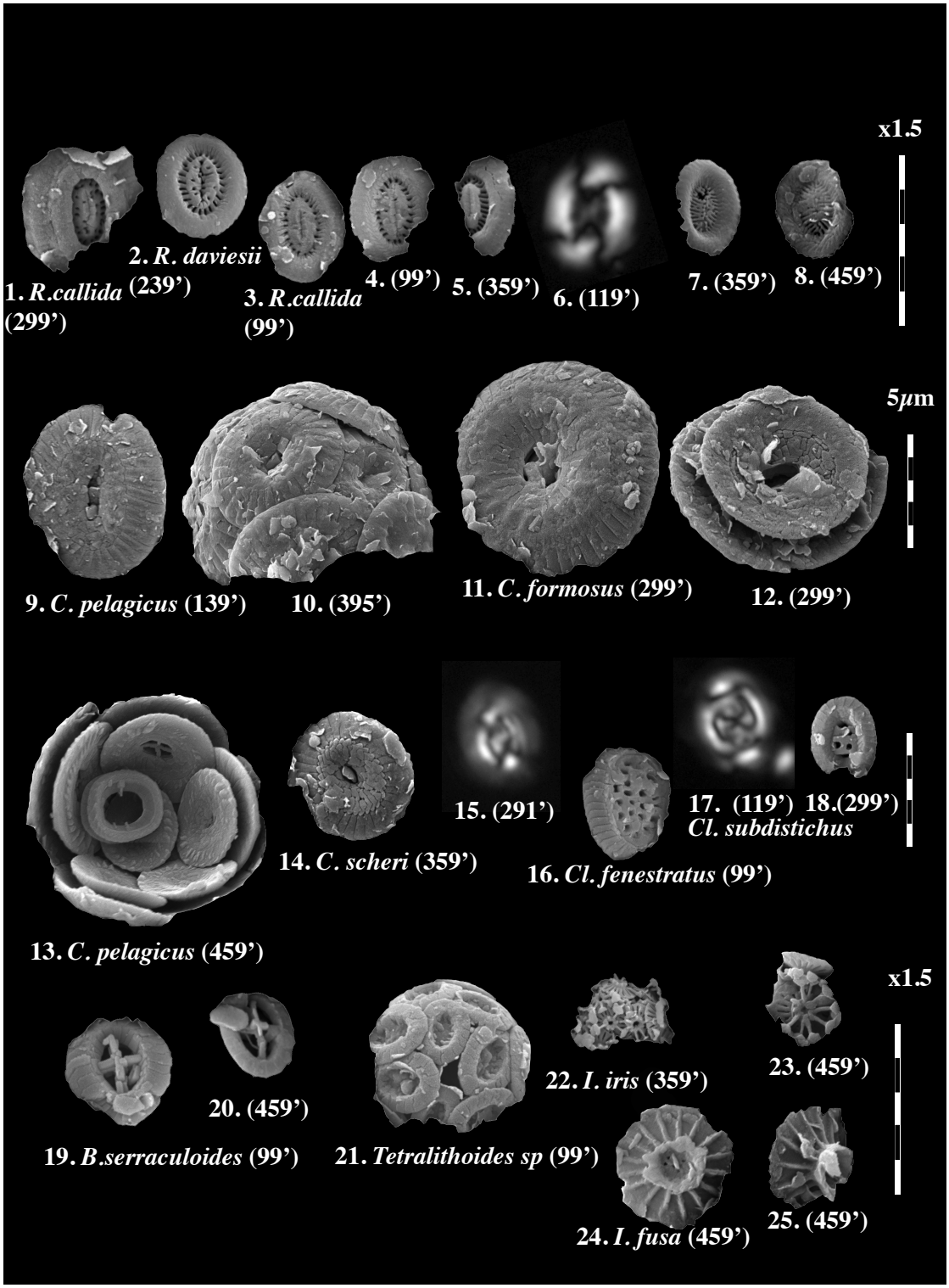
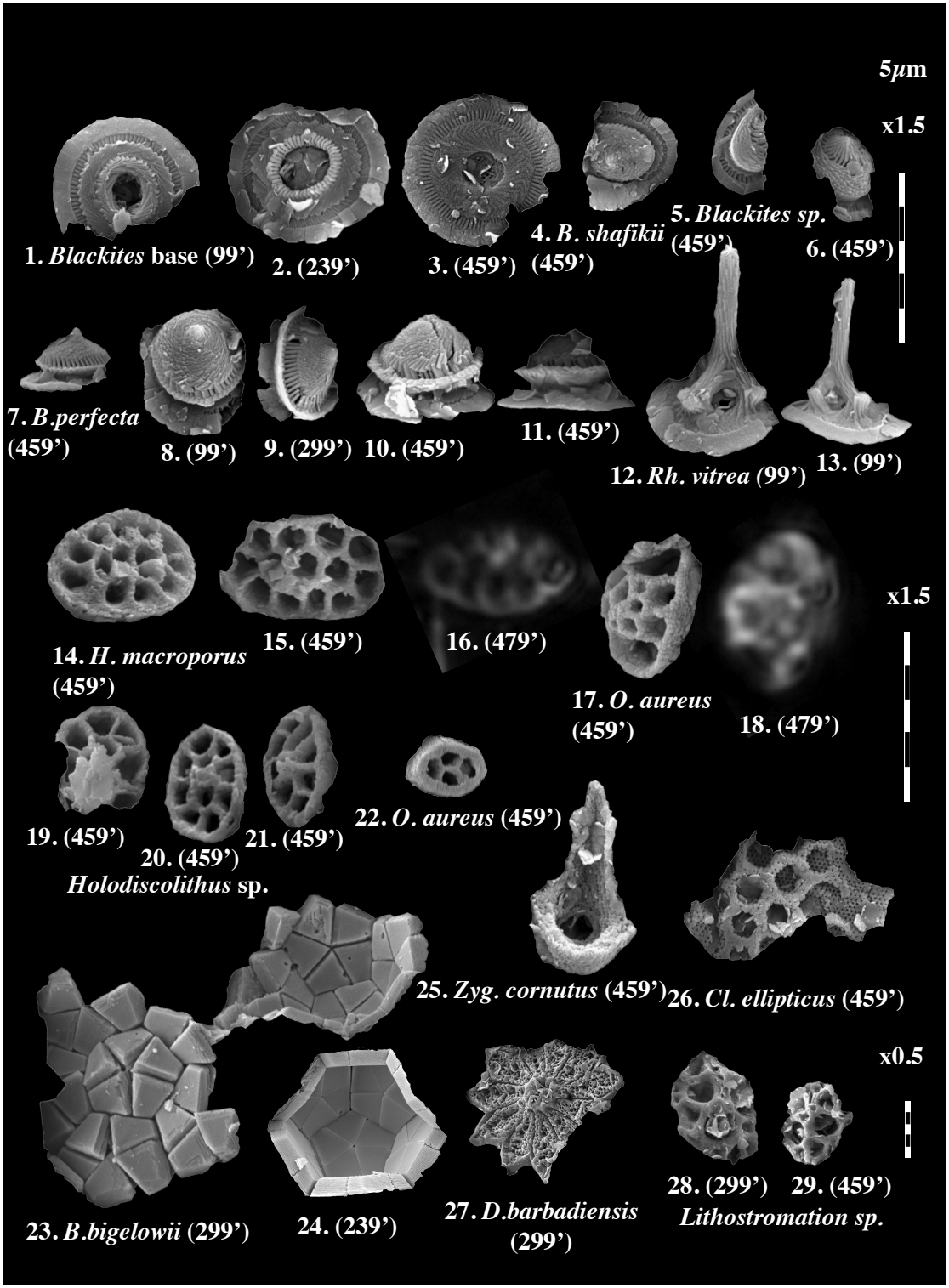
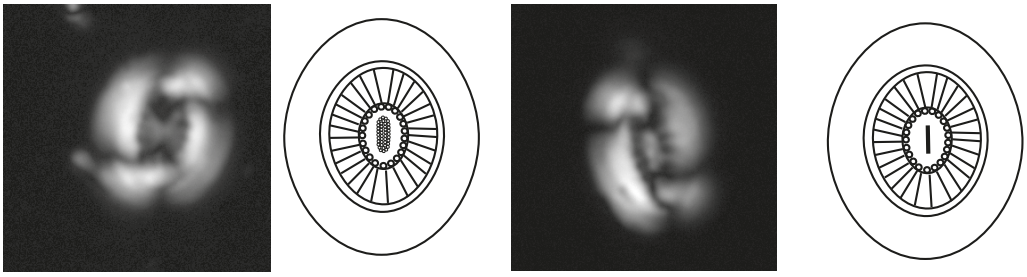


Plate 2.11:

Rhabdosphaeraceae,Holococcoliths, Nannoliths (SEM taken from Tamsin)





R. daviesii (291')

R. callida (119')

Figure 2.2: Sketched diagram of *R. daviesii* and *R.callida* showing the different between both species. *R. daviesii* have been distinguished from *R. callida* by the central area net, whilst wide central area plug in *R. callida*.

Chapter 3

Calcareous Nannofossil Assemblages through Eocene/Oligocene Transition in the Mossy Grove Core

3.1 Introduction

As outlined in Chapter 1, the Eocene-Oligocene Transition is the point of transition from the greenhouse climates of the early Cenozoic to the modern icehouse climates. The EOT is a geologically abrupt step-like transition in the long-term trend towards more positive deep-ocean benthic foraminifera oxygen isotope values (Zachos et al., 2001). Taken as representing high-latitude and deep-water temperatures, as well as global continental ice volume, the EOT is interpreted to represent the rapid expansion of Antarctic ice sheets with an associated sea-level fall at the end of the long-term Eocene trend of high-latitude cooling. Here we present new calcareous nannofossil assemblage data from the Mossy Grove core on the US Gulf Coast. The marine clays recovered in this core represent an apparently complete section through the latest Eocene and into the EOT (Dockery III et al., 1991), although increasing the stratigraphic constraints on this core is an objective of this thesis.

The most detailed descriptions of middle to late Eocene calcareous nannofossil assemblages from the US Gulf Coast remain the monograph published by William Seisser from onshore Paleogene outcrops sequences of the US Gulf Coast (Siesser, 1983). His work included multiple images of very well preserved nannofossil specimens, especially from the late Eocene Yazoo Formation of Alabama and Mississippi. These late Eocene to early Oligocene sequences have, more recently, been extensively studied to provide palaeoclimate and sequence stratigraphic constraints on the Eocene/Oligocene transition of the Gulf Coast

(Miller et al., 2008; Wade et al., 2012). All of these studies, however, focus on the St Stephen's Quarry Section and Core in Alabama. Although this section has intermittently good calcareous microfossil preservation during the very latest Eocene, through the Eocene/Oligocene transition, the vertical thickness of the section is relatively thin compared to the Mossy Grove core (Miller et al., 2008). In particular, there is a significant condensed section in the St Stephen's core section between ~36.4 and ~34 Ma, which is represented by the lithified high carbonate Cocoa Sand Member of the Yazoo Formation (Miller et al., 2008). Within the St Stephen's succession, Miller et al., (2008) identify two significant unconformities, between 35.9 and 35.4 Ma and 35.0 and 33.9 Ma. This missing time severely hampers the ability to assess the rates and timings of biotic and climatic evolution through the late Eocene at this location. This critical late Eocene interval is now known to include a number of cool phases that could precondition the system for the onset of Antarctic glaciation (Persico & Villa, 2004), but are also potentially significant in the progressive loss of coccolithophore diversity from the warm climates and peak diversities of the early Eocene to the icehouse / low diversity conditions of the earliest Oligocene (Bown et al., 2008).

This chapter will focus on the calcareous nannofossil assemblage variability through this succession, providing the first detailed records of coccolithophore community change from the US Gulf Coast through this critical interval. It also provides an additional record of tropical to sub-tropical marine ecosystem change before and through the EOT, the dynamics of which are still constrained from only a limited number of locations (Coxall & Pearson, 2007).

3.2 Methods and materials

Calcareous nannofossils were counted, at species level, in simple smear slides using polarizing light microscope (Zeiss AxioScope) at 1250x magnification. A total of 135 smear slides (from 31 feet (~9.4 m) to 519 feet (~158.1 m), with 2/3 feet (~0.6/0.9 m) intervals) are prepared from raw sediment samples, with only 6 samples being barren of calcareous nannofossils, all of which are from the upper part of the section. Different slides amount and magnification used in this chapter is intentionally to examine in details of each species assemblages, rather than specific species identification on Chapter 2. Clean surfaces of the raw samples were scraped with a toothpick to loosen a small amount of sediment that was then diluted with distilled water and smeared onto a thin cover glass. The cover glass was dried on a hotplate and then mounted onto a microscope slide using Norland 61 Optical Adhesive, which was cured under UV light. For the quantification of nannofossil assemblages, at least 400 specimens were counted per slide, with the percentage of individual taxa then calculated in relation to this total number counted. Where necessary, individual specimens were imaged at 2000x magnification, with a QImaging Qicam and Q-capture Pro 7.

Within the summary range chart (in Appendix A), the total calcareous nannofossil abundance was recorded within sediments as follows (Palike et al., 2010); D for dominant, more than 90% sediment particles, A for abundant, 50-90% of sediment particles, C for common 10-50% of sediment particles, F for few, 1-10% sediments particles, R for rare, less than 1% sediment particles and B for barren, none present. And the total abundance for individual calcareous nannofossil taxa was recorded as follows; dominant (D), more than 100 specimens per field of view (FOV), abundant (A), for 10 to 100 specimens per FOV, common

(C) for 1 to 10 specimens per FOV, few (F) for 1 specimen per 1 to 10 FOV and rare (R) for less than 1 specimen per 10 FOV. During counting (Appendix B), calcareous nannofossil preservation state was also recorded using a following qualitative assessment; good (G) for assemblages with little or no recrystallization and/or dissolution, with specimens able to be identified to species level, moderate (M) for assemblages dominated by specimens that show some alteration, but where the majority can still be identified to the species level, poor (P), for assemblages where specimens are highly altered by dissolution and/or recrystallization with identification at the species and/or generic level difficult or impossible.

Calcareous nannofossil assemblage diversity was modelled using the SHE analysis of Buzas & Hayek (1996), which is now a common statistical expression of biodiversity in both marine and terrestrial ecology. The analysis includes the two basic components of diversity, species richness (S) and the evenness of the numerical distribution across taxa (E). These two aspects of biodiversity are combined in the summary statistic, the Shannon Index (H). Calculations of the diversity index were made within Excel by using the equations $H = -\sum_{1}^{N} p_i \ln p_i$ and $H = \ln S + E$ $H = \ln S + E$, where H is Shannon's diversity index, S is total number of species in the community (richness), p_i is the proportion of S made up of the *í*th species and E is evenness. The H index increases (or decreases) when either species richness (S) or evenness (E) increase (or decrease).

In addition to diversity analyses, multivariate statistical modelling has been applied to simplify and understand the patterns of assemblage change across tens of individual taxa, including similarities and differences of behaviour between species subject to the same external environmental forcing. This modelling included Principal Component Analysis (PCA) and classical cluster analysis, both of which were performed using the PAST software

(PAlaeontological STatistic; Hammer et al., 2001). The additive log transformation of primary taxon percentage abundance data have been done before the multivariate analyses were undertaken, to convert these to normally-distributed proxy variables. The PCA was also performed on a reduced relative abundance data set, with the removal of rare species defined as having a standard deviation of primary relative abundance of less than 1% (Dunkley Jones et al., 2008). PCA scores of individual taxa can be useful in determining similar ecological preferences, and the plotting of whole assemblage scores through a succession can summarise the direction, rate and magnitude of the dominant ecological changes through time. To support this interpretation, cluster analysis was performed to test the robustness of the grouping of species into units with similar palaeoecological preferences. The combination of these two statistical analyses, together with existing studies of the biogeographic distribution of late Eocene calcareous nannofossils, allows for palaeoecological inferences and a discussion of palaeoenvironmental change through the late Eocene and EOT of the US Gulf Coast.

3.3 Results

3.3.1 Biostratigraphy

Based on detailed light microscope observations, the abundance and preservation within sediments and of individual taxa were recorded. All raw data and species counts are provided in the Appendix. Out of 135 samples 6 were barren of calcareous nannofossils, all of which occur above 55 feet (~16.8 m) depth in the topmost Yazoo Clay, thus assemblage count data is available from 55 feet (~16.8 m) to 519 feet (~158.2 m).

The biostratigraphy of the Mossy Grove core presented here follows the calcareous nannofossil biozonation of Martini (1971). A detailed age model is constructed using biohorizons defined by the observed first (base) and last (top) up section occurrences of taxa (Figure 3.1). The age of bioevents corresponding to these biohorizons were taken from recent compilations (Agnini et al., 2014; Expedition 320/321 Scientists, 2010) using the Geological Timescale 2012 (GTS2012; Gradstein et al., 2012). The late Eocene stratigraphy of the Mossy Grove core is constrained by the biohorizon base (B) *Isthmolithus recurvus,* top (T) *Coccolithus formosus,* top (T) *Discoaster saipanensis,* top (T) *Discoaster barbadiensis,* top (T) *Reticulofenestra reticulate,* (B) *Reticulofenestra isabellae* and base (B) *Chiasmolithus oamaruensis*. Of these seven biohorizons, only four are within the Mossy Grove succession.

From the base of the succession up, the first recorded biohorizon is the B *R. isabellae* at 499 feet (~152.1 m). This marks the base of the undifferentiated zone CNE17-CNE19 (NP19/20), with sediments below this level assigned to CNE18. The last observed of *I. recurvus* at 487 feet (~148.4 m), is suggested due to reworking and expected to be deeper than 500 feet. The rare occurrence of *Chiasmolithus oamaruensis* in this succession was observed in samples 299 feet (~91.1 m) and 431 feet (~131.4 m), which is consistent with a transition to more temperate calcareous nannofossil assemblages through the succession.

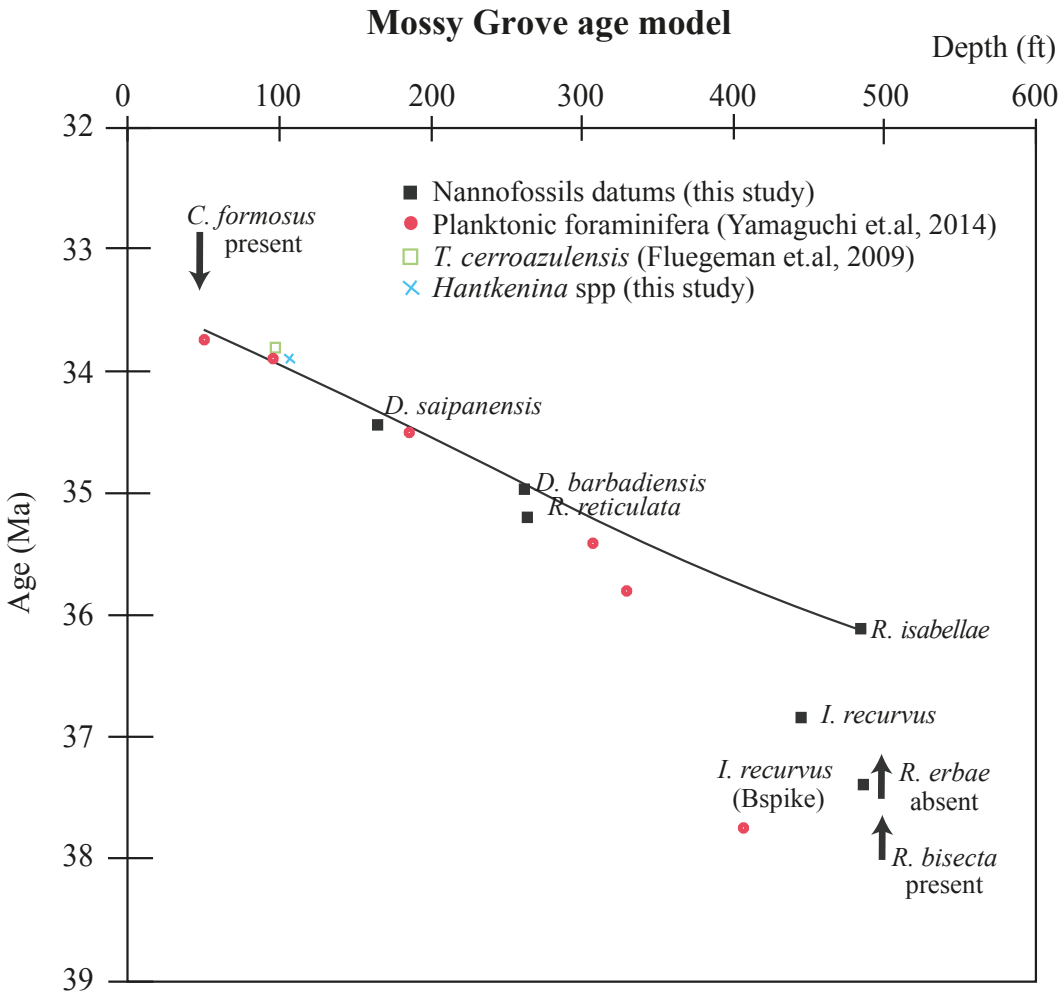


Figure 3.1: The age model of Mossy Grove based on calcareous nannofossil assemblages in this study and previous study from Yamaguchi et al., (2014) and Fluegeman et al., (2009).

Within NP19-20, the T *R. reticulata* occurs at 263 feet (~80.1 m), with a marked abundance decline prior to this at 363 feet (~110.6 m), and assigned as CNE19-CNE20 boundary. The T *D. saipanensis* (base of CNE21/NP21) and T *D. barbadiensis* occur at the same depth, 164 feet (~50 m), which marks the top of NP19/20, however *D. barbadiensis* is suggested to be reworked at 164 feet (~50 m) and the common occurrence are at 263 feet, within CNE20. Zone CNE20/NP19-NP20, the *Discoaster saipanensis* Zone, thus spans the middle of the core, between 263 feet (~80.1 m) to 164 feet (~50 m), from the interval started

from the T *Reticulofenestra reticulate* and *Discoaster barbadiensis* to the T *Discoaster saipanensis. Discoaster saipanensis* is present with rare abundance through this zone, whilst *Discoaster barbadiensis* is only consistently present below 263 feet (~80.1 m). Rare specimens of *Reticulofenestra reticulata* are present in samples at 263 feet (~80.1 m) and 266 feet (~81.1 m), and the biohorizon T *R. reticulata* is tentatively placed at 263 feet (~80.1 m). Below this level, however, below this level, down to 363 feet (~110.6 m), *R. reticulata* is absent, only consistently occurring below 363 feet (~110.6 m) down to the base of the Yazoo Clay.

The topmost section of the Yazoo Clay within the Mossy Grove core, from 164 feet (~50 m) to 55 feet (~16.8 m), is assigned to Zone CNE21/NP21, the *Coccolithus formosus* Zone. The consistent presence of *Coccolithus formosus* up to the top of the recovered Yazoo Clay, at 55 feet (~16.8 m), constrains the top of this Zone (biohorizon T *Coccolithus formosus*), whilst the base is placed at the biohorizon T *Discoaster saipanensis* at 164 feet (~50 m). The occurrence of T *Pemma papillatum* at 112 feet (~34.1 m) suggested that the Eocene-Oligocene Boundary lies within CNE21/NP21, and so should occur somewhere between 55 feet (~16.8 m) to 164 feet (~50 m), or above the top of the recovered Yazoo Clay, as the top of CNE21/NP21 is unconstrained. The Eocene-Oligocene Boundary is tentatively placed at ~90-100 feet (~27.4-30.5 m) based on the age model of calcareous nannofossil assemblages and the absence of *Hantkenina* spp (plantktonic foraminifera) above 106 feet (~32.3 m) as further discussed in Chapter 4. It should be noted, however, that the low abundances of *Discoaster* species and planktonic foraminifera – especially marker taxa - and the potential for nannofossil reworking with sea level fall, make biostratigraphy difficult in this interval.

3.3.2 Nannofossil Assemblages

Calcareous nannofossil assemblages at Mossy Grove core are very well preserved. They are mainly dominated by small coccolith, such as *R. dictyoda* small and *R. minuta*. Within the Yazoo Clay, the preservation of calcareous nannofossil varies from moderate to excellent preservation with little recrystallization. Relative abundance, in percent, of key species are shown in Figures 3.2 to 3.13. From an initial examination of these data it is clear that there are different responses to late Eocene environmental change within different species, with some showing long-term decreases and increases through this interval. For example, *Coccolithus formosus*, holoccocolith species, as well as *Helicosphaera*, *Sphenolith* and *Discoaster* species show a general trend of decreasing abundance, whilst *Reticulofenestra daviesii* and *Isthmolithus recurvus* both show increasing abundance. The grouped holococcolith species shown in Figure 3.10 is the most abundant of these taxonomic groups showing declining abundance, with mean 2% in the Eocene and 1.2 % in the Oligocene followed by the helicosphaerid group, sphenolith group, *Coccolithus formosus* and *Discoaster* spp, with mean abundance of 1% in the late Eocene for all decreasing species and groups, and 0.7%, 0.6%, 0.3% and 0.1% respectively in the earliest Oligocene. The holococcolith group (Figure 3.10), even though shows a declining pattern from the late Eocene to the early Oligocene, can be divided into two groups; one with a more marked decline and the other one of low abundance species with more sporadic occurrences. The later group consists of *Holodiscolithus macroporus, Holodiscolithus minolettii and Orthozygus aureus*, whereas the more abundant *Lanternithus minutus, Zygrhablithus bijugatus* and *Zygrhablithus bijugatus cornutus* show a consistent decline that is most marked in the lower part of the core, between ~400’ and 450’. Similarly, other taxonomic groups that show declining abundance trends up-

section - the Helicosphaerid group (Figure 3.7) (*Helicosphaera compacta* and *Helicosphaera gartneri*), *Coccolithus formosus* (Figure 3.4), and *Discoaster* spp (Figure 3.11) (*Discoaster barbadiensis, Discoaster saipanensis, Discoaster deflandrei, Discoaster tanii* and *Discoaster distinctus*) also show a clear declining trend from the late Eocene to the early Oligocene. In the same way, there are other taxa which show a clear declining trend in the same interval, such as *Pontosphaera versa* (Figure 3.9) and total *Pemma* species (Figure 3.12).

Taxonomic groups that show an increasing trend in abundance up-section, include *Reticulofenerstra daviesii, R. lockeri* and *Pontosphaera multipora*. *Reticulofenerstra daviesii* (Figure 3.3) shows a clear increasing trend near to the top of the Yazoo Clay, with mean relative abundance of 1% below the Eocene/Oligocene boundary (EOB), increasing to 8.8% above. *R. lockeri* shows a similar broad increase into the earliest Oligocene, although over a slightly longer interval ~250' to 100'. The mean relative abundance of *Pontosphaera multipora* (Figure 3.9) also increases through the EOB, from 1% below to 5% above. The other species that increased from the late Eocene to the early Oligocene is *Isthmolithus recurvus* (Figure 3.9). This increase in abundance up-section is significantly earlier than the other taxa, occurring some way below the EOB, but does show a consistent increase from rare occurrences in the late Eocene (below 375 feet (~114.3 m)), to a consistent value of ~5% relative abundance in the late Eocene to the early Oligocene (above 371 feet (~113.1 m)).

3.3.3 Multivariate assemblage analyses

Statistical analyses were carried out using principal component analysis (PCA) to differentiate species and subspecies that have similar responses through the stratigraphy. This is shown by their weightings on the first and second principal components (PC1 and PC2).

Table 3.1 shows the taxonomic groups used within this analysis and Table 3.2 shows the value result of PCA analysis for 6 selected species, and 13 groups, and these are also shown as plots in Figure 3.14 and 3.15. PC1 and PC2 explain 23.5% and 17.9% of the observed variance respectively. The selection of taxonomic groups are chosen based on the importance and the abundance of species and group. The PC1 loadings are positive for all selected species and groups (Figure 3.14).

The *R. dictyoda* group, *Sphenolithus* group, *Cyclicargolithus formosus*, *R. bisecta* group, *Umbilicosphaera* group, *Reticulofenestra westerholdii, Discoaster* spp., *R. reticulata* group, total holococcoliths and total braarudosphaerids all have high positive PC1 loadings (Figure 3.14). Whereas *Isthmolithus recurvus, R. daviesii* group, *R. bisecta* group*, R. dictyoda,* group and total rhabdosphaerids all show a high PC2 loadings (Figure 3.15). All the species and subspecies grouping are shown in Table 3.1.

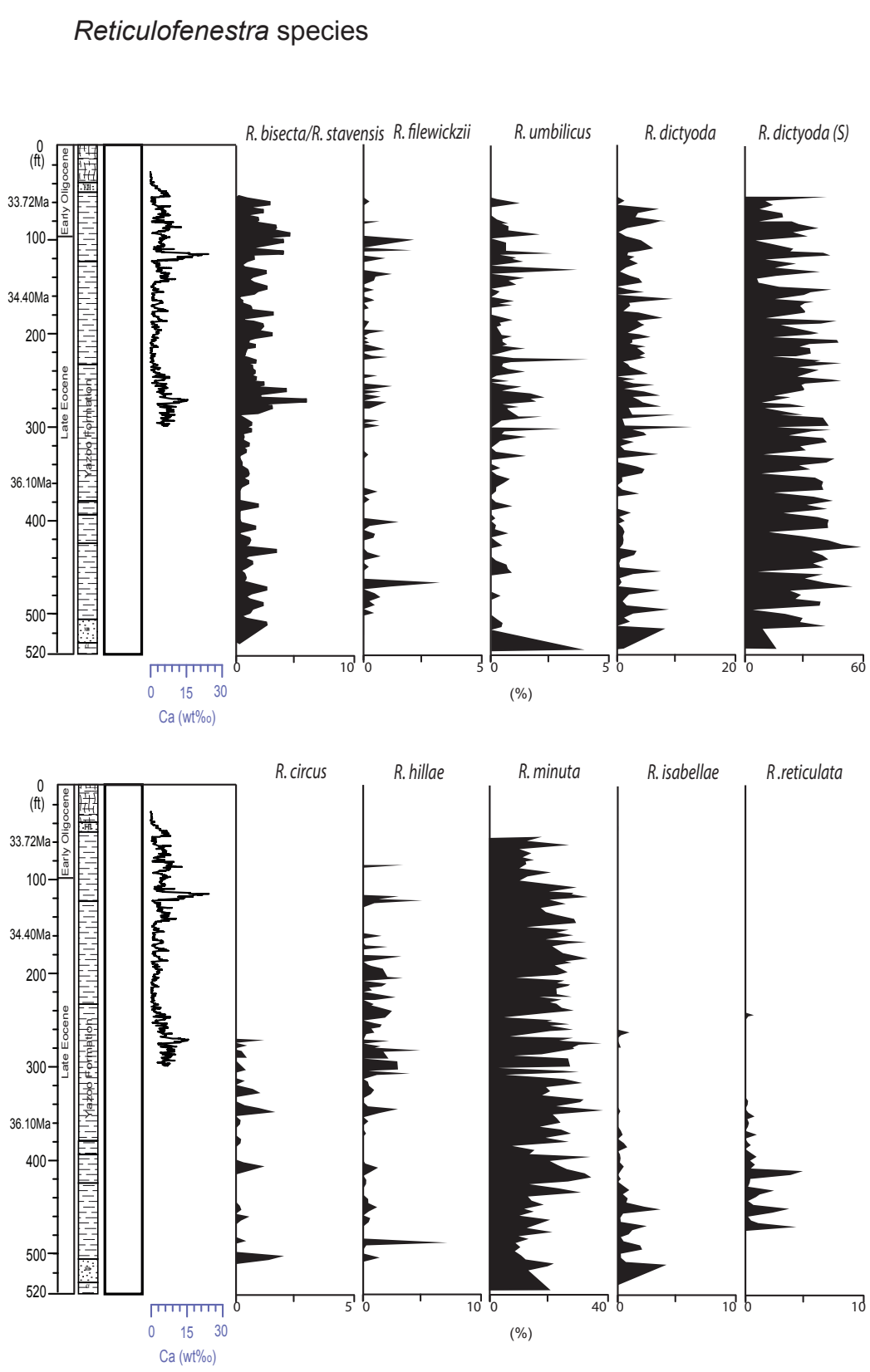


Figure 3.2: Plotted graph of calcareous nannofossil assemblages.

Reticulofenestra species

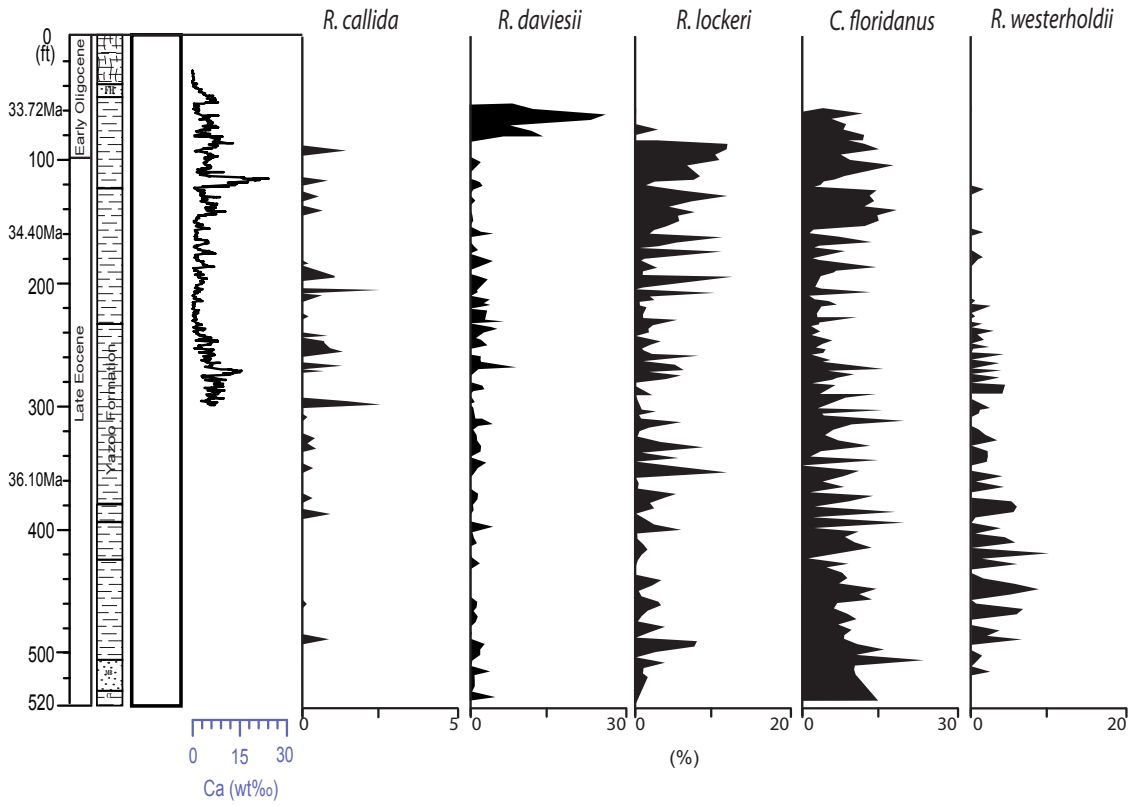


Figure 3.3: Plotted graph of calcareous nannofossil assemblages (continued).

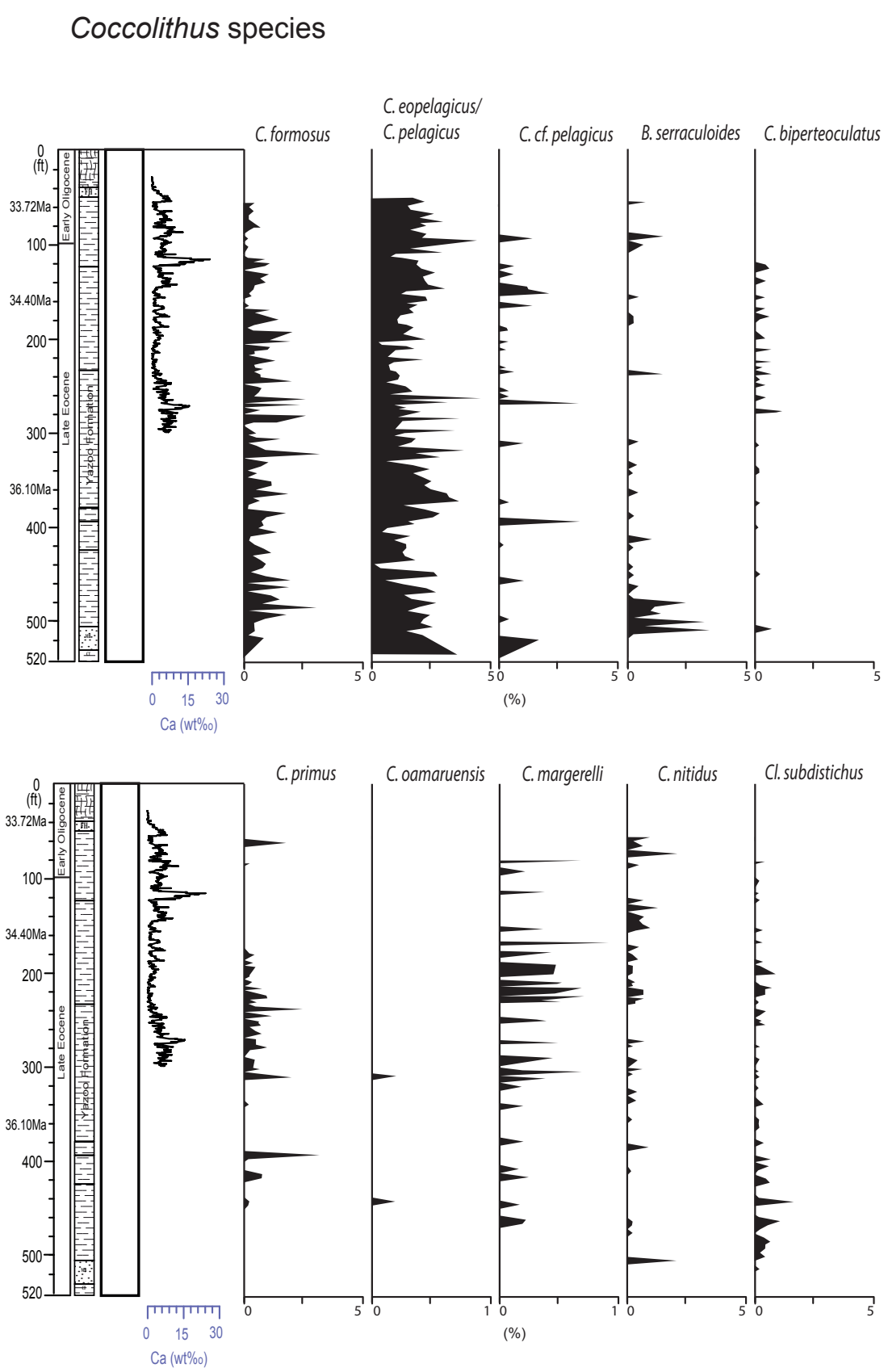


Figure 3.4: Plotted graph of calcareous nannofossil assemblages (continued).

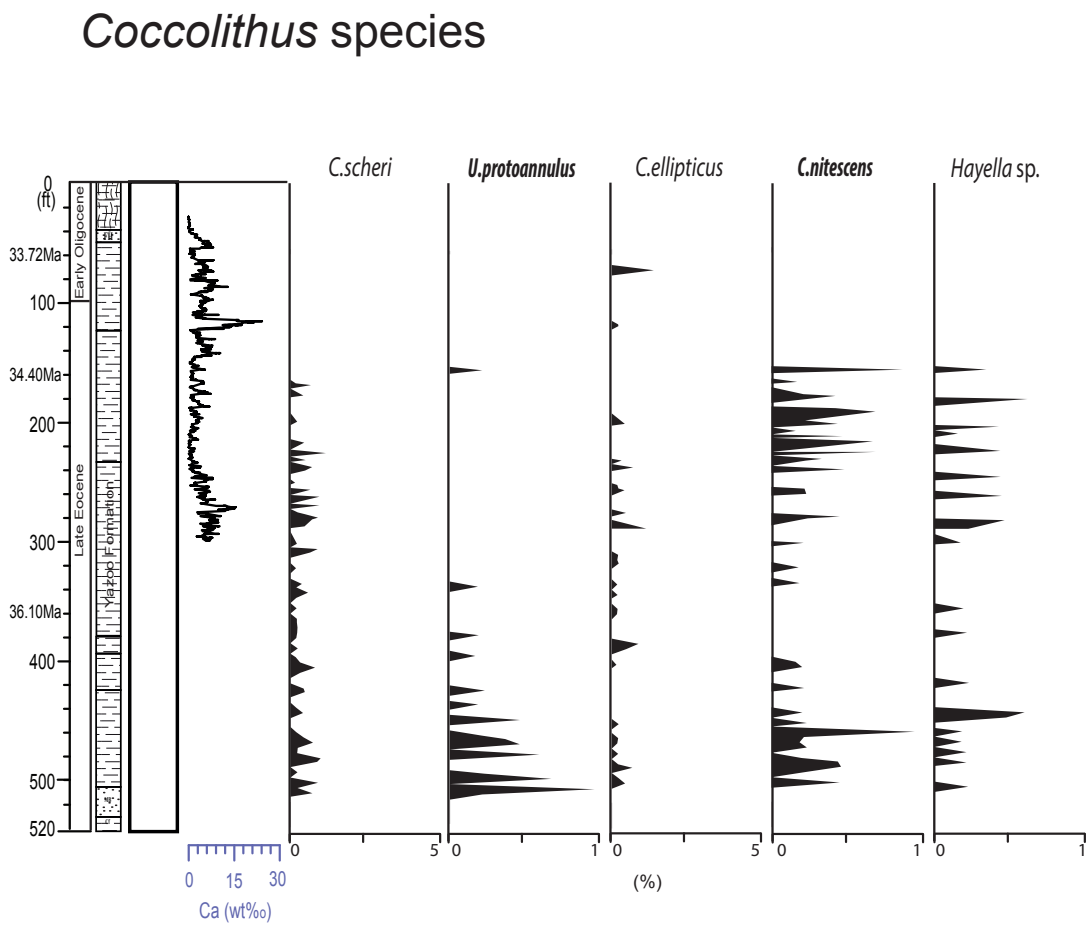


Figure 3.5: Plotted graph of calcareous nannofossil assemblages (continued).

Blackites species

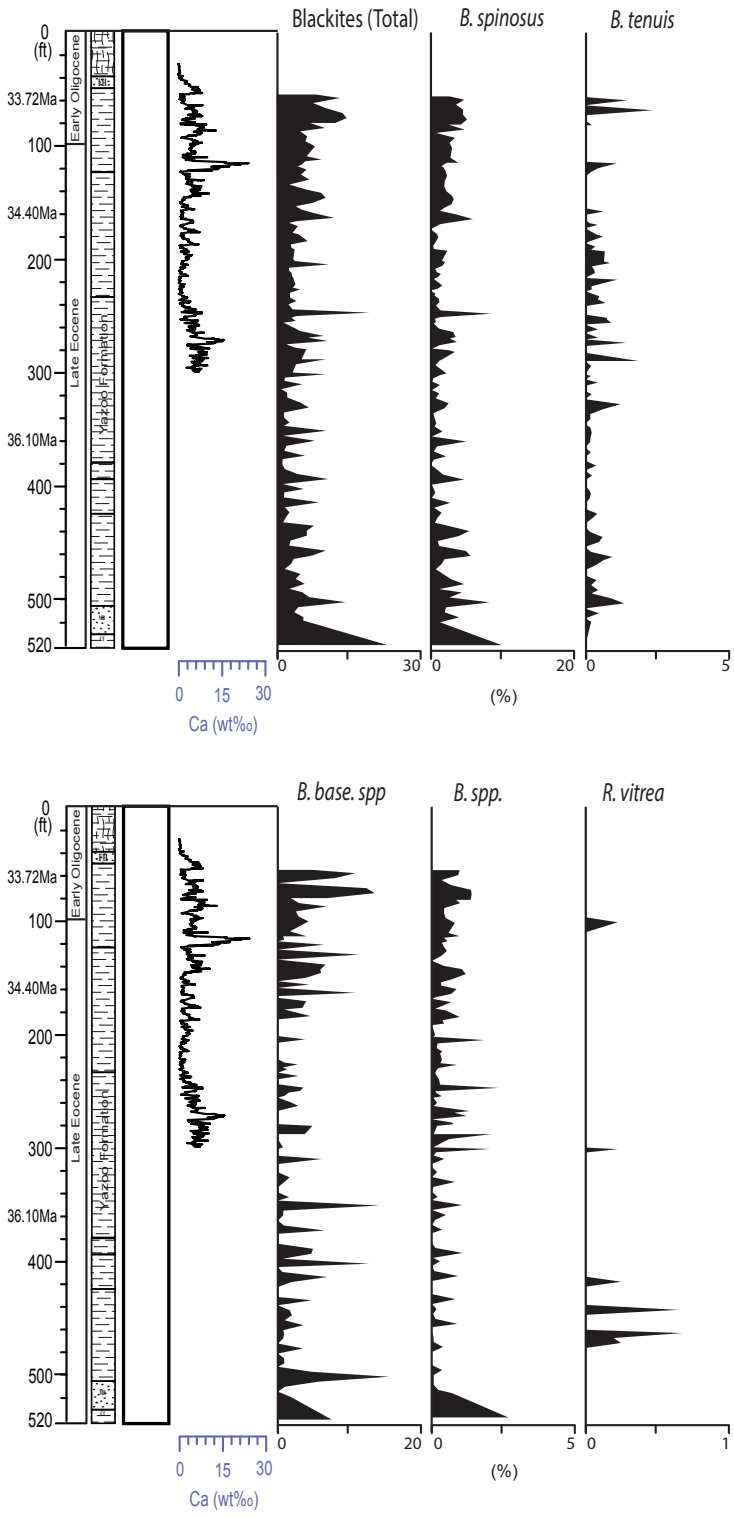


Figure 3.6: Plotted graph of calcareous nannofossil assemblages (continued).

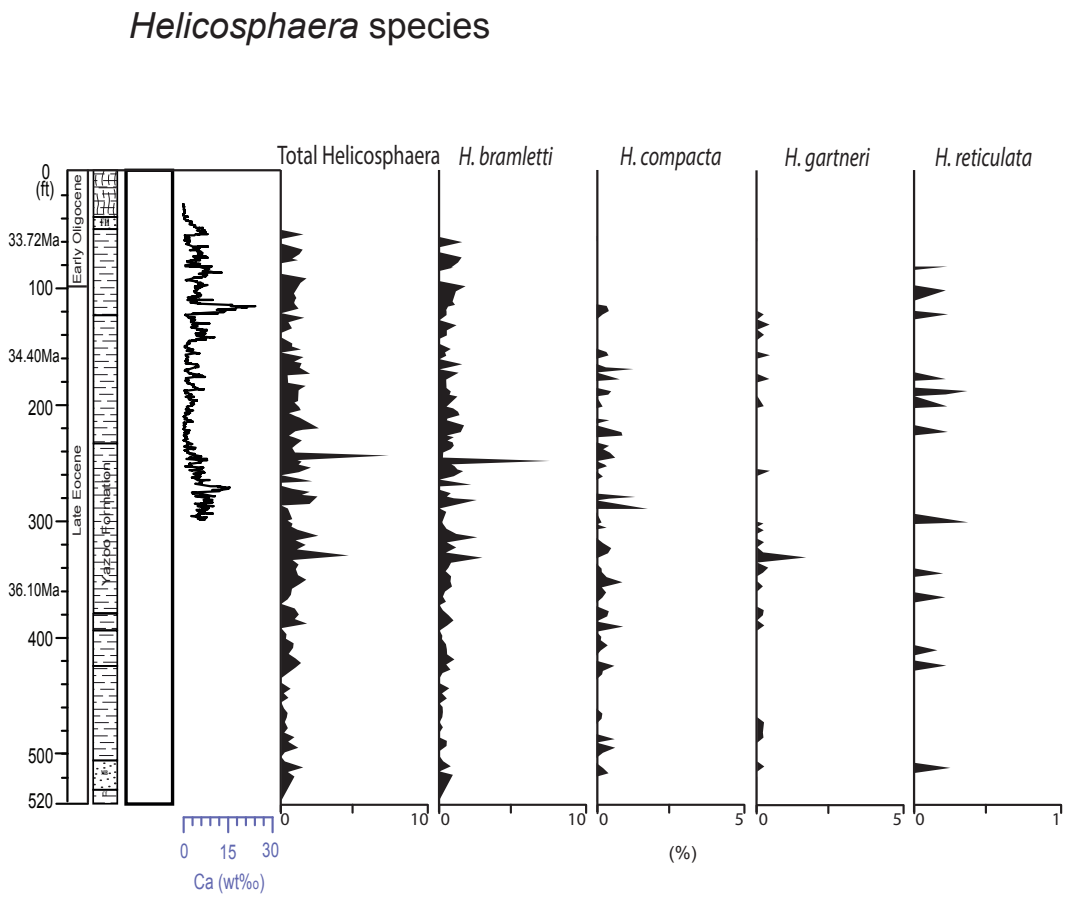


Figure 3.7: Plotted graph of calcareous nannofossil assemblages (continued).

Umbilicosphaera species

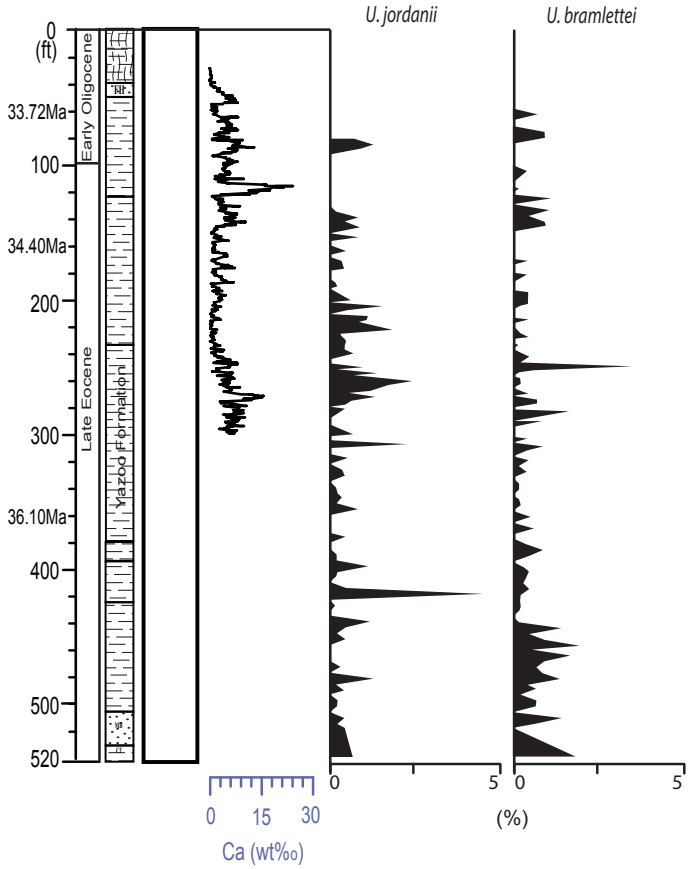


Figure 3.8: Plotted graph of calcareous nannofossil assemblages (continued).

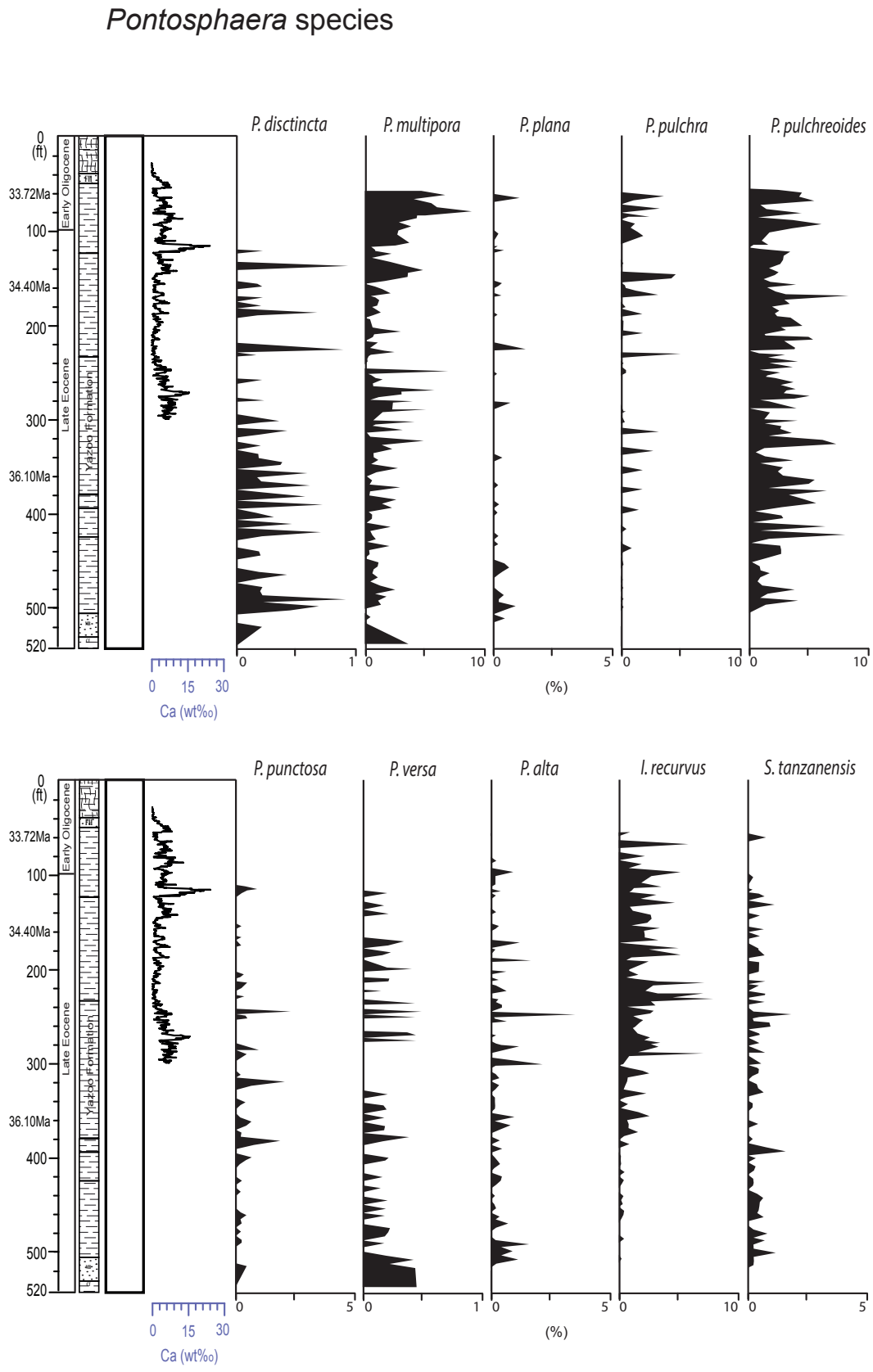


Figure 3.9: Plotted graph of calcareous nannofossil assemblages (continued).

Holoccolithus species

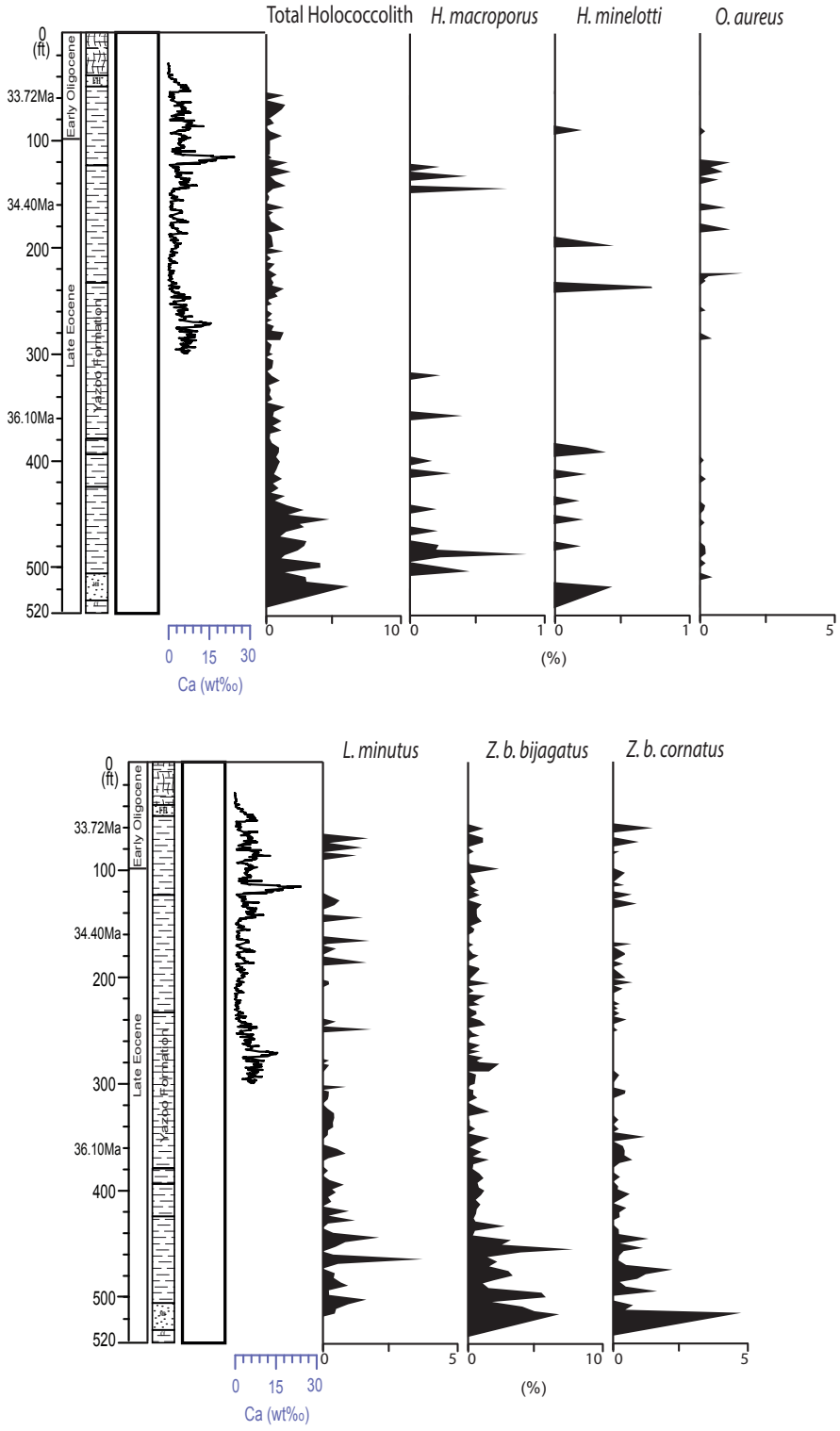


Figure 3.10: Plotted graph of calcareous nannofossil assemblages (continued).

Discoaster species

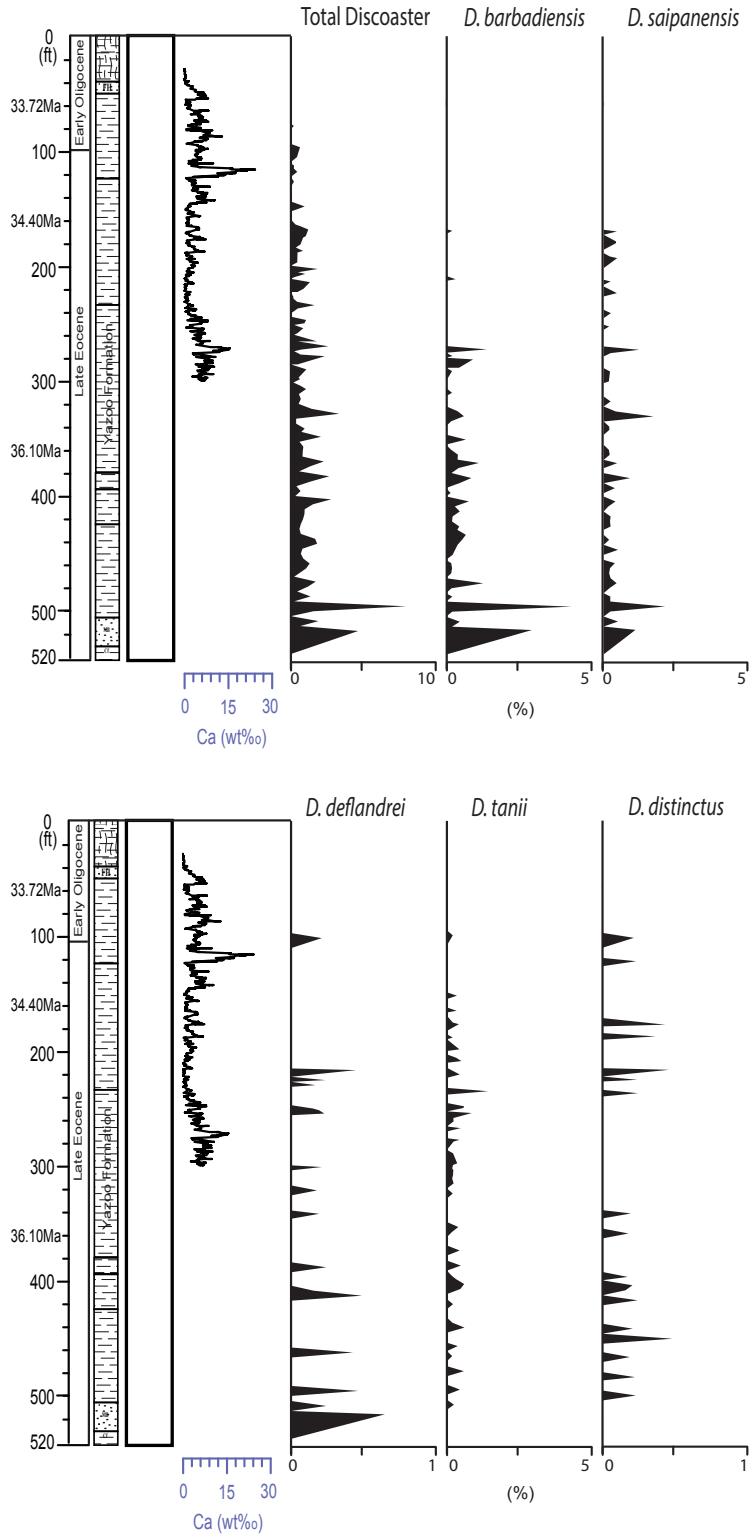


Figure 3.11: Plotted graph of calcareous nannofossil assemblages (continued).

Braarudosphaera species

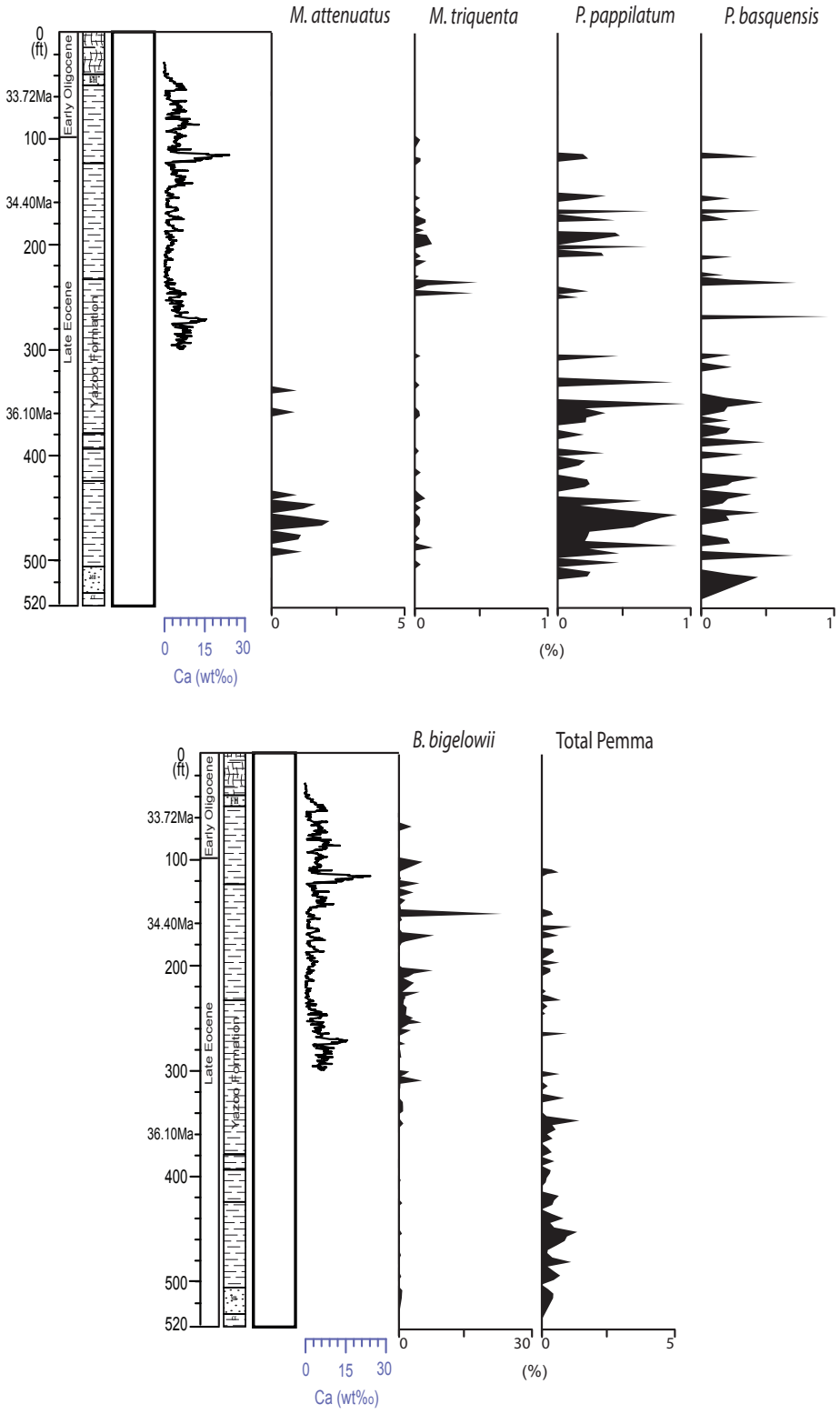


Figure 3.12: Plotted graph of calcareous nannofossil assemblages (continued).

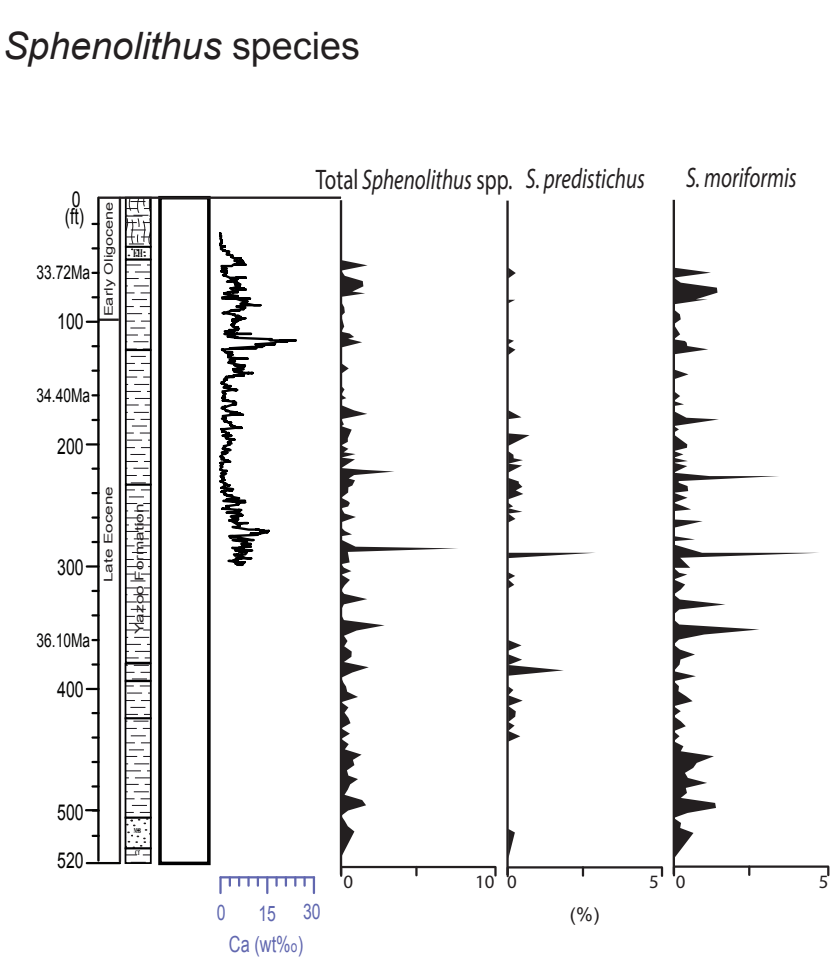


Figure 3.13: Plotted graph of calcareous nannofossil assemblages (continued).

Table 3.1: Species and group of species used in PCA analysis, based on the genus level and the importance.

Taxonomic grouping used in PCA analysis	**Taxa included**
Reticulofenestra dictyoda group	*R. dictyoda*, *R. circus*, *R. hillae,* and *R. umbilica*
Sphenolithus spp.	*S. moriformis, S. predistichus,* and *S. grandis*
Coccolithus formosus	*Coccolithus formosus*
Reticulofenestra bisecta group	*R. bisecta, R. filewiczii* and *R. stavensis*
Umbilicosphaera group	*U. jordanii, U. bramlettei, U. protoannula and Coronocyclus nitescens*
Reticulofenestra westerholdii	*R. westerholdii*
Discoaster spp. group	*D. saipanensis, D. deflandrei, D. barbadiensis, D. tanii, D. distinctus, D. spinescens, D.* cf. *williamsii,* and *D. nodifer*
Reticulofenestra reticulata group	*R. reticulata* and *R. isabellae*
Total holococcoliths	*Holodiscolithus macroporus, H. minolettii, Orthozygus aureus, Lanternithus minutus, Zygrhablithus bijugatus bijugatus* and *Z. bijugatus cornutus*
Total Pentaliths	*Braarudosphaera bigelowii, Micrantholithus attenuatus, M. triquentra, Pemma basquense* and *P. papillatum*
Isthmolithus recurvus	*Isthmolithus recurvus*
R. daviesii group	*R. daviesii, R. callida* and *R. lockeri*;
Rhabdosphaerids	*Blackites spinosus, B. tenuis, Blackites* spp., Blackites spines, and *Rhabdosphaera vitrea*

Table 3.2: The values of the PCA analysis for all 6 selected species, and 13 subspecies

Axis	Eigenvalue	Percent
1	1860	23.49
2	1419.8	17.931
3	851.82	10.758
4	571.16	7.2134
5	517.12	6.5309
6	416.55	5.2608
7	364.96	4.6092
8	332.27	4.1964
9	292.17	3.6899
10	276.54	3.4926
11	218.31	2.7571
12	203.05	2.5644
13	194.05	2.4508
14	136.68	1.7262
15	122.73	1.55
16	52.021	0.657
17	38.848	0.49063
18	29.45	0.37194
19	20.498	0.25887

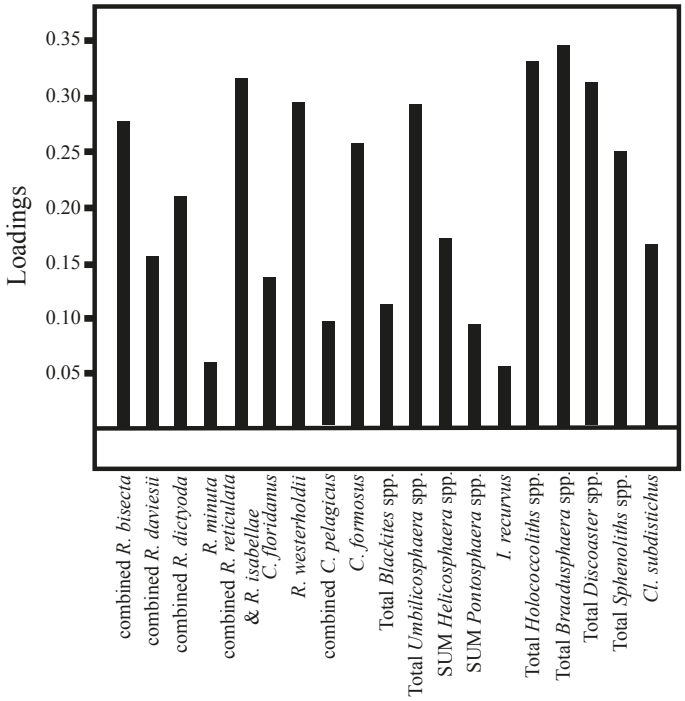


Figure 3.14: PC1 loadings based on selected species/subspecies/group of species for PCA analysis. All species of calcareous nannofossils show positive loadings.

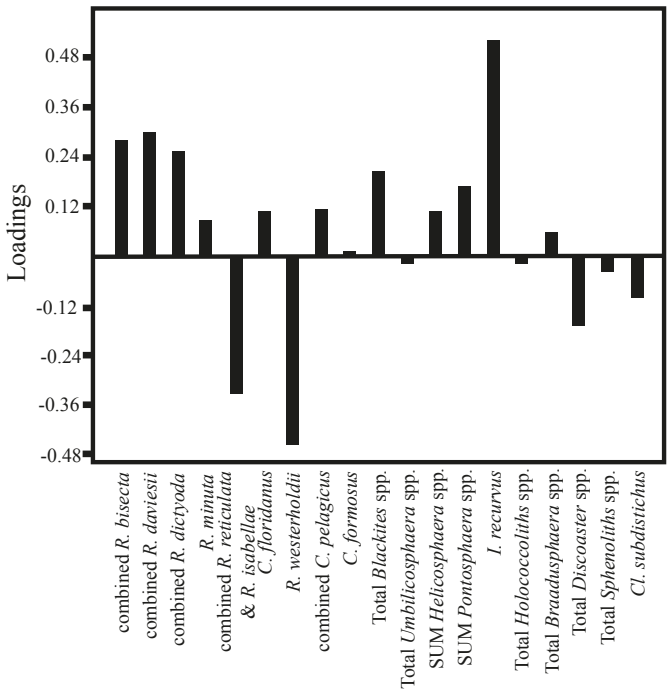


Figure 3.15: PC2 loadings on selected species/subspecies/group of species for PCA analysis.

Plots of the PC1 and PC2 principal component scores for each sample by depth are shown in Figure 3.16. These can be used to split the stratigraphic succession into several intervals based on the mean values of PC1, which alternate between intervals with more positive and negative values. The first broadly positive interval, with the most positive PC1 values of the whole succession, is at the bottom part of the core, from 519 feet to 400 feet (~158.2 to 121.9 m) with mean PC1 value 2.07. The second positive series is between 343 feet (~104.5 m) to 266 feet (~81.1 m) with a mean PC1 value of 0.14. Both positive series lie in the late Eocene. Separating these two intervals is the first succession with a negative mean, from 399 feet (~121.6 m) to 347 feet (~105.8 m) with a mean PC1 value of -0.33. There are similar intervals between 263 feet (~80.1 m) to 182 feet (~55.5 m) with mean of -0.16 and 179 feet (~54.6 m) to 55 feet (~16.8 m) with mean value -1.32. These intervals with negative PC1 scores lie in the late Eocene, around the EOB and in the early Oligocene. Over the long-term, there appears to be a general trend to more negative values, with the EOB and the early Oligocene negative intervals having more negative mean values compared to the late Eocene section. In contrast to PC1 scores, PC2 is stable in the late Eocene succession at the bottom of the core between 519 feet to 367 feet (~158.2 to 111.9 m). However, it then shows a significant and systematic shift between 363 feet to 300 feet (~110.6 to 91.4 m) towards positive values, before stablising with more positive values between 299 feet to 55 feet (~91.1 to 16.8 m).

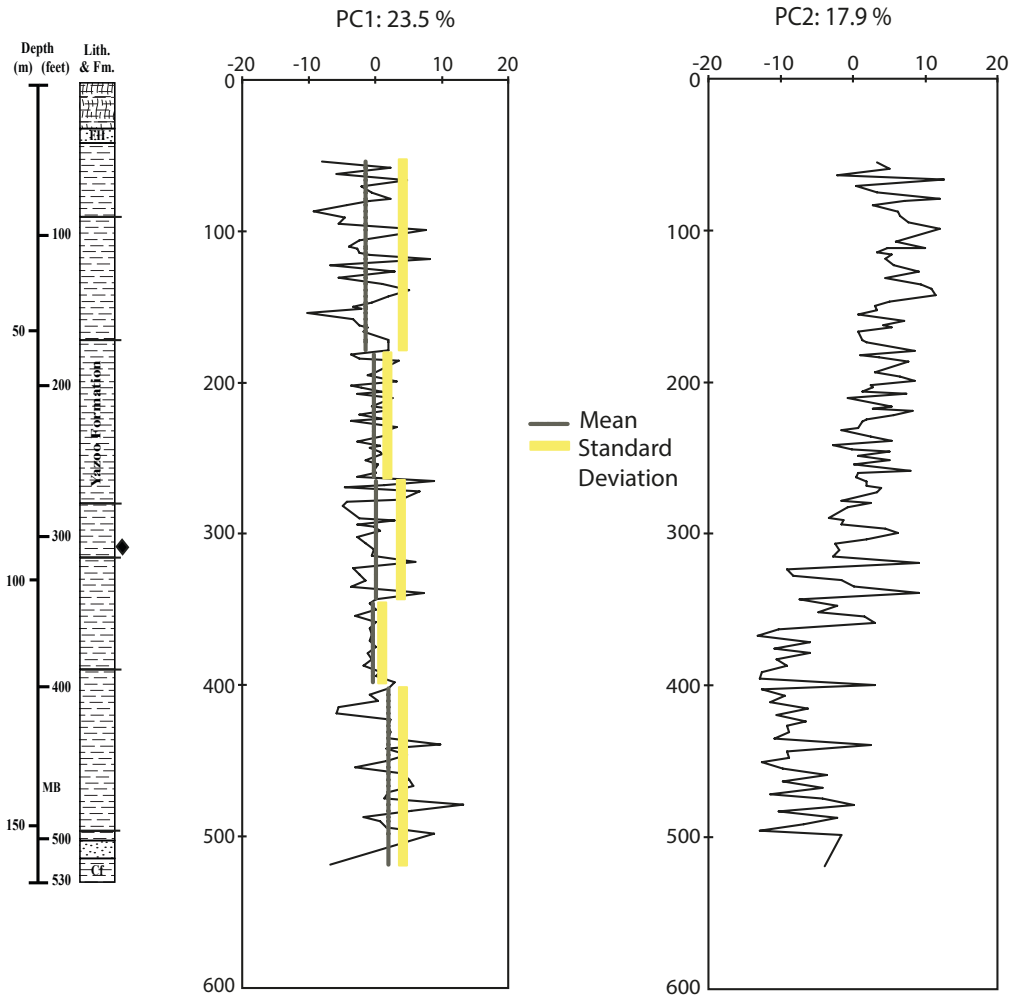


Figure 3.16: The PC1 (left) PC2 loadings of multivariate analysis PCA with mean and standard deviation values and 23.5% variance for PC1 and 17.9% variance for PC2.

3.4 Discussion

The Mossy Grove core provides a unique picture of low latitude coccolithophore ecology and evolution through the late Eocene, in the lead up to and through the onset of the greenhouse-icehouse transition. The studied succession provides an apparently continuous record though this interval, with the consistent presence of well-preserved calcareous nannofossil

assemblages throughout the Yazoo Clay. An integrated discussion of both calcareous nannofossil assemblage data along with the other palaeoclimate proxy and biotic data gathered from the Mossy Grove core will be presented in Chapter 5. Here I focus on a discussion of species abundance variations that can be useful in determining palaeoenvironmental change through the late Eocene succession recovered within the Mossy Grove core. This discussion focuses on two stratigraphic intervals, the late Eocene succession towards the base of the core and the Eocene/Oligocene transition. This is followed by a summary discussion of the palaeoenvironmental preferences of certain key taxa.

3.4.1 Late Eocene cooling phase

The dominant nannofossil assemblage change in the base of the Mossy Grove succession, below ~280 ft, is the distinct shift in PC2 values towards more positive values between ~360 ft and 280 ft. This is driven by a shift from species and taxonomic groups with large negative PC2 loadings (*R. westerholdii*, *R. reticulata* group, *Discoaster* spp.), to those with more positive values (*R. daviesii* group, *I. recurvus*). Based on late Eocene biogeography (Wei and Wise, 1990) and patterns of assemblage change at high-latitudes during late Eocene cooling (Persico and Villa, 2004) taxa with the most negative PC2 loadings are consistently considered to be warm-water, tropical to sub-tropical species, whilst those with the most positive PC2 loadings are high-latitude, cool-water taxa. For example, the discoasters are consistently found to favour tropical and sub-tropical open ocean environments (Wei & Wise 1990; Persico & Villa 2004; Villa & Persico 2006; Villa et al., 2014; Fioroni et al., 2015). The structured shift in assemblages represented by this change in PC2 values is a loss of tropical / sub-tropical taxa and increase in cooler water high-latitude assemblages into the US Gulf

Coastal waters. In its position, with a palaeo-latitude of ~30ºN, the Mossy Grove core is potentially able to detect a wider biogeographic contraction of the range of tropical assemblages during this time that is not recorded at lower latitude, fully tropical locations. For example, the cooler-water *I. recurvus* is consistently absent from assemblages throughout the EOT succession from Tanzania (~8ºS), even during the earliest Oligocene glacial maximum (Dunkley Jones et al., 2008). This is most consistent with a significant sub-tropical cooling phase in the latest late Eocene, immediately prior to the onset of the EOT and the onset of the major phases of Antarctic glaciation.

PC1 values are more difficult to interpret, but as noted in the results above, do show coherent variation between stratigraphic intervals with more positive mean values and higher variability (e.g. 519 ft to 400 ft; 343 feet (~104.5 m) to 266 ft) and intervals with more negative mean values and less variation (e.g. 400 ft to 343 feet (~104.5 m)). Taxonomic groups with the most positive loadings for PC1 are the braarudosphaerids, discoasters, sphenoliths, holococcoliths and the *R. reticulata* group. Taxonomic groups with more negative loadings are *R. minuta*, *I. recurvus*, *Pontosphaera* spp. and the *C. pelagicus* group. There is also a consistent trend through the whole core towards more negative mean values of PC2 through the late Eocene and into the earliest Oligocene. Of the taxonomic groups with positive PC1 loadings the discoasters, sphenoliths and holococcoliths are all associated with warm-water conditions (Dunkley Jones et al., 2008; Persico and Villa, 2004; Wei and Wise, 1990). The braarudosphaerids have a long-recognised ecology of being shelf-sea and/or opportunist taxa (Bown, 2005), whilst increased abundances of holococcoliths have been linked to oligotrophic conditions (Dunkley Jones et al., 2008). Given these associations, a reasonable interpretation of intervals with positive PC1 scores are those where warm-water taxa dominant, in potentially more oligotrophic conditions, but with contributions of distinct

warm-water shelf-sea taxa. In contrast, *R. minuta*, *I. recurvus* and *C. pelagicus* are most associated with temperate to cool-water conditions, and/or higher productivity regimes (Dunkley Jones et al., 2008; Persico and Villa, 2004; Wei and Wise, 1990). Together, this would suggest that the PC1 scores reflect alterations between more dynamic intervals with influxes of distinct assemblages with tropical / oligotrophic associations (e.g. 519 ft to 400 ft; 343 ft to 266 ft) and intervals of more continuously temperate and higher nutrient conditions (e.g. 400 ft to 343 ft). Over the whole succession, an integrated assessment of both PC1 and PC2 scores indicates a shift from a sub-tropical shelf sea environment subject to the influence of tropical and oligotrophic water masses towards one dominated by higher nutrient and temperate water assemblages. This is consistent with the patterns of ostracod assemblages, which indicate deeper-water (~more open ocean) assemblages during the interval when PC1 scores are more positive between 343 ft to 266 ft (Yamaguchi et al., 2014).

Table 3.3: Ecological preferences of different species based on PCA analysis.

Cold	**Warm**	**Eutrophic**	**Oligotrophic**
R. daviesii *I. recurvus*	*R. westerholdii* *R. reticulata* group *Discoaster* spp. *Sphenolithus* spp. *Holococcolithus* spp.	*R. minuta* *I. recurvus* *C. pelagicus*	*Holococcolithus* spp.

3.4.2 Eocene/Oligocene Transition

The Eocene-Oligocene Transition, occurring between ~34.2 to 33.5 Ma, includes both the major positive $\delta^{18}O$ shift in marine carbonates (Zachos et al., 2001; Coxall et al., 2005; Katz et al., 2008) and dramatic deepening of the carbonate compensation depth (Coxall et al., 2005) that are closely coupled to Antarctic ice sheet expansion. On a planetary scale, there is evidence for global cooling (Zachos et al., 2001; Lear et al., 2008; Liu et al., 2009; Miller et al., 2009) and changes in ocean circulation that impact both high-latitude and tropical marine biotic communities (Dunkley Jones et al., 2008; Pearson et al., 2008; Villa et al., 2008; Wade & Pearson 2008), potentially through an increase in upwelling driven productivity (Diester-Haass & Zahn 1996; Salamay & Zachos 1999). Here, this research adds to this picture by providing a unique new record of sub-tropical marine environmental change.

Within the Mossy Grove core, the changes in assemblage through the EOT appear to be relatively smaller compared to the distinct shifts observed in the latest Eocene. In general the changes that are observed are the continuation of the trends observed in this earlier interval – broadly towards more temperate and cool-water taxa and away from tropical, oligotrophic assemblages. The later group, which shows continued decreasing species abundances, include *C. formosus*, total holoccocoliths, *Helicosphaera* spp., *Sphenolith* spp. and *Discoaster* spp. whilst the cool-water taxa showing increased species include *Reticulofenestra daviesii, Pontosphaera multipora* and *Isthmolithus recurvus*. From the results of the PCA analysis, PC1 shows the most negative mean values during and after the EOT, whilst PC2 has the most positive values during this interval, together indicating the presence of an "end-member" calcareous nannofossil assemblage, that is distinctly different from that preserved at the base of the Yazoo Clay.

The most notable individual taxon response to the EOT is shown by *R. daviesii*, which is well documented high-latitude, cool-water taxon (Wei & Wise 1990; Persico & Villa 2004; Villa & Persico 2006; Villa et al., 2014; Fioroni et al., 2015). This shows a clear increase in abundance across the EOT and into the earliest Oligocene. Coupled with this change, there is also a clear increase in the abundance of *P. multipora*, on the basis of which is here also proposed to have temperate to cool-water affinities. The other individual taxa with the clearest cool-water ecology based on previous biogeographic studies is *I. recurvus* (Wei & Wise, 1990, Persico & Villa 2004; Villa et al., 2014). This species is more abundant with increasing latitude in the South Atlantic (Wei & Wise 1990), although may have a cool-temperate water abundance peak, as it is not dominant in high-latitude Southern Ocean locations during early Oligocene cool phases (Persico & Villa 2004). In the Mossy Grove core, this species does not increase significantly across the EOT, as it has already shifted to higher abundance someway before the EOT, with a shift from rare to consistent occurrences at ~370 ft.

3.4.3 Palaeoecological preferences of calcareous nannofossil

In the previous discussion, species with declining abundance are dominated by warm-water taxa including discoasters, holococcoliths, helicosphaerids, sphenoliths and *C. formosus* (Wei & Wise 1990; Persico & Villa 2004; Villa & Persico 2006; Villa et al., 2014; Fioroni et al., 2015). There are, however, subtleties on this general theme of declining abundance of warm water taxa through the succession, especially considering the impact of sea level change on this inner shelf palaeolocation. For example, compared to open ocean sites (e.g. Wei & Wise, 1990), the total abundance of discoasters in the Mossy Grove assemblages is low, even towards the base of the Yazoo Clay, and become rarer up-section. Although this is interpreted

as consistent with the general trend of a shift from tropical to temperate and cool-water assemblages, the impact of global scale eustatic sea level lowering is also highly likely to impact discoaster abundance, with a shift to shallower water inner shelf conditions in the early Oligocene. With this decline in water depth, and the major base level lowering with increasing erosion from the nearby continental landmass, a shift to increasingly eutrophic conditions through the EOT at the Mossy Grove location is also likely.

In contrast to the more uniform drop in abundance of discoasters, the total abundance of *Helicosphaera* and *Sphenolith* species groups are more persistent in abundance through the EOT with some species even increasing in relative abundance in the earliest Oligocene, such as *S. moriformis* (Fig. 3.13). Overall, however, the abundance of both groups is still higher in late Eocene compared to early Oligocene. Taken together, this suggests that the helicosphaerids and sphenoliths are warm-water taxa but with a greater resilience to the more dynamic and higher nutrient conditions of shallow shelf environments. This is consistent with the warm-water affinity of sphenoliths observed in the Atlantic and Indian Oceans records of the late Eocene and early Oligocene (Wei & Wise 1990; Wei et al., 1992). In terms of nutrient preference, sphenoliths have been associated with oligotrophic conditions based on orbital-scale cycles in sphenolith abundance, closely and positively coupled to discoaster and *Florispheara profunda* abundance in mid-Pliocene sediments from the tropical Atlantic (Gibbs et al., 2004). Nevertheless, sphenoliths also have been considered to adapt to mesotrophic/eutrophic conditions in high-productivity and diatom rich Messinian sediments (Wade & Bown 2006), in the early Oligocene interval (Wade & Palike 2004) and across the EOT (Dunkley Jones et al., 2008). This variability in abundance patterns between environments and external forcing conditions clearly shows that sphenoliths are capable of thriving across a range of tropical and sub-tropical environments, with a broadly

cosmopolitan behaviour (Wade & Bown 2006; Dunkley Jones et al., 2008). The helicosphaerids associated with near shore and shelf sediments have been assigned as warm water taxa in Atlantic Ocean (Wei & Wise 1990) as in Mossy Grove core. As with the sphenoliths, biogeographic studies (Wei & Wise 1990) support a sub-tropical to tropical affinity for helicosphaerids, including in the modern Atlantic (Ziveri et al., 2004). Although they are more commonly found in continental margin deposits (de Kaenel and Villa, 1996), this may be a factor of their relatively high susceptibility to dissolution rather than primary ecological preference (Gibbs et al., 2004). In this study, sea level lowering across the EOT at the Mossy Grove site does not appear to negatively impact helicosphaerid abundance to the same extent as the discoasters, which are more constrained to pelagic environments. Although holococcoliths are even more dissolution susceptible than helicosphaerids (Young et al., 2005) the decline in abunance through the Mossy Grove core is not associated with any decline in the quality of preservation, or increase in dissolution. Instead, this pattern is attributed to an affinity of holococcoliths for warm and oligotrophic conditions (Cros et al., 2000), which decline through the late Eocene and the EOT.

Chapter 4

Geochemical proxies for palaeoenvironemtal change and planktonic foraminifera from the Mossy Grove core

4.1 Introduction

Over the past decades, there has been increasing interest in the climate switch, from largely ice-free greenhouse to glaciated icehouse states, across the Eocene-Oligocene transition (Coxall and Pearson, 2007; Pearson et al., 2009). The EOT is prominent as the most significant climate transition of the Cenozoic era and occurs geologically fast, in less than 1 Ma, driven by the dynamics and positive feedbacks of Antarctic ice sheet formation (De Conto and Pollard, 2003). Although both the tectonic configuration of southern ocean gateways, the Drake Passage and Tasmanian gateway, and long-term cooling likely driven by declining levels of atmospheric CO_2, are all justified as playing a role in preconditioning the system for the shift into a glaciated state (DeConto & Pollard 2003; Katz et al., 2008; Goldner et al., 2014), the timing and magnitude of changes to the Earth system immediately before the EOT, and hence acting as the potential "trigger" for the transition are still poorly constrained. This is largely due to the poor recovery of complete sections through the latest Eocene with good microfossil carbonate and / or biomarker preservation.

In this chapter, I outline initial efforts to use the Mossy Grove core to develop new geochemical proxy records of climate and carbon cycle dynamics through this late Eocene interval. Key to this is the presentation of a new high-resolution fine fraction coccolith-fraction bulk isotope record for the whole core. Developing from this I also present planktonic foraminiferal assemblage and initial isotope analyses undertaken as part of this thesis. These

are discussed relative to existing but unpublished benthic foraminiferal isotopic and trace metal data, that provide a temperature record of bottom waters for the upper part of the cored succession. Finally, to compare to the planktonic foraminifera oxygen isotopic estimates of sea surface temperature, I present pilot organic geochemical analyses of the TEX_{86} temperature proxy to identify the palaeoenvironment during the EOT.

Using these data, I will examine two key questions regarding the EOT:

i). First, is there any sign of significant sub-tropical cooling prior to or through the event, which, being far from high-latitude ice-sheets is most likely to reflect CO_2 driven global climate change rather than local ice-sheet / climate dynamics (Liu et al., 2009). If there is evidence for cooling, what is its magnitude and timing relative to the main phase of ice-sheet growth, as constrained by bulk isotope stratigraphy?

ii). Second, are the climate fluctuations found within the core coupled to any significant perturbations in the carbon cycle, as shown by systematic changes in bulk carbonate carbon isotope signatures. Rapid glaciation, together with long term silicate weathering and orbital forcing trigger a changes of carbon cycle responses, which cause of positive $\delta^{13}C$ shifts through the EOT itself (Merico et al., 2008) as well as the potential for precursor global negative shifts in $\delta^{13}C$ that would both relate to major changes in storage between global carbon reservoirs, the deepening of CCD and the rapid declining of atmospheric carbon dioxide (ρCO_2) (Coxall and Pearson, 2007).

4.2 Methodology

4.2.1 Fine-fraction (<20μm) bulk isotope analyses

As detailed in Chapter 2, the Mossy Grove core sediments contain very well preserved calcareous nannofossil assemblages. Light microscope observations (Chapters 2 and 3) demonstrate that cocolith carbonate dominates the the <20 μm size fraction carbonates. On this basis, this size-fraction was targeted for bulk isotope analyses to reduce noise from the mixing of planktonic and benthic foraminifera, or ostracod carbonate that is also abundant in this section, or other allochthonous carbonate which can complicate the geochemical signals. Recent work has also focused attention on the utility of coccolith carbonate isotope analyses for the purposes of reconstructing both external palaeoenvironments and the biological responses of coccolithophore algae to environmental change (Coxall and Pearson, 2007). A total of 440 samples of bulk sediment were prepared by wet sieving using deionized water at 63μm and 20μm. The filtrate was then collected on standard filter paper, and oven dried overnight at 40ºC. The residue was checked for the presence of coccolith carbonate using light microscopy, and was shown to be dominated by nannofossil material. The collected <20μm residue was stored in small plastic vials and sent to NERC Isotope Geosciences Library (NIGL) in Keyworth, Nottingham for bulk isotope analysis. Samples were analysed for carbon and oxygen isotope composition ($\delta^{13}C$ and $\delta^{18}O$) at the NERC Isotope Geosciences Laboratory (NIGL). Sample material was powdered to yield CO_2 from the equivalent of 10 mg of 100% calcite and reacted with anhydrous phosphoric acid *in vacuo* overnight at a constant 25°C. Liberated CO_2 was separated from water vapour under vacuum and collected for analysis. Measurements were made on a VG Optima mass spectrometer (standard reproducibility of < ±0.2‰).

4.2.2 Planktonic foraminifera assemblages and isotope analyses

Washed micropalaeontological residues were provided at 4 feet (~1.2 m) resolution for the top ~350 feet (~106.7 m) of the Mossy Grove core by collaborator Tatsu Yamaguchi. These residues were split into the following size fractions 63-125 μm; 125-250 μm; 250-500 μm. The >125 μm fractions were observed using reflected stereomicroscopy and picked and sorted for planktonic foraminifera. Particular attention was paid to species within the genera *Turborotalia, Globoturborotalita* and *Hantkenina*, which were the primary target for isotopic analyses. Where possible these genera were split down to species level. Selected specimens were imaged using the JEOL 6000 field-emission scanning election microscope. Semi-quantitative abundance counts were made of key taxa, to document any major assemblage changes through the EOT.

Grouped taxa within the following categories were isolated for isotopic analysis, with grouping dependent on the relative abundance of species and the resultant number of tests / mass of carbonate available for isotopic analysis: *Globoturborotalita* spp., *G. ouachitanensis*, *Hantkenina alabamensis*, *H. nanggulensis*, *Turborotalia ampliapertura*, *T. increbescens*, *T. pomeroli*. The picked formaniniferal tests were cleaned using the deionized water, and ultrasonicated for 2s before being weighed using a six-point microbalance and then sent to NIGL for isotopic analysis as above.

4.2.3 TEX_{86} analyses

Pilot analyses to determine the TEX_{86} sea surface temperature (SST) proxy was undertaken for seven samples, to determine an independent measure of SST for comparison to

those based on planktonic foraminiferal oxygen isotope data. The TEX_{86} temperature proxy was first proposed by Schouten et al., (2002) on the basis of the relative ratios of glycerol dialkyl glycerol tetraethers (GDGTs) present in marine sediments. These archaeal tetraether lipids are biosynthesized by marine crenarchaeota, with a structure that is dependent on the temperature of the growth environment, which in the case of marine archaeota can be correlated to SSTs (Bolton and Stoll, 2013; Hemoso et al., 2014).

Organic biomarkers were extracted from raw sediment samples prior to analyses. First, raw sediment was freeze-dried overnight and then homogenized using a spatula or, for harder sediments, an agate mortar and pestle. The samples were then ultrasonically extracted with the solvent dichloromethane (DCM)/methanol(MeOH) (3:1, v/v). This was repeated 3 to 4 times until the solvent remained clear. The total lipid extract (TLE) was then extracted from this solvent using a polyvap and then dried over a Na_2SO_4 column. The TLE was then separated into three fractions N1, N3 and N4 using a silica gel column. The N1 contains aliphatic hydrocarbon which were obtained by eluting the column with 4 ml of hexane. The N3 fraction contains alcohols aldehydes and ketones which were obtained by eluting with 4 ml of DCM. The N4 fraction contains the sterols, hopanols and GDGTs fractions and was obtained by eluting with 5 ml MeOH. The N4 fraction was then redissolved in *n*-hexane:iso-propanol (99:1, v/v) and filtered using a 0.45 μm, 4 mm diameter PTFE to get the GDGT fraction. The samples were then run in the GC mass spectrometer to determine the relative concentrations of the following GDGT compounds: GDGT-0, GDGT-1, GDGT-2, GDGT-3 and Crenarchaeol and its regioisomer. Sea surface temperature (SST) were determined following the Kim et al., (2010) calibration for TEX_{86}^{H}, TEX_{86}^{L}, and 1/ TEX_{86}.

4.2.4 Benthic foraminifera isotope and trace metal analyses; bulk XRF analyses.

In addition to the geochemical data generated as outlined above, raw trace element and isotopic data from the benthic foraminifera species *Uvigerina jacksonensis*, were provided by project collaborator Tatsu Yamaguchi (between samples depths 62 feet (~18.9 m) to 216 feet (~65.8 m)). Alongside this, he also provided high-resolution (~1 cm) bulk rock elemental data based on hand-held XRF scanning for the upper ~358 feet (~109.1 m) of core.

4.3 Results

4.3.1 Fine-fraction (<20μm) bulk isotope analyses

The results of fine-fraction carbon and oxygen isotopes are shown in Figures 4.1 and 4.2 respectively (raw data in Appendix C). Through the succession, both $\delta^{13}C$ and $\delta^{18}O$ show similar patterns of stratigraphic variation from the late Eocene through the earliest Oligocene Yazoo Clay. Within the late Eocene interval of the Yazoo Clay, between ~500 feet (~152.4 m) and 300 feet (~91.4 m), $\delta^{13}C$ values show little long-term trend, with values mostly between ~ 0 and 1 ‰. Within this long-term stability, however, there are patterns of short-term, potentially cyclical variations, with a period of ~20 feet (~6.1 m). In this same interval $\delta^{18}O$ values vary between -1 and -2 ‰, also with hints of cyclical behaviour. Above 300 feet (~91.4 m), there is a major coupled shift in both $\delta^{13}C$ and $\delta^{18}O$ to more negative values, with $\delta^{13}C$ reaching a minimum value of ~ -3 ‰, and $\delta^{18}O$ of ~ -4 ‰ at ~275 feet (~83.8 m). The one extreme negative value of -10.5 ‰ in $\delta^{13}C$ and -7.88 ‰ in $\delta^{18}O$ was recorded at 279.5 feet (~85.2 m) is unlikely to reflect primary coccolith calcite, but maybe

due to reworking of other fine carbonate material in an interval with relatively low coccolith abundance (Chapter 3).

From 275 feet (~83.8 m) to 250 feet (~76.2 m), $\delta^{13}C$ recovers back to more positive values, but remains ~1 ‰ more negative that the basal late Eocene succession, with values typically between 0 and -1 ‰ from 250 feet (~76.2 m) to 150 feet (~45.7 m). In the same interval, $\delta^{18}O$ shifts back to more positive values of ~ -1 ‰, but with greater variability than seen at the base of the core, or in $\delta^{13}C$ during the same interval. At ~190 feet (~57.9 m) there is another, more minor shift towards positive values in $\delta^{18}O$, with values between ~180 feet (~54.9 m) and 50 feet (~15.2 m) largely between 0 and -1 ‰. This shift in $\delta^{18}O$ occurs when values of $\delta^{13}C$ remain relatively stable, but is followed by another transient negative shift in $\delta^{13}C$ between 150 feet (~45.7 m) to 125 feet (~38.1 m). Within this interval $\delta^{13}C$ reaches a minimum value of ~ -3 ‰ and then, similar to the first perturbation, recovers to more positive values, between 0 and 1 ‰, above 125 feet (~38.1 m).

4.3.2 Planktonic foraminifera assemblages and stable isotope analyses

Planktonic foraminifera within the Yazoo Clay of the Mossy Grove core are notably less abundant and diverse compared to open ocean successions. The decreased diversity of planktonic foraminifera is associated with shoreline proximity during deposition of Moodys Branch Formation and Yazoo Clay (Fluegeman et al., 2009). The calcareous nannofossils however seem to be abundant and diverse in Mossy Grove core, which contrasts with planktonic foraminifera assemblages. The main aim of this study was to identify and pick all available mixed-layer dwelling planktonic foraminifera suitable for isotopic analysis from the Mossy Grove core. In this process, I document both the taxonomy of the identified species, and the low numbers patterns of abundance through the study interval (Table 4.1). As noted

previously, only residue samples between ~338 feet (~103 m) and 50 feet (~15.2 m) with low resolution results, provided by Tatsu Yamaguchi, were available for analysis at this time.

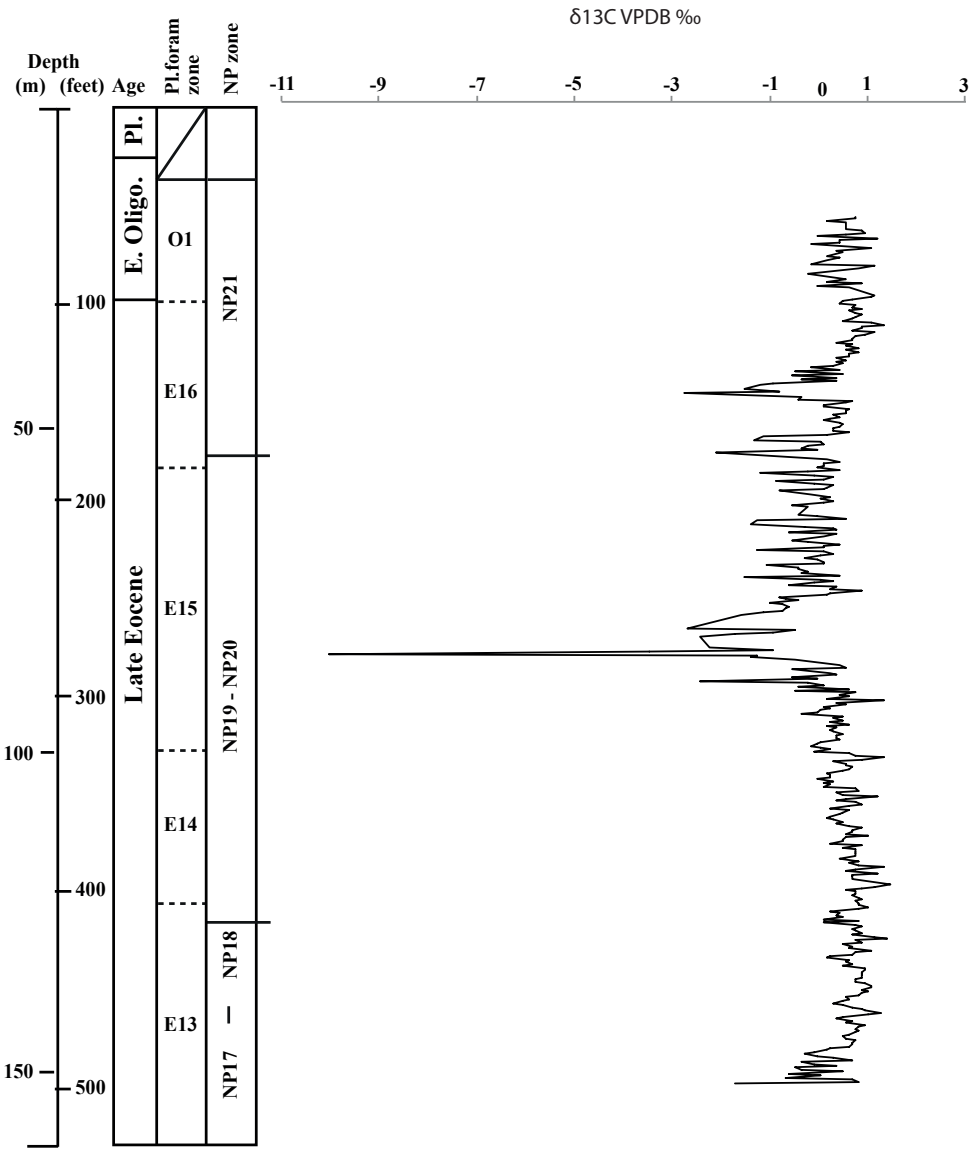


Figure 4.1: The carbon isotope data from the bulk sediments

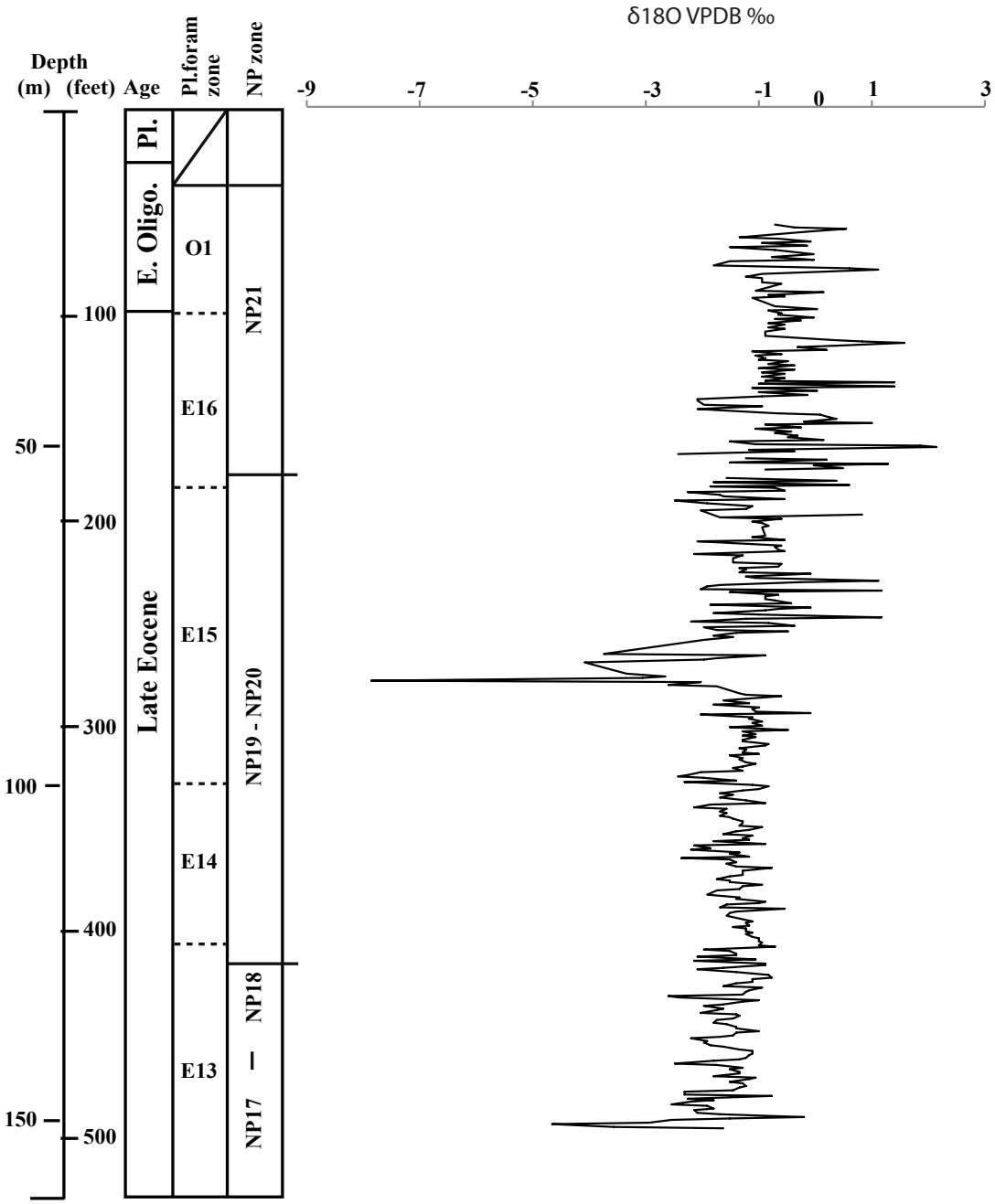


Figure 4.2: The oxygen isotope data from the bulk sediments

Table 4.1: The counting of planktonic foramifera in Mossy Grove core.

PF biozone	Depth (feet)	*T. ampliapertura*	*T.increbescens*	*T.pomeroli*	*G.ouachitaensis*	*G.angulioffícinalis*	*G.gnaucki*	*G.martini*	*H.alabamensis*	*H.compressa*	*H.nanggulanensis*	*H.primitiva*
OI	62											
	66		1		1	1	3					
	70		2		2							
	74						2					
	78											
	82											
	84											
	88				2							
	90	9			5	2	6					
	92	4										
	94		1		1		1					
Upper E16	96	4			3							
	98	35	17		2		4					
	100											
	102											
	106	6			7		1					1
	110		1		1		1					
	112											
	114											
	118	2			11	3	6	1				
	122									1		
	126	6	1		13	1	1	1	1			
	130											
	132	9	5		12				2			
	134		1									1
	138											
	142		2		3		5		2	1	2	
	146											
	150	2			5		3	1				
	154											
	158											
	162	4	2		7		1		4			
	170											
	174		4		2							
	178											
	182											
E15-E16	186											
	190						1					
	194											
	198											
	202											

Table 4.1: The counting of planktonic foramifera in Mossy Grove core (continued).

PF biozone	Depth (feet)	*T. ampliapertura*	*T.increbescens*	*T.pomeroli*	*G.ouachitaensis*	*G.angulioffícinalis*	*G.gnaucki*	*G.martini*	*H.alabamensis*	*H.compressa*	*H.nanggulanensis*	*H.primitiva*
E15 - Lower E16	206											
	214											
	218											
	222											
	226											
	230											
	234											
	238											
	242											
	246											
	250											
	254											
	258											
	262											
	266											
	274											
	278											
	282											
	292											
	294			1	1							
	298											
	302			1								
	306											
	310											
	314											
	318			1			1					
	322											
	326		1					1				
	330		2									
	334		6	2	7		3	1				
	338		19	2			1		2			1
E14	342		4	4	1							
	346		4		7			1				
	350		1		1							
	354											
	358		1									

Eleven species of surface dwelling planktonic foraminifera were identified - *Turborotalia ampliapertura, Tubrorotalia increbescens, Turborotalia pomeroli, Globoturborotalita anguliofficinalis, Globoturborotalita gnaucki, Globoturborotalita martini, Globoturborotalita ouachitaensis, Hantkenina alabamensis, Hantkenina compressa, Hantkenina primitiva* and *Hantkenina nanggulanensis* – with SEM images shown in Plates 4.1-4.3. *G. ouachitaensis* is the most diverse species within the Yazoo Clay, followed by *T. ampliapertura*, *T. increbescens, G. gnaucki, G. martini, T. pomeroli, H. alabamensis, G. anguliofficinalis, H. primitiva, H. compressa* and *H. nanggulanensis* with most species preserved as glassy and few frosty. The intergraded species of *T. ampliapertura* and *T. pomeroli* (Pearson et al., 2006) observed by the appearance of both species, where *T. ampliapertura* only found from the upper section to 170 feet (~51.8 m) followed by *T. pomeroli* only found below 292 feet (~89 m) to bottom section (Table 4.1). These changes were also shown in planktonic foraminifera distribution by Fluegeman et al, 2009. The morphologies and identifying features of these species are summarized below, following the taxonomy of (Pearson et al., 2006):

Globoturborotalita anguliofficinalis **Blow 1969**

(Plate 4.1)

Description: This species is characterized by a small test, globular chambers, low trochospiral and spinose; 4 and half globular chambers in spiral view, 4.5 to 5 globular chambers in umbilical view; chambers with depressed suture, straight, globular in shape and increase in size moderately; umbilical open aperture with low rounded arch, thick rim and narrow lip in the aperture; final chambers decrease in size and partially cover the umbilicus.

***Globoturborotalita gnaucki* Blow & Banner 1962**

(Plate 4.1)

Description: This species has a small lobulated test, low trochospiral, globular chambers; 4.5 globular in spiral view, 4 to 4.5 globular in umbilical view; chambers straight with depressed sutures; large umbilicus, open and moderately increasing in size; aperture umbilical, with rounded arch and thin thickened rim; chambers globular in shape in edge view.

***Globoturborotalita martini* Blow & Banner 1962**

(Plate 4.1)

Description: This species characterized by small test and moderately low trochospiral, globular chambers, lobute in outlined; 4 globular in spiral view, 4.5 to 5 globular in umbilical view; chambers with depressed suture, straight, globular in shape and rapidly increase in size; small umbilicus, partially covered by chamber, aperture umbilical, with rounded arch and thickened rim; globular in shaper in edge view.

***Globoturborotalita ouachitaensis* Howe & Wallace 1932**

(Plate 4.1)

Description: This *globoturborotalita* species is characterized by small size, moderately low trochospiral, outline lobulated; 4 globular in spiral view, 4 globular in umbilical view; chambers with globular shape, suture depressed, straight and increase moderately in size; large umbilicus and open; umbilical aperture with rounded arch and thickened rim; slightly elevated in initial spire of chambers.

***Turborotalia ampliapertura* Bolli 1957**

(Plate 4.2)

Description: *T. ampliapertura* has a compact globular test with 3-4 chambers, with trochospiral arrangement; inflated, appressed, embracing and moderately increasing size of the chambers; in side view the outline is lobate or rounded; slightly curved and depressed dorsal; high arch aperture with nearly circular in umbilical-extraumbilical position; umbilicus wide and deep; ventral sutures moderately curved, depressed. Smooth to weakly cancellate wall, with densely pustulose; have tendency to defoliate. Distinguished from *T.increbescens* by centered aperture, more globular in shape, wider and large open umbilicus.

***Turborotalia increbescens* Bandy 1949**

(Plate 4.2)

Description: A compact rounded test with 3.5 to 4 chambers in the final whorl and moderate to high trochospiral arrangement; appressed, embracing, radially compressed and moderately increasing chambers size; final chamber commonly radially flattened; rounded periphery with final chamber arching towards umbilicus in side view; curved, depressed dorsal sutures; broad arch aperture in an intra-extraumbilical position, often irregular and elongate; an imperforate or pustulose lip is usually visible; umbilicus usually narrow to moderately open; ventral sutures slightly curved, depressed; usually a strong tendency for sinistral coiling. The wall usually weakly cancellate and coarsely pustulose, often smooth on final chamber; have tendency to defoliate. Distinguished from *T. pomeroli* by its compact morphology.

***Turborotalia pomeroli* Toumarkine & Bolli 1970**

(Plate 4.2)

Description: Turborotalia species with large and globular test; 4 (rarely 5) chambers in the final whorl and high to moderate trochospiral; inflated, strongly radially compressed, appressed, and chambers moderately increase in size;.the final chamber arching towards umbilicus, with slightly curved dorsal suture; smooth wall with cylindrical pustules around umbilicus, weakly cancellate on earlier chambers; tendency to defoliate.

***Hantkenina alabamensis* Cushman 1925**

(Plate 4.3)

Description: Hantkenina with rounded to polygonal in shape and inflated moderately, globular final stage; 5-6 chambers in adult whorl; depressed suture, sigmoidal slightly restricted and deep umbilicus; adult chambers extend into a hollow tubulospine with variety of long and slender to short and stout; high equatorial arch for primary aperture, narrow at the top, broadening at the base into lateral lobes, bordered by an often crenulated and pustulose imperforate lip.

***Hantkenina compressa* Parr 1947**

(Plate 4.3)

Description: Subtriangular or polygonal in shape; 5-6 chambers and increase in shape rapidly, straight suture and sigmoidal slightly; adult chambers extend into a hollow tubulospine with straight, long and slender or short and triangular; lobed, continuous and slightly angular peripheral; elongated narrow equatorial arch flaring into lateral lobes for aperture with wide flaring lip.

***Hantkenina nanggulanensis* Hartono 1969**

(Plate 4.3)

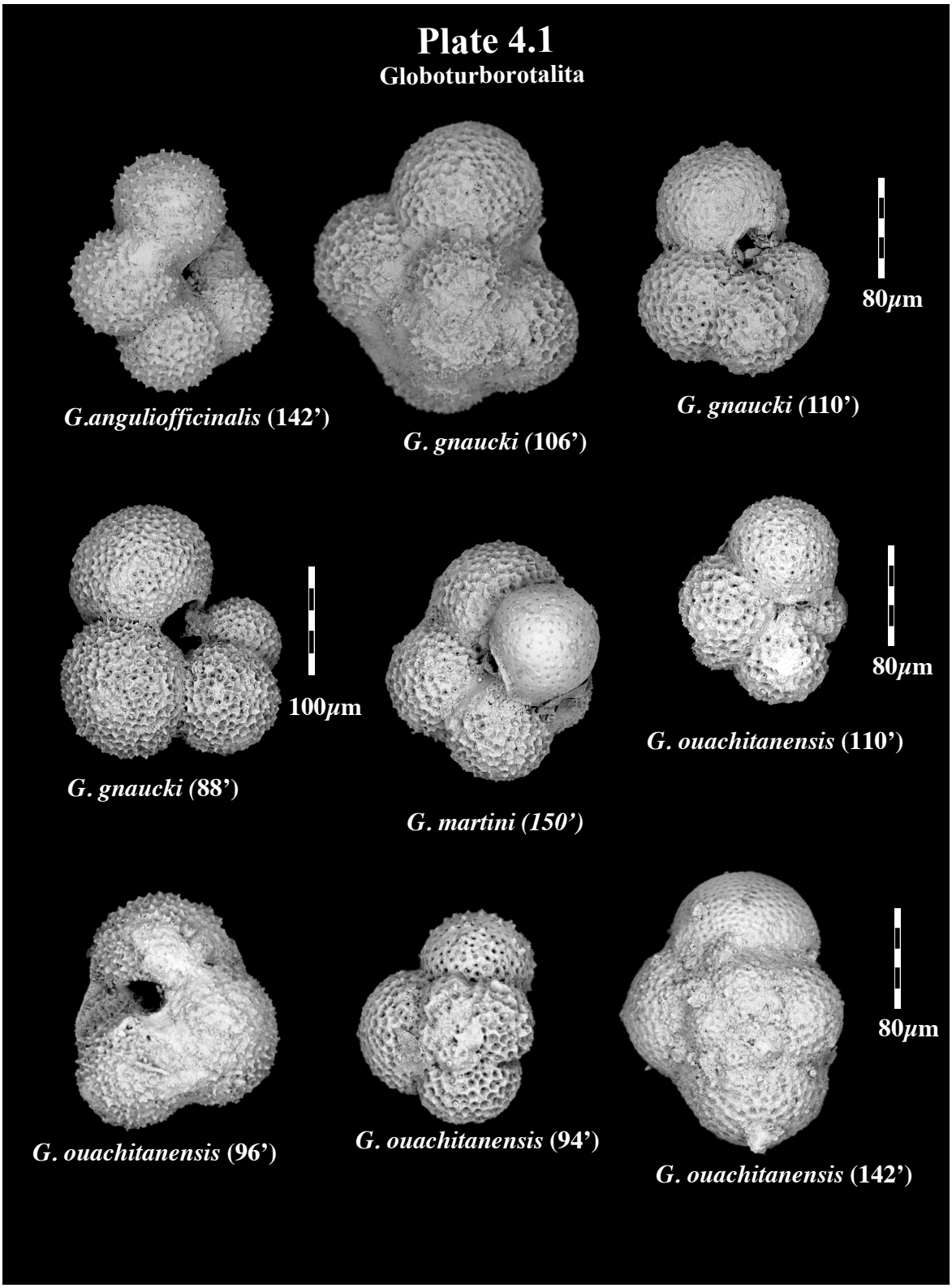
Description: Hantkenina species with biumbilicate and very large size; 5-6 chambers with spherical or polygonal shape, rapidly increasing in size; variable shape of aperture, symmetrical (as is typical for earlier hantkeninids) or asymmetrical; adult chambers extended into a hollow tubulospine; sutures depressed and curved; umbilicus deep and restricted.

***Hantkenina primitiva* Cushman & Jarvis 1929**

(Plate 4.3)

Decription: This species characterize by 5-7 chambers closely appressed, adult whorl chambers is rounded or polygonal and size increasing gradually; aperture with wide imperforate lip, arch, laterally pinched into a narrow slit; 1-3 of the first adult whorl chambers are rounded and pustulose, final 2-5 chambers extend into hollow tubulospines.

The relative abundance of foraminifera species are shown in Figure 4.3. The biggest feature of the planktonic foraminifera assemblages is the absence of all planktonic foraminifera in residues between ~290 feet (~88.4 m) and 200 feet (~61 m). Across this interval there is also a shift in the abundance of species, including the complete loss of *T. pomeroli* and significant reduction in the abundance of *T. increbescens*, whilst *T. ampliapertura* and *G. angulioffícinalis* appear for the first time above ~170 feet (~51.8 m), and *G. ouachitaensis* increases in abundance between ~170 feet (~51.8 m) and 90 feet (~27.4 m).


Plate 4.1
Globoturborotalita
G.angulioficinalis (142')
G. gnaucki (106')
G. gnaucki (110')
80μm
G. gnaucki (88')
100μm
G. martini (150')
G. ouachitanensis (110')
80μm
G. ouachitanensis (96')
G. ouachitanensis (94')
G. ouachitanensis (142')
80μm

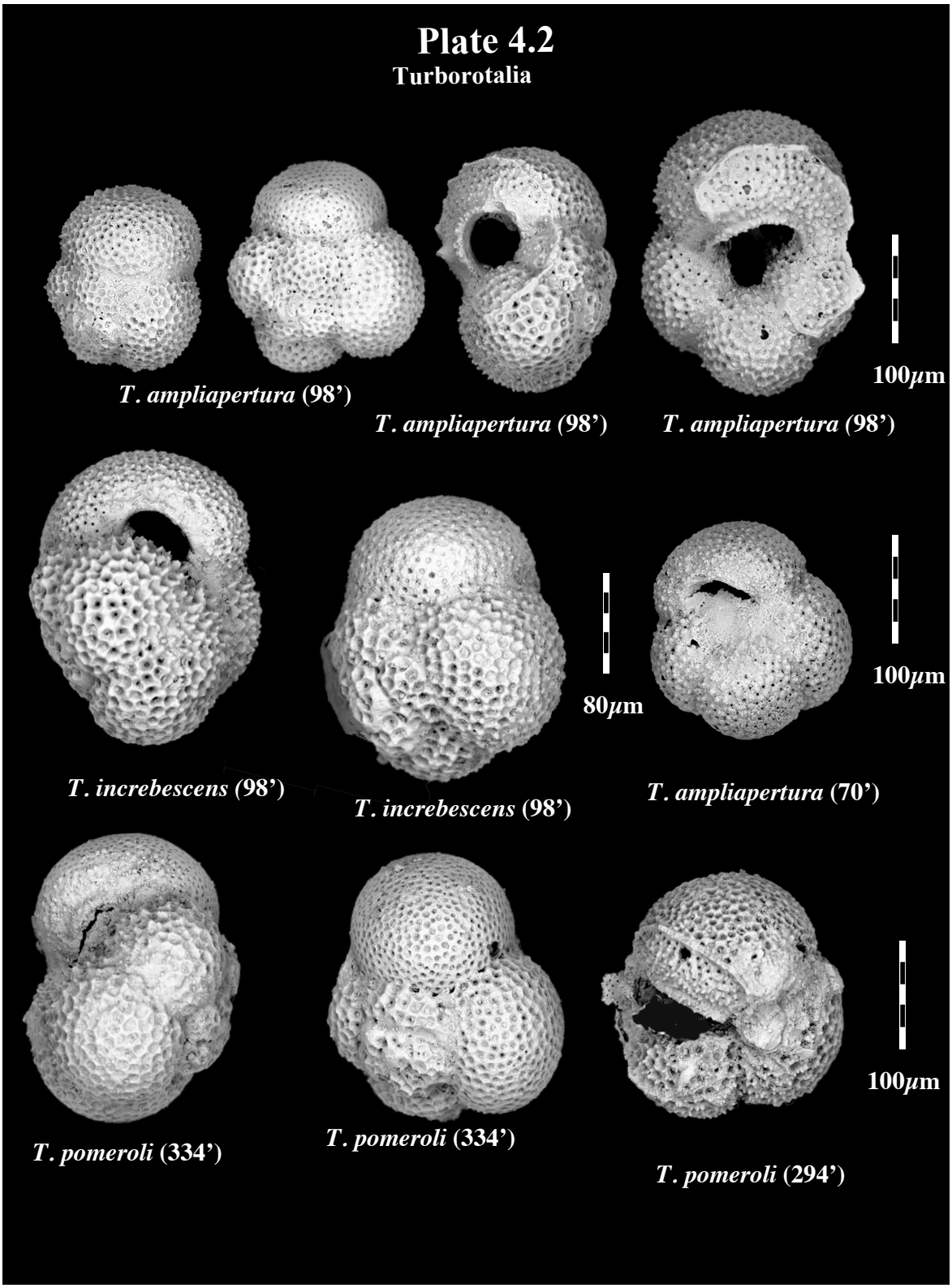
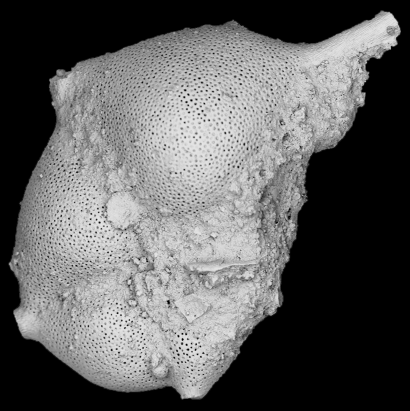

Plate 4.2
Turborotalia
T. ampliapertura (98')
T. ampliapertura (98')
T. ampliapertura (98')
100μm
T. increbescens (98')
T. increbescens (98')
80μm
T. ampliapertura (70')
100μm
T. pomeroli (334')
T. pomeroli (334')
T. pomeroli (294')
100μm

Plate 4.3

Hantkenina & Globigerinatheka index



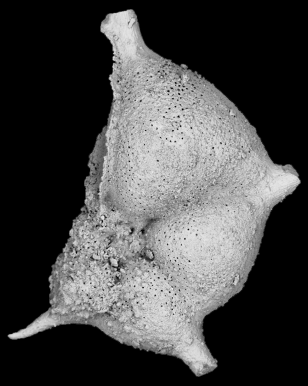
***H. alabamensis* (162')**



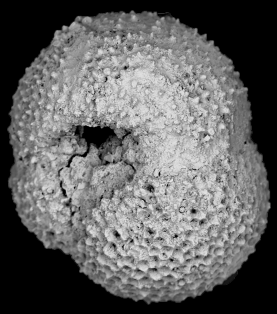
***H. nanggulensis* (142')**



200μm



***H. primitiva* (134')**



***Globigerinatheka index* (358')**



100μm

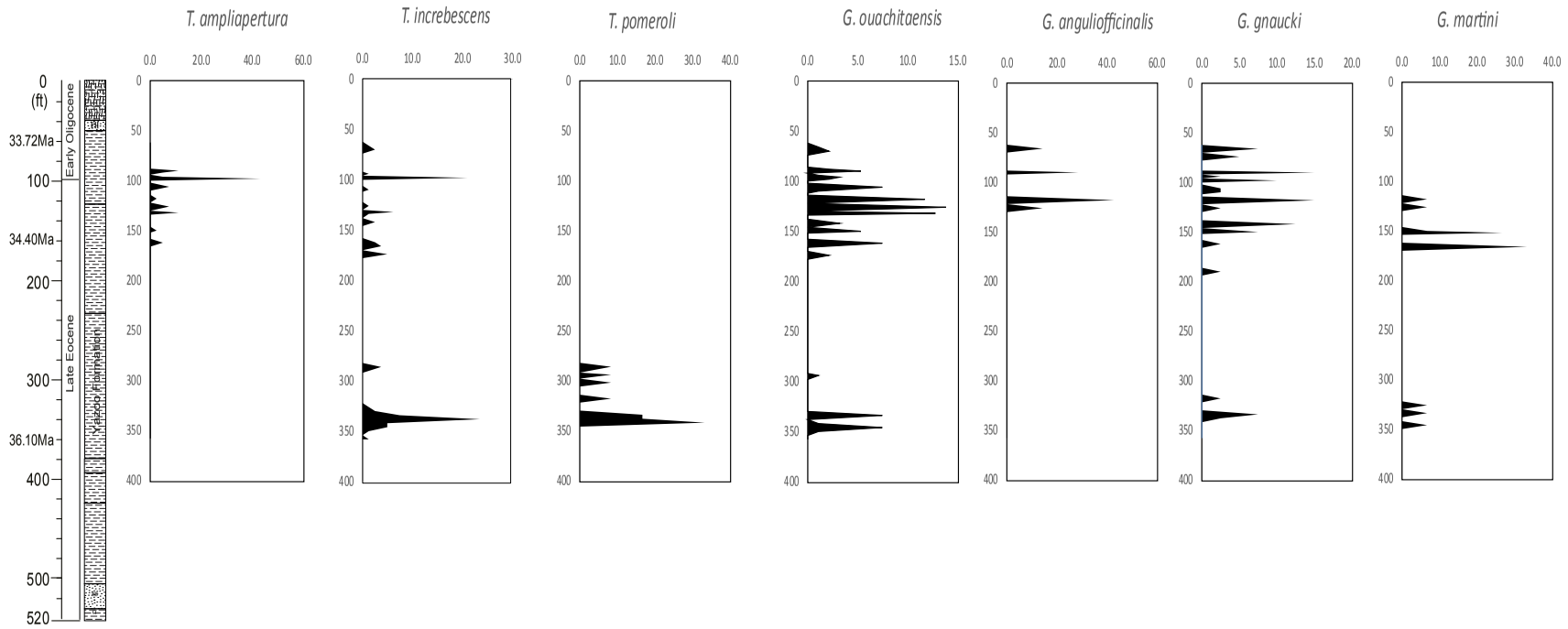


Figure 4.3: Relative abundance of planktonic foraminifera (%) for all genus except Hantkaninae spp due to least abundance observed.

4.3.3 Planktonic foraminifera isotopes

The oxygen and carbon isotopes for planktonic foraminifera have been recorded in multispecies cross plots (Figure 4.4) in two separated ages ranges, Eocene and Oligocene. The Eocene is considered to be below 106 feet (~32.3 m) depth, and Oligocene at 105 feet (~30 m) depth and above. *Hantkanina* spp were observed at 106 feet (~32.3 m). In the late Eocene, $\delta^{18}O$ values range between −1.68 ‰ to −3.67 ‰ and the $\delta^{13}C$ value range between a maximum of +0.72‰ for *Turborotalia increbescens* and minimum of -0.80‰ for *Hantkaninae alabamensis*. In the earliest Oligocene *Turborotalia ampliapertura* shows the lightest $\delta^{18}O$ value of −2.18 ‰ whereas *Globoturborotalita* spp (marked as combined *Globoturborotalita* in Figure 4.4) has the lightest $\delta^{13}C$ value of -0.32 ‰ (raw data in Appendix D). The overall oxygen isotope values for planktonic foraminifera fluctuate between −3.7 to −1.30 ‰, with more positive values in the earliest Oligocene interval. Carbon isotopes for the whole section are variable, ranging between +1.16 to −0.80 ‰ (Figure 4.5), which is likely due to species-specific photosymbiotic and ecological effects on $\delta^{13}C$.

Oxygen isotope values for all species are converted to temperature estimates using the calibration of Kim & O'Neil (1997) for inorganic calcite, in the form presented in Bemis et al., (1998):

$$T = 16.1 - 4.64 (\delta^{18}O_c - \delta^{18}O_{sw}) + 0.09(\delta^{18}O_c - \delta^{18}O_{sw})^2$$

The oxygen isotopic composition of seawater is estimated from paired benthic foraminifera $\delta^{18}O$ and Mg/Ca measurements. The mean value for seawater $\delta^{18}O$ in the interval for which there is planktonic foraminiferal data is 1.21 ‰, which was used for all temperature

calculations. This assumes that there is minimal difference between surface and bottom water $\delta^{18}O$, within the relatively shallow shelf environment (<300 m water depth). The resulting temperatures range from 16.5ºC (98 ft; *T. ampliapertura*) to 28.1ºC (142 feet (~43.2 m); *H. alabamensis*), with a mean value of 20.7 ºC. The underlying $\delta^{18}O$ values of these planktonic foraminifera analyses are in the same range as data from the EOT of St Stephen's Quarry Core in Alabama (1997). Within the interval analyzed - 338 feet (~103 m) to 90 feet (~27.4 m) – there is no clear trend of either warming or cooling of sea surface temperatures, with the assumption of no large systematic change in underlying seawater $\delta^{18}O$.

4.3.4 TEX_{86} analyses

The pilot TEX_{86} analyses of seven samples, between depths 259 feet (~78.9 m) and 139 feet (~42.4 m) (raw data in Appendix E), give a range of the TEX_{86} proxy from 0.64 to 0.73 (Figure 4.6). The estimated palaeo-sea surface temperature for these values, using the Kim et al., (2010) calibration for TEX_{86}^{H} are between 25.2 °C and 29.4 °C (Figure 4.6), with a mean value of 28.2 ºC. The coolest SST is recorded from the deepest sample, at 259 feet (~78.9 m), with the remaining samples in a relatively tight, and warmer range of temperatures, between 27.3 ºC and 29.4 ºC. It is noticeable that, across the same stratigraphic interval, TEX_{86}^{H} derived SSTs are consistently ~5 ºC warmer than those based on planktonic foraminiferal $\delta^{18}O$. This is consistent with similar offsets between TEX_{86}^{H} and $\delta^{18}O$ SSTs reported from both the high and mid-latitude locations in the early Eocene (Wade et al., 2012).

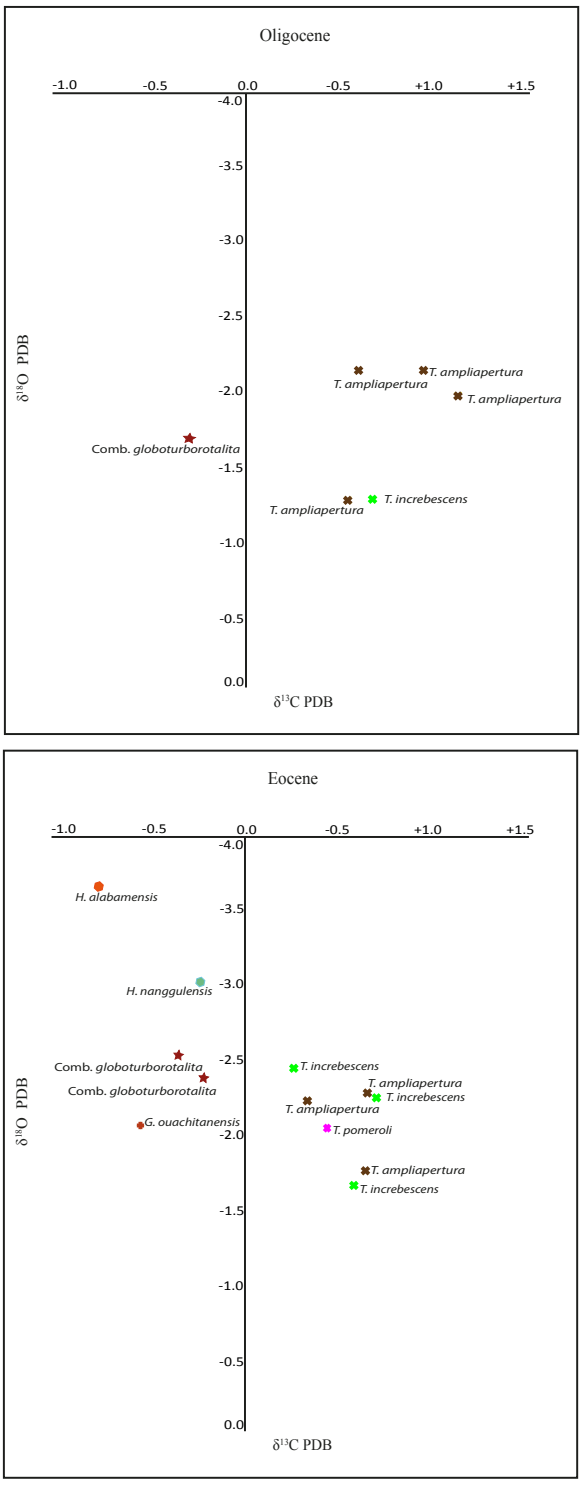


Figure 4.4: The cross plotting multispecies of planktonic foraminifera's stable isotope record for the Eocene (below 106 ft), and Oligocene (above 105 ft).

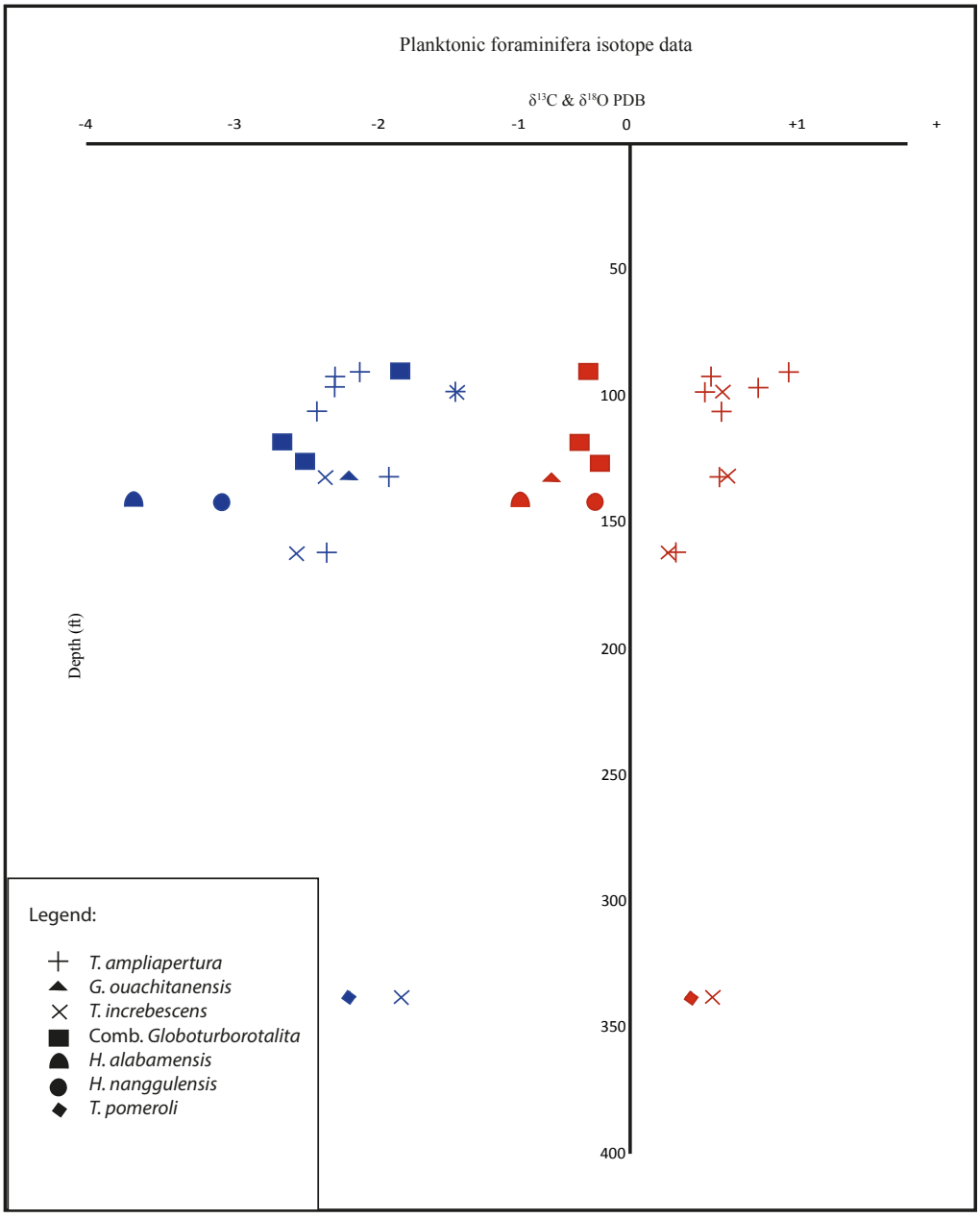


Figure 4.5: The stable isotope records for planktonic foraminifera through the whole section of Mossy Grove core (Blue marks indicate the δ18O and Red marks indicate the δ13C).

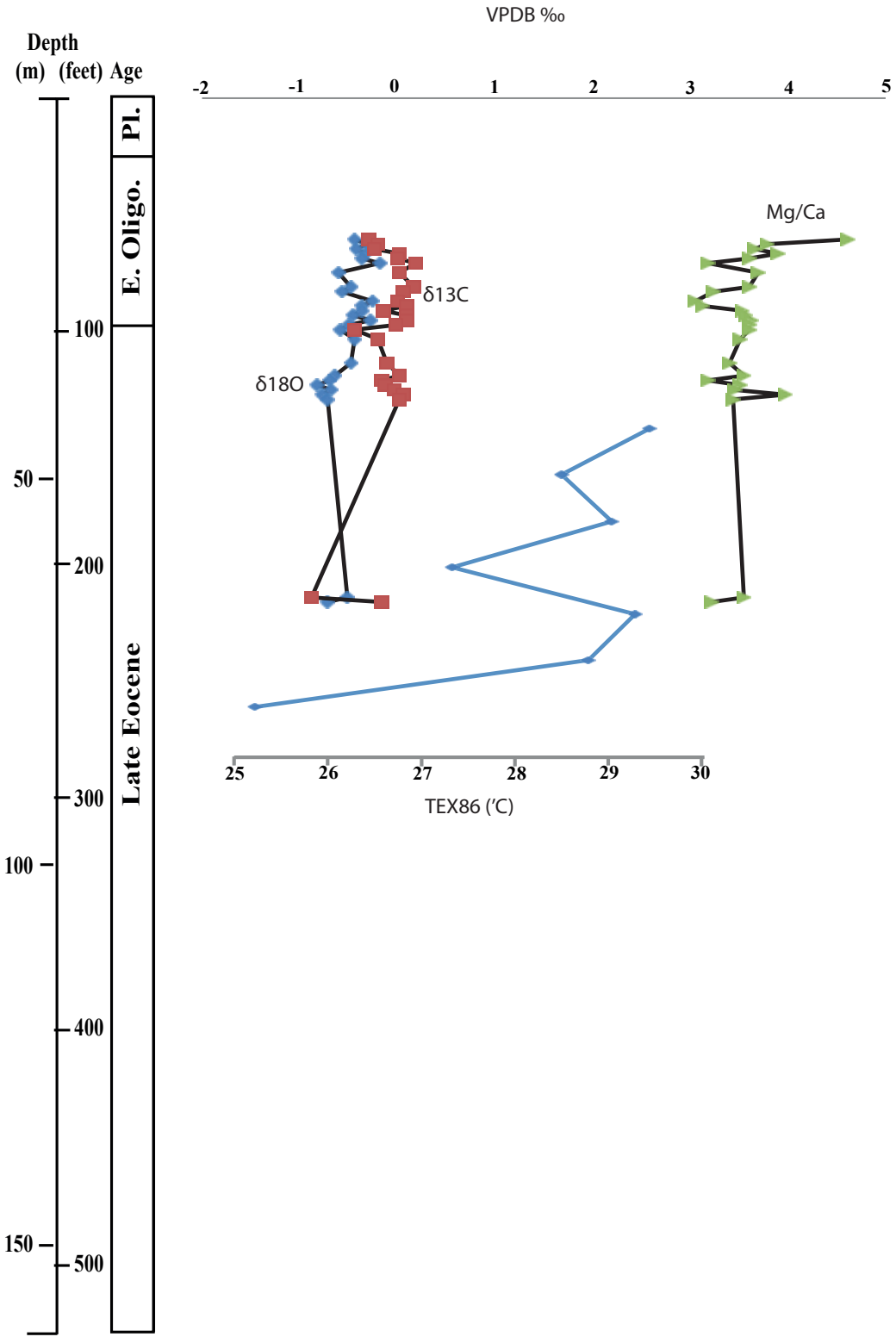


Figure 4.6: The oxygen and carbon isotope data from benthic foraminifera *U.jacksonensis* and the TEX_{86} temperature data from 7 samples of the pilot study.

4.3.5 Benthic foraminifera isotope and trace metal analyses; bulk XRF analyses

The stable isotopic analysis of benthic foraminifera has been undertaken by project partner Tatsu Yamaguchi (Yamaguchi et al., unpublished). The benthic foraminifera, *Uvigerina jacksonensis*, was used for both stable isotopic and trace metal analyses (Mg/Ca). In the interval 216 feet (~65.8 m) to 120 feet (~36.6 m), $\delta^{18}O$ values are roughly constant at ~ -0.7 ‰ before shifting to more positive values of -0.19 to -0.59 ‰ above 114 feet (~34.7 m). Values of benthic foraminifera test Mg/Ca across the interval analyzed – between 216 feet (~65.8 m) and 62 feet (~18.9 m) – are more stable, with an average value of 3.54 mmol/mol. There is a marked shift to a much higher Mg/Ca value, of 4.61 mmol/mol, in the topmost sample, at 62 feet (~18.9 m). Bottom water temperatures are estimated using the *O. umbonatus* temperature calibration of Lear et al., (2002), with estimated seawater Mg/Ca of 4 mol/mol. These temperatures are relatively stable, from 11.9 ºC to 14.3 ºC but then shift up to 15.5 ºC at 62 feet (~18.9 m). These values were then combined with benthic foraminifera $\delta^{18}O$, from the same species and sample, to estimate seawater $\delta^{18}O$. The benthic foraminiferal calcite $\delta^{18}O$ to temperature relationship used is a linear form of the Kim and O'Neil equation used above for planktonic foraminifera. Between ~250 feet (~76.2 m) and 100 feet (~30.5 m), these estimates are between -1.0 and -1.5 ‰, but then show a significant shift above 100 feet (~30.5 m) towards more positive values, reaching a maximum of -0.56 ‰ at 62 feet (~18.9 m).

4.4 Discussion

4.4.1 Coccolith-fraction stable isotope stratigraphy and environmental interpretation

The clearest signals in all the available geochemical data from the Mossy Grove core are the two distinct transient shifts to negative $\delta^{13}C$ and $\delta^{18}O$ within the coccolith fraction bulk isotope records. The largest of these transients, above ~300 feet (~91.4 m), shows a major negative excursion of over 2 ‰ in both $\delta^{13}C$ and $\delta^{18}O$. The second is more muted, but again has closely coupled negative perturbations in both $\delta^{13}C$ (~1.5 to 2 ‰ excursion) and $\delta^{18}O$ (~1 ‰ excursion), centered on ~144 feet. Within the context of the EOT, two interpretations for this data are likely.

First, is that the biostratigraphy of the Mossy Grove core is slightly in error, and these two shifts represent the first and second step of the EOT itself. Although these are known to consist of two positive isotope shifts, in both $\delta^{13}C$ and $\delta^{18}O$, there are indications that the onset of the first step in the EOT is preceded by a negative transient excursion in both stable isotope systems (Coxall et al., 2005). This, potentially global transient, could then also be amplified by the effect of sea level fall during both steps, which could modify the global positive signal, into a negative transient followed by small positive isotopic shift, if the effects of increasing freshwater (low $\delta^{13}C$ and $\delta^{18}O$), erosion of terrestrial carbon (low $\delta^{13}C$) and local warming with sea level fall (trend to lower $\delta^{18}O$ in biogenic calcite) outweighed the global signal. If this is the case, then both the the *Hantkenina* and multi-rayed discoaster extinction horizons are placed somewhat too high – the former being placed at 106 feet (~32.3 m) and the later at ~164 feet (~50 m). In previous studies of the EOT in low latitude locations, the discoaster extinction is found before the first step and the *Hantkenina* extinction with the plateau phase between the two steps (Pearson et al., 2008). If the coccolith fraction isotope

excursions represent the two steps of the EOT in the Mossy Grove succession, then the top of the multi-rayed discoasters would be expected below ~290 feet (~88.4 m), and the top of *Hantkenina* spp. below ~145 feet (~44.2 m). In relatively shallow shelf sections, this mismatch could be explained by reworking, especially during a major sea level regression. This interpretation is supported by the absence or very low abundance of both calcareous nannofossil and planktonic foraminifera taxa concerned immediately below their picked topmost occurrence. However, even given the potential for reworking, the mismatches seem large, and there is good evidence for higher abundances of *Hantkenina* spp at and below 142 feet (~43.2 m), and multi-rayed discoasters below ~263 feet (~80.2 m). If these are the true tops of each, both would still be somewhat offset too young relative to the isotope stratigraphy.

The second interpretation, which is more consistent with the available biostratigraphy, is that the first major negative shift in bulk isotope values is associated with the late Eocene Chesapeake Bay impact event (~35.3 Ma). Microspherules have been reported from foraminiferal residues within the Mossy Grove core, at a depth of 308 feet (~93.9 m) (Fluegeman et al., 2009), which is close to, although still preceding, the base of the first major negative isotopic excursion. The magnitude of the negative isotopic excursion, and the association with a dramatic and prolonged decline in abundance of planktonic foraminifera, indicate a major perturbation of local seawater isotopic composition and environments. In this scenario, negative shifts in fine fraction coccolith calcite $\delta^{13}C$ and $\delta^{18}O$ would be driven by extensive terrestrial erosion due to the loss of vegetation across the eastern North American continent, through impact induced burning and/or local transient climate shock. In this second scenario, the two-step transition through the EOT interval is most likely represented by the moderate positive shift in $\delta^{18}O$ at 190 feet (~57.9 m) to 175 feet (~53.3 m) followed by the

positive shift in $\delta^{13}C$ at 145 feet (~44.2 m) to 135 feet (~41.1 m). Although coccolith-fraction $\delta^{18}O$ does not show a significant shift at this second level, there is a systematic positive trend in benthic $\delta^{18}O$ above ~120 feet (~36.6 m). At present the limited stratigraphic coverage of paired benthic foraminiferal $\delta^{18}O$-Mg/Ca data makes the shift difficult to place in context – there could be larger positive shifts in benthic $\delta^{18}O$ through the excursion intervals in coccolith fraction isotope data noted above, that would be consistent with the EOT, but data is currently not available in this interval.

Although significant caution should be employed in making inferences about SSTs from bulk $\delta^{18}O$ isotope data, it is notably that these values through the lower part of the core show no long-term shift towards more positive values, which could be indicative of significant cooling prior to the EOT. This contrasts with the interpretation of the nannofossil assemblage data in Chapter 3, which does indicate a shift to more temperate-water taxa between ~ 370 feet (~112.8 m) and 300 feet (~91.4 m). As with coccolith fraction $\delta^{18}O$, nannofossil assemblages are also not direct proxies of SSTs. In this case either could be subject to other influences that either damp or create a false cooling signal during this interval. The resolution of this issue awaits independent SST data, such as TEX_{86} proxy data – which although problematic for absolute values, is useful in documenting the dynamics and direction of change of SSTs. Late Eocene palaeotemperature reconstructions are important because they may indicate the preconditioning and proximal causes of the more rapid EOT (Scher et al., 2011).

4.4.2 Palaeotemperature estimation through the late Eocene and EOT

Marine palaeotemperature estimates come from three sources: for sea surface temperatures (SSTs) from planktonic foraminifera $\delta^{18}O$ and TEX_{86} estimates; and benthic foraminifera $\delta^{18}O$ and Mg/Ca palaeothermometry. All of these are remarkably stable through the various intervals for which data is available. Although these data are limited by being pilot studies (TEX_{86}), limited by the abundance of planktonic foraminifera, or only targeted to the upper part of the core (benthic foraminifera), together they give a consistent pattern of relatively stable temperatures through the upper ~250 feet (~76.2 m) of the cored interval. This is actually consistent with the nannofossil assemblage data, where the major shift from warm to more temperate assemblages happens at depths greater than 300 feet (~91.4 m), or near the very top of the core <100 feet (~30.5 m).

Absolute temperature values derived for bottom waters of 12-13ºC, and mixed-layer SSTs from planktonic foraminiferal isotopes of ~21ºC, indicate a water column temperature gradient of ~8-9ºC. It should be noted that these $\delta^{18}O$-derived SSTs are significantly cooler, by >5 ºC, than associated TEX_{86}^{H} SSTs through the same interval. This data supports the suggestion that TEX_{86}^{H} estimates of Paleogene SSTs give values that are consistently too warm compared to other proxy data (Dunkley Jones et al., 2013; Taylor et al., 2013). Reconciling these differences in proxy SST estimation is an area of ongoing active research, and this and further data from the Mossy Grove core will be useful in contributing to future comparisons of proxies behaviour from successions through the Paleogene.

Chapter 5

The Eocene/Oligocene Transition on the US Gulf Coastal Plain

5.1 Introduction

The late Eocene is considered as a time of global cooling prior to the onset of major Antarctic glaciation across the EOT (Zachos et al., 2001). The dynamics and magnitude of this cooling, including whether there was any major cooling event immediately prior to the triggering of glaciation is still poorly known. Associated with this is the potential role of late Eocene impact events in accelerating any cooling trend driven by a decline in atmospheric greenhouse gas concentrations (Pagani et al., 2011). The effect of both of these events on sub-tropical marine ecosystems is also poorly known. Although the EOT clearly marks a major decline in long-term diversity trends in both calcareous nannofossils (Bown, 2005b) and planktonic foraminifera (Ezard et al., 2011), the relative impact of cooling, sea level, productivity changes and late Eocene impact events cannot be resolved with this long-term, multi-million year record through the Cenozoic. In this thesis I have developed new records of the assemblages of calcareous nannofossil preserved in a continuous succession of the Yazoo Clay, recovered in the Mossy Grove Core, near Jackson, Mississippi. These demonstrate the presence of very well-preserved to exceptionally well-preserved nannofossils within this clay-rich succession. I have used these to document the taxonomy of these late Eocene assemblages as discussed in Chapter 2. These assemblages also proved an excellent opportunity to develop detailed assemblage records of ecological variability through this critical interval of the late Eocene. These assemblage data are combined with a range of

geochemical climate proxy data to constrain aspects of the marine environment of the US Gulf Coast through the late Eocene and into the EOT.

5.2 The Eocene-Oligocene Transition boundary at Mossy Grove

The initial stratigraphy of the Yazoo Clay recovered within the Mossy Grove Core, based on the planktonic foraminifera assemblages and radiometric dating of bentonite layers, placed the Eocene / Oligocene boundary, as defined by the top of *Hantkenina* spp., at the top occurrence of *H. alabamensis* at 120 ft (Fluegeman, 2003; Fluegeman et al., 2009). This position was supported by of the top occurrence of *Turborotalia cocoaensis* and *Turborotalia cerroazulensis* at 96ft, whose extinctions are also associated with the EO boundary (Pearson et al., 2006). Ostracods also show a species turnover in this upper section of the core, above ~100 ft (Yamaguchi et al., 2011). This is also supported by the palynological analysis of Burgess (unpublished MSc Dissertation, University of Birmingham, 2015) which placed the EO boundary in Mossy Grove close to ~87 ft as marked by the tops of *Heteraulacysta porosa* and *Thlassiphora fenestrata* together with an increasing abundance of *Enneadocysta arcuata* occurred above this depth.

In this study, the examination of planktonic foraminifera assemblages showed that *Hantkenina* spp., when present in the Yazoo Clay interval examined (above 338 ft), are always in low to very low abundance. This low abundance is typical of somewhat restricted shelf environments and makes reliable biostratigraphy based on typical pelagic foraminiferal species difficult. The identification of the top occurrence of *Hantkenina* spp. is based on only one observed *H. primitiva* specimen at 106 ft. This level is consistent with the calcareous nannofossil biostratigraphy presented here, as the Eocene/Oligocene boundary should and

does lie between the top of the multi-rayed discoasters, *D. saipanensis* at 164 ft, and the top of *Coccolithus formosus*, which lies above the top of the Yazoo Clay formation recovered in the Mossy Grove core. These biohorizons through the EOT are consistent with the planktonic foraminifera zonation proposed by Fluegeman et al., (2009) and with the patterns of ostracod assemblage change noted by Yamaguchi et al., (2014).

Assuming this biostratigraphy is correct, the bulk coccolith-fraction stable isotope data show major perturbations prior to the main phase of the EOT. In particular, the large negative excursions in both $\delta^{18}O$ and $\delta^{13}C$ in the late Eocene, at around ~290 ft, or ~35.2 Ma based on the biostratigraphic age model, has not previously been recognized in any succession. The magnitude of this event, and its absence, or muted expression in far-field deep-ocean successions (Coxall and Pearson, 2007) strongly indicate that this is due to a regional-scale environmental change, magnified by the sensitivity of the potentially restricted shallow shelf environment of the US Gulf Coast. The close coupling in age with the Chesapeake Bay impact event (~35.3 Ma) and with reported microspherule layers within the Mossy Grove Core at ~308 ft (Fluegeman et al., 2009) are intriguing, and would, at first suggest that this is the primary driver of this transient isotopic excursion. Counter to this, however, are three observations that are hard to reconcile with the observed pattern as a response to an impact horizon. First, the proposed impact horizon somewhat precedes the most rapid phase of the isotope excursion at ~285 ft. Second, there is a prolonged stratigraphic interval that shows a gradual negative shift in the isotopes, especially through the period of cyclicity in $\delta^{13}C$ from ~400 ft to 300 ft, prior to the most rapid phase of the isotope excursion. This suggests that the condition of the system is gradually moving towards this excursion as an end-member event, rather than this being completely driven by an external, stochastic impact on the system. Third, the timescales of recovery of this perturbation, which persists up to ~250 ft and is on

the order of 200-300 ka based on the biostratigraphic age model, are long if this perturbation is purely regional / continental in scale. For comparison, recovery from the major global perturbation to the carbon cycle at the Paleocene Eocene Thermal Maximum (PETM), was largely complete within ~100 ka (Bowen et al., 2015), whilst recovery time at the end Cretaceous mass extinction was on the order of 500 ka (Norris et al., 2013).

If this is not the first step of the EOT, or directly related to the Chesapeake Bay impact, it would suggest that there is a significant precursor climatic event prior to the onset of the EOT, and that this is represented by the isotopic shift in the Mossy Grove core, as well as the loss of planktonic foraminifera and dinoflagellates within the same interval, and an increase in terrestrial derived fern spores (Burgess, MSc 2015; Marcelo Mota pers. comm.). The loss of pelagic microfossils and increase in terrestrial-derived material indicates a shoaling, sea-level fall event. As argued for the EOT, this could also drive a shift to more *negative* $\delta^{13}C$ and $\delta^{18}O$, associated with the local effects of freshwater and terrestrial organic matter input. Candidates for a large late Eocene sea-level lowering, prior to the onset of the EOT, include evidence of valley down-cutting in Egypt, at ~36 to 35.8 Ma (Peters et al., 2010). This is older than the estimated age of the Mossy Grove event, but correlation between these two successions is subject to some uncertainty, and awaits a full tuning and correlation of bulk isotopes and new XRF data from Mossy Grove to unpublished reference curves from the deep ocean (Expedition 320, Wilson et al., in prep; Expedition 342, Bohaty et al., in prep). There is also evidence for some short term climate variability, including potential precursor transient glacial events from Southern Ocean isotopic (Scher et al., 2014; Scher et al., 2011) and biotic records (Persico and Villa, 2004). The data from Mossy Grove, once tied into the deep-ocean stratigraphy, could be the first clear evidence from the low latitudes of the magnitude of these events – in terms of global eustatic sea level fall – and hence provide a

discrimination between ocean cooling and ice volume expansion in existing late Eocene $\delta^{18}O$ from the Southern Ocean (Persico and Villa, 2004; Scher et al., 2014).

With either interpretation of the Mossy Grove stratigraphy, the entire main phase of the EOT is represented within the Mossy Grove core. Further, regardless of the exact positioning of the two steps of the EOT, the long-term patterns of the bulk coccolith-fraction isotope records are clearly influenced by a combination of global seawater isotopic signals – positive shifts of up to 1 ‰ in both $\delta^{13}C$ and $\delta^{18}O$ (Coxall et al., 2005) – with local sea-level controlled effects that tend to drive both stable isotope systems towards negative values during intervals of sea-level fall. This later effect is likely a combination of changing seawater isotopic composition (water and dissolved inorganic carbon) due to increased freshwater and terrestrial-derived organic carbon flux – with negative $\delta^{18}O$ and $\delta^{13}C$ respectively - into the Mississippi embayment. With sea level fall, there is also the potential for local seawater warming, or at least the damping of any wider planetary cooling associated with the onset of Antarctic glaciation. Evidence for little temperature change, or even warming, comes from the planktonic and benthic foraminifera geochemical records and TEX_{86} temperature proxies. For example the stable isotopic composition of the lower mixed-layer dwelling (Wade & Pearson 2008) *Turborotalia ampliapertura* and *T. increbescens* are similar in late Eocene and early Oligocene. TEX_{86} SST data supports this stability between ~239 ft and 139 ft, with the only change being a *warming* into this interval from the lowermost data point at 259 ft. Benthic foraminifera trace metal data also indicate no cooling up-section through the interval studied, but if anything a slight warming of bottom waters in the earliest Oligocene.

5.3 Phytoplankton changes during the EOT

The EOT has been associated with significant shifts in coccolithophore assemblages on long-time scales (Bown, 2005a), in the high latitudes (Persico and Villa, 2004) and the tropics (Dunkley Jones et al., 2008). It is also closely coupled with a major extinction event in the planktonic foraminifera (Wade & Pearson 2008; Pearson et al. 2008) and a large species turnover of radiolarian (Funakawa et al., 2006). In general, these extinctions and assemblage changes are consistent with a widespread change in upper ocean thermal structure and productivity regimes, marked by a shift from higher diversity, specialist flora and faunas to lower diversity and more cosmopolitan assemblages in the earliest Oligocene (Funakawa et al., 2006; Dunkley Jones et al., 2008; Pearson et al., 2008).

This research project made use of well-preserved and abundant calcareous nannofossil assemblages, preserved in the continuously deposited Yazoo Clay Formation of the Mossy Grove core, to quantify assemblage changes within the northern sub-tropics through the late Eocene and EOT. This draws upon existing work that has associated late Eocene calcareous nannofossil assemblages with patterns of surface ocean temperature, nutrient availability and other environmental parameters (e.g. Gibbs et al., 2006; Kalb and Bralower, 2012; Villa et al., 2014). Variations in calcareous nannofossil assemblages in the Mossy Grove core been documented by the relative abundance of taxa, diversity metrics for the combined assemblage and the use of multivariate statistical analyses to extract general trends that are expressed in the behavoiur of more than one taxa (Chapter 3). In summary, calcareous nannofossil assemblages across the EOT itself show relatively little change. Instead there is a prominent decline in the abundance of warm-water taxa, and associated increase in more temperate and cool-water taxa, prior to the EOT, between ~400 ft and 300 ft, in the late Eocene Yazoo Clay.

Warm-water taxa that decline in abundance include discoasters, holococcoliths, helicosphaerids, sphenoliths and *Coccolithus formosus*. This trend, and the taxa affected, are consistent with global biogeographic studies and existing assemblage data across the broader late Eocene to early Oligocene transition (Wei and Wise, 1990; Tremolada & Bralower 2004; Gibbs, N. J. Shackleton, et al., 2004; Villa et al., 2008; Dunkley Jones et al., 2008; Bordiga et al., 2015; Villa et al., 2014; Fioroni et al., 2015). The timing of this assemblage shift within the Mossy Grove core, is however, distinct from tropical locations where assemblage changes are closely coupled to the EOT (Dunkley Jones et al., 2008). Instead, the change in assemblage prior to the EOT, has similarities with the longer-term assemblage shifts from warm-water to cool-water assemblages in the high latitudes through the late Eocene (Persico and Villa, 2004).

Through the EOT and into the earliest Oligocene, this trend of loss in abundance of warm-water taxa continues, although there is a distinction between known warm-water taxa that show large declines (e.g. discoasters, holococcoliths) and others that show more moderate declines (e.g. *Sphenolithus* and *Helicosphaera* spp.). Here, this is interpreted to represent the combined effects of some cooling, mostly towards the base of the Mossy Grove core prior to the EOT, with the effects of sea level fall and potential increase in nutrient availability across the EOT itself. We propose the latter effect causes the difference in response between warm-water taxa with an open-water, oceanic preference (discoasters, holococcoliths), which decline through the EOT, and those with more tolerance to more marginal and higher nutrient conditions (e.g. *Sphenolithus* and *Helicosphaera* spp.). This is supported by past studies that identify *Sphenolithus* and *Helicosphaera* as warm-water genera (Wei & Wise 1990), where *Sphenolithus* adaptable in mesotrophic/eutrophic conditions (Dunkley Jones et al., 2008;

Wade and Bown, 2006), whilst *Helicosphaera* is related to warm surface waters and near-shore environment (Bukry et al., 1971; Krhovský et al., 1993).

Taxa that increase in abundance through the EOT in the Mossy Grove core are broadly considered to have a temperate- or cool-water preference, including; *Reticulofenestra daviesii, Pontosphaera multipora* and *Isthmolithus recurvus. Reticulofenestra daviesii* in particular shows a notable increase after the EOT, and is one of the key cool-water taxa identified in Southern Ocean ODP Sites 689 (Persico & Villa 2004) and 748 (Villa et al., 2008). Therefore is widely considered as a cold-water species with some eutrophic affinity (Perisco and Villa, 2004; Villa et al., 2008; 2014; Fioroni et al., 2015). The peak in abundance of *R. daviesii* in the earliest Oligocene of the Mossy Grove core, indicates the potential for a second phase of cooling towards the very top of the Yazoo Clay, stratigraphically above the range of the available SST proxies (Chapter 4). Associated with this, is an increase in abundance of *Pontosphaera multipora*, which may also have temperate to cool-water affinities. The other well-documented temperate- to cool-water taxon within the Mossy Grove assemblages, *Isthmolithus recurvus* (Wei &Wise, 1990; Persico & Villa 2004), does not dramatically increase in abundance across the EOT, but rather appears and then increases in abundance during the major shift in nannofossil assemblage in the late Eocene prior to the EOT.

5.4 Comparison with ostracod assemblages and palynology from the Mossy Grove core

In contrast to the calcareous nannofossil assemblages, ostracod assemblages show a significant turnover during EOT, with an extinction of ~50% at the species level, which mainly occurred in EOT-1 and EOT-2 rather than the Oi1 (Oxygen Isotope event 1) and associated with glacioeustatic sea level changes (Yamaguchi et al., 2014). Fourteen species

disappeared between the upper Eocene and lower Oligocene successions in the Mossy Grove core. Ten species disappeared between 33.96 and 33.81 Ma (~67 feet to 91 feet), two others have last occurrences before 34.18 Ma (~111 to 123 feet) and two others survived during the EO event. These extinctions appear to be associated with sea level fall through the EOT, and prior to the early Oligocene glacial maximum, by which time there is some repopulation by taxa that temporarily disappear through the EOT (Figure 5.1). This pattern of ostracod assemblage change is similar to that of benthic foraminifera in Mossy Grove core (Fluegeman et al., 2003), where four species of benthic foraminifers disappeared between 33.90 Ma and 33.83 Ma (~67 feet to 91 feet). Initial palynomorph studies are more similar in response to the calcareous phytoplankton, with no significant turnover through the EOT, but longer-term more gradual changes through the succession (Burgess, MSc 2015). Taken together this suggests that sea level fall through the EOT impacted bottom water communities, whilst was not of such significant magnitude through the EOT itself to dramatically change surface water environments. Instead, surface water environments experienced more change in the late Eocene prior to the onset of the EOT, as shown in PCA analyses of calcareous nannofossil assemblages, with a dramatic shift in PC2 between 400 feet and 300 feet, which at 300 feet is associated with a rapid influx of inner shelf palynomorphs and the loss of planktonic foraminifera (Burgess, MSc 2015) (Figure 5.1). There is a shallowing signal in ostracod assemblages at the same time, and together would support the presence of a significant transient glacial event in the late Eocene, prior to the accepted onset of the EOT (Peters et al., 2010).

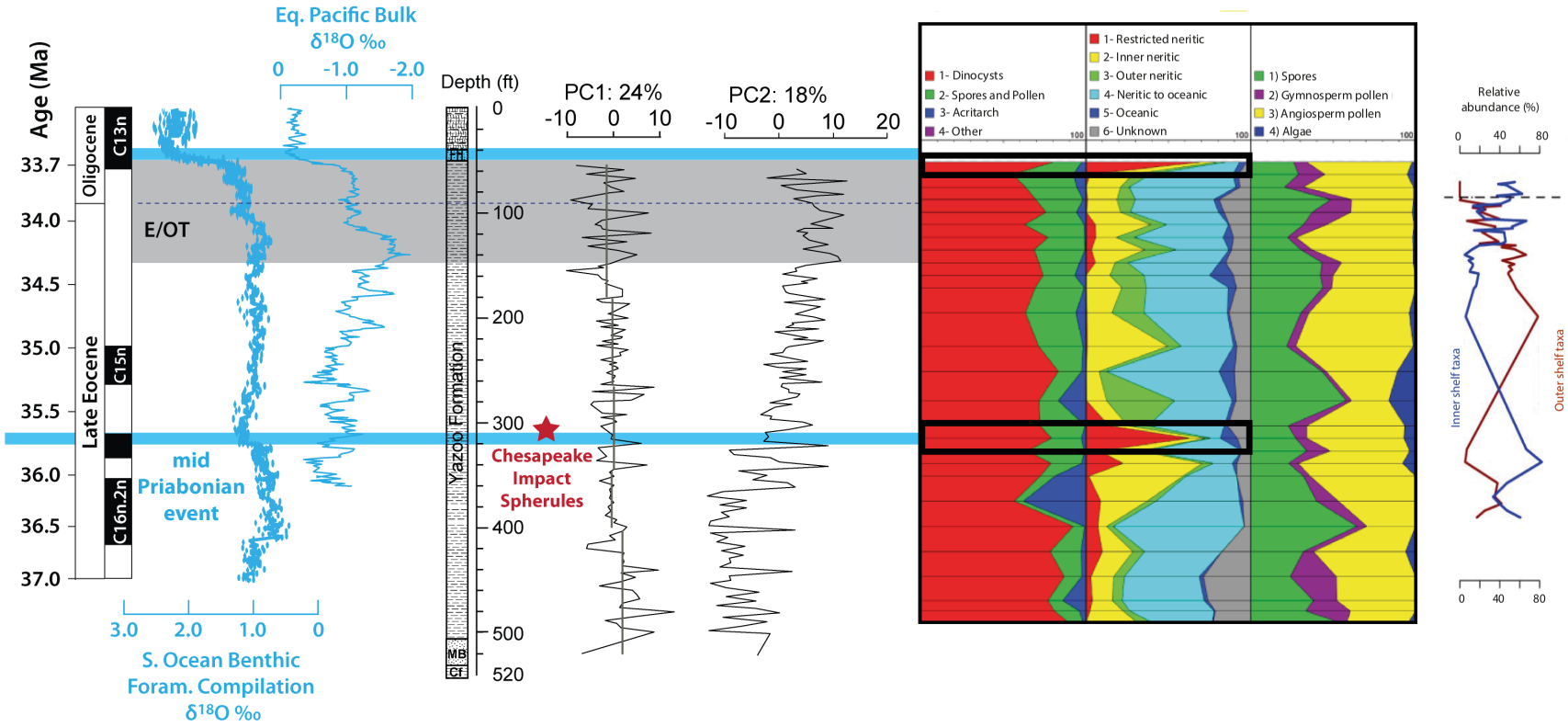


Figure 5.1: The compilation data of the PCA analysis from calcareous nannofossil and the palynology data from Burgress 2015, which been correlated with the EOT and Priabonian event from Southern Ocean compilation and Pacific Ocean, together with ostracod data by Yamaguchi et al., 2014.

Chapter 6

6.1 Conclusion

This study documents the calcareous nannofossil assemblages, assemblage changes, and a range of geochemical palaeoenvironmental proxy data, through the late Eocene and Eocene/Oligocene Transition recovered in the Mossy Grove Core, western Mississippi. The calcareous nannofossil assemblages of the late Eocene show a distinct shift through this interval, which is interpreted as representing the increasing influence of more temperate and higher productivity conditions within this sub-tropical shelf sea environment. The progression is most marked *before* the main phase of the EOT, in the latest Eocene, with a shift from more tropical and oligotropic taxa towards temperate and cool-water taxa. After this there is relatively minor change through the EOT itself, although there is a further shift to cool-water species (e.g. *Reticulofenestra daviesii*) in the earliest Oligocene. Calcareous nannofossil taxa have been assigned to major palaeoecological groups based on the patterns of coordinated change through this section, including multi-variate analyses, and through a consideration of their late Eocene biogeography. The two most notable cool water taxa, *R. daviesii* and *I. recurvus* are clearly associated with temperate to cool-water conditions, based on extensive studies of biogeography and their abundance patterns in high-latitudes during the late Eocene to early Oligocene cooling phase (Wei & Wise 1990;Persico & Villa 2004; Villa & Persico 2006; Villa et al., 2014; Fioroni et al., 2015). In this section, there is a temporal offset in response between these two species, with a marked increase in *I. recurvus* abundance in the late Eocene, whilst *R. daviesii* remains in low abundance until the earliest Oligocene. This is consistent with progressive cooling, as *R. daviesii* and *I. recurvus* reach peak abundance at high-latitudes and mid-latitudes respectively (Villa & Persico 2006). On the basis of a similar

response to *R. daviesii, P. multipora* is proposed to have similar temperate and cool-water affinities. By contrast, warm water generally oceanic taxa, even though following the general trends of declining towards the EOT, are also impacted by eustatic sea level changes. The abundance of discoasters in the Mossy Grove sediments, for example, are low compared to open ocean sites (Wei & Wise, 1990), which is presumed to be related to the relatively shallow shelf palaeoenvironment. On the other hand, sphenoliths and *Helicosphaera* spp. are proposed to be more tolerant of higher nutrient conditions in shallow shelf environments due to their higher abundance and persistence through the succession.

The interpretation of coccolith-fraction stable isotope data is complex, and is not fully resolved. These data show two prominent negative transient excursions in $\delta^{13}C$ and $\delta^{18}O$, followed by less pronounced shifts to more positive values. These could be correlated with the standard two-step isotopic transition through the EOT, associated with a two-phase growth of the Antarctic ice sheet (Coxall et al., 2005). This correlation would require that the initial planktonic foraminiferal biostratigraphy of Mossy Grove core is slightly in error, with the recovered interval spanning less of the late Eocene than initially reported (i.e. being a more expanded section). The higher than expected placement of both the biohorizon top of *Hantkenina* spp. and the multi-rayed discoasters (Pearson et al., 2008) could be explained by reworking within the major regression across the EOT. This is possible as both groups are present at very low abundance throughout the succession, making the separation of genuine and reworked occurrences very difficult. The other evidence of reworking is the occurrence of few late Cretaceous to middle Eocene taxa, *C. margereli, Bomolithus* sp. and *D. spinescens.* The Mesozoic survivor *C. margereli* was ranged from middle Jurassic to early Palaeocene, *Bomolithus* sp. aged from middle Palaeocene to early Eocene, whilst the age of *D.*

spinsescens is middle Eocene. The negative transients in both $\delta^{13}C$ and $\delta^{18}O$ of coccolith fraction carbonates are also most likely related to local sea level fall, with the increased flux of relatively negative $\delta^{13}C$ terrestrially-derived organic material and the increased influence of fresh (more negative $\delta^{18}O$) water in this shallow shelf environment. An alternative interpretation, which is more consistent with initial biostratigraphy, is that the negative first shift of bulk isotope reflected the late Eocene Chesapeake Bay impact event (~35.3 Ma). This is suggested by the reported (but not figured or evidenced) presence of microspherules in foraminiferal residue around the start of the first negative isotope shift (Fluegeman et al., 2009).

Geochemical-based paleotemperature estimations, suggest the US Gulf Coast sea surface temperatures are on the order of ~21ºC based on the $\delta^{18}O$ isotopic values of mixed-layer planktonic foraminifera. Benthic foraminifera $\delta^{18}O$ isotopic values indicate temperatures of 12-13ºC for local bottom waters, with a water column temperature gradient of ~8-9ºC. On the other hand, SSTs derived from the organic biomarker proxy TEX_{86}^{H}, indicate SSTs >5ºC warmer during the same interval. This is consistent with growing evidence that Paleogene SST's derived from TEX_{86}^{H} are consistently too warm compared to other proxy data (Dunkley Jones et al., 2013; Taylor et al., 2013)

6.2 Recommendation for future study

Directions for future research include the further development of geochemical proxy data to generate fuller coverage across the stratigraphy with multi-proxy temperature data. In particular, a high-resolution study of SST proxies derived from TEX_{86}^{H}, would be of high

value, in determining the patterns of late Eocene sub-tropical cooling prior to the onset of Antarctic glaciation. This should be integrated with an improved stratigraphic scheme that should be possible with the correlation of the high-resolution Mossy Grove isotope record to similar deep-ocean records, once they become available, from the eastern Equatorial Pacific (IODP Expedition 320) and Newfoundland (IODP Expedition 342).

REFERENCES

Agnini, C. et al., 2014. Biozonation and biochronology of Paleogene calcareous nannofossils from low and middle latitudes. *Newsletter on Stratigraphy*, 47(2): 131-181.

Alegret, L. et al., 2008. Effects of the Oligocene climatic events on the foraminiferal record from Fuente Caldera section (Spain, western Tethys). *Palaeogeography, Palaeoclimatology, Palaeoecology*, 269(1–1): 94–102.

Anagnostou, E. et al., 2016. Changing atmospheric CO2 concentration was the primary driver of early Cenozoic climate. *Nature*, 533: 380-384.

Aubry, M.-P., 1986. Palaeogene calcareous nannofossil biostratigraphy of northwestern Europe. *Palaeogeography Palaeoclimatology Palaeoecology*, 55: 267-334.

Backman, J., 1978. Late Miocene - Early Pliocene nannofossil biochronology and biogeography in the Vera Basin, SE Spain. *Stockholm Contributions in Geology*, 32: 93-114.

Bemis, B., Spero, H., Bijma, J., and Lea, D., 1998, Reevaluation of the oxygen isotopic composition of planktonic foraminifera: Experimental results and revised paleotemperature equations. *Paleoceanography*, 13(2):150-160.

Billard, C. & Inouye, I., 2004. What is new in coccolithophore biology? *In: J.R. Young and H.R. Thierstein (Editors), Coccolithophores: From molecular process to global impact. Springer, Berlin,* 1–29.

Bohaty, S.M. & Zachos, J.C., 2003. Significant Southern Ocean warming event in the late middle Eocene. *Geology*, 31(11): 1017–1020.

Bolton, C.T. and Stoll, H., 2013. Late Miocene threshold response of marine algae to carbon dioxide limitation. *Nature,* 500: 558-562.

Boudreaux, J.E. & Hay, W.W., 1969. Calcareous nannoplankton and biostratigraphy of the late Pliocene-Pleistocene-Recent sediments in the Submarex cores. *Revista Española de Micropaleontología*, 1(3): 249-292.

Bowen, G. J. et al., 2015, Two massive, rapid releases of carbon during le onset of the Palaeocene-Eocene thermal maximum. *Nature Geoscience*, 8(1); 44-47.

Bown, P.R. & Dunkley Jones, T., 2006. New Paleogene calcareous nannofossil taxa from coastal Tanzania: Tanzania Drilling Project Sites 11 to 14. *Journal of Nannoplankton Research*, 28(1): 17-34.

Bown, P.R. & Dunkley Jones, T., 2012. Calcareous nannofossils from the Paleogene equatorial Pacific (IODP Expedition 320 Sites U1331-1334). *Journal of Nannoplankton Research*, 32(2): 3-51.

Bown, P.R. et al., 2008. A Paleogene calcareous microfossil Konservat-Lagerstätte from the Kilwa Group of coastal Tanzania. *Bulletin of the Geological Society of America*, 120(1): 3–12.

Bown, P.R. et al., 2009. A Paleogene record of extant lower photic zone calcareous nannoplankton. *Palaeontology,* 52(2): 457-469.

Bown, P.R. et al., 2004. Calcareous nannoplankton evolution and diversity through time. *In: H.R. Thierstein and J.R. Young (Editors), Coccolithophores: From Molecular Processes to Global Impact. Springer, Berlin*, 481-508.

Bown, P.R., Dunkley-Jones, T. & Young, J.R., 2007. Umbilicosphaera jordanii Bown 2005 from the Paleogene of Tanzania: confirmation of generic assignment and a Paleocene origination for the family Calcidiscaceae. *Journal of Nannoplankton Research*, 29(1): 25-30.

Bown, P.R. & Young, J.R. 1998. Techniques. In: P.R. Bown (Ed.). Calcareous Nannofossil Biostratigraphy. British Micropalaeontological Society Publications Series. Chapman & Hall/Kluwer Academic, London: 16–28.

Bown, P.R., 2005. Selective calcareous nannoplankton survivorship at the Cretaceous-Tertiary boundary. *Geology*, 33(8): 653-656.

Bown, P., 2005, Calcareous nannoplankton evolution: a tale of two oceans. *Micropaleontology,* 51(4): 299.

Bramlette, M.N. & Riedel, W.R., 1954. Stratigraphic value of discoasters and some other microfossils related to Recent coccolithophores. *Journal of Paleontology*, 28: 385-403.

Bramlette, M.N. & Sullivan, F.R., 1961. Coccolithophorids and related nannoplankton of the Early Tertiary in California. *Micropaleontology*, 7: 129-188).

Bramlette, M.N. & Wilcoxon, J.A., 1967. Middle Tertiary calcareous nannoplankton of the Cipero section, Trinidad, W.I. Tulane Studies in Geology and Paleontology, 5: 93-131.

Bronnimann., P. & Stradner, H., 1960. Die Foraminiferen- und Discoasteriden-zonen von Kuba und ihre interkontinentale Korrelation. *Erdoel-Zeitschrift ffd Bohr- und Foerdertechnik*, 76: 364-369.

Bukry, D. & Bramlette, M.N., 1968. Stratigraphic significance of two genera of Tertiary calcareous nannofossils. *Tulane Studies in Geology and Paleontology*, 6: 149-155.

Bukry, D. & Percival, S.F., 1971. New Tertiary calcareous nannofossils. *Tulane Studies in Geology and Paleontology*, 8: 123-146.

Bukry, D., 1971. Cenozoic calcareous nannofossils from the Pacific Ocean. *San Diego Society of Natural History Transactions*, 16: 303-327.

Bukry, D., 1973. Coccolith stratigraphy, eastern equatorial Pacific, Leg 16, Deep Sea Drilling Project. *Initial Reports of the Deep Sea Drilling Project,* 16: 653-711.

Burgess, R., 2015. Analysis of the palynomorph assemblage through the Eocene/Oligocene transition within the Mossy Grove core, Mississippi. *Master dissertation-unpublished*.

Coccioni, R. et al., 2000. Marine biotic signals across a late Eocene impact layer at Massignano, Italy: Evidence for long-term environmental perturbations? *Terra Nova*, 12(6): 258–263.

Coxall, H.K. et al., 2005. Rapid stepwise onset of Antarctic glaciation and deeper calcite compensation in the Pacific Ocean. *Nature*, 433(January): 53–57.

Coxall, H.K. and Pearson, P.N., 2007. The Eocene-Oligocene transition. In: M. Williams, A.M. Haywood, J. Gregory and D.N. Schmidt (Editors), Deep-time perspectives on climate change: Marrying the signal from computer models and biological proxies. *The Micropalaeontological Society Special Publication*, 351-387.

Cramer, B.S. et al., 2011. Late Cretaceous-Neogene trends in deep ocean temperature and continental ice volume: Reconciling records of benthic foraminiferal geochemistry (δ18O and Mg/Ca) with sea level history. *Journal of Geophysical Research*, 116(C12023):

Cros, L. et al., 2000. New example of holococcolith-heterococcolith combination coccospheres and their implication for coccolithophorid biology. *Marine Micropaleontology*, 39: 1–34.

Cushing, E.M., Boswell, E.H., Hosman, R.I. 1964. General Geology of the Mississippi Embayment. *Geological Survey Professional paper*, 448-B:1-27.

DeConto, R.M. & Pollard, D., 2003. Rapid Cenozoic glaciation of Antarctica induced by declining atmospheric CO2. *Nature*, 421(2001): 245–249.

de Kaenel, E. & Villa, G., 1996. Oligocene-Miocene calcareous nannofossil biostratigraphy and paleoeecology from the Iberian Abyssal Plain. *Proceedings of the Ocean Drilling Program. Scientific Results*, 149: 79-145.

Deflandre, G. & Fert, C., 1954. Observations sur les coccolithophoridho actuels et fossiles en microscopie ordinaire et éet naire et. *Annales de Pal Patologie*, 40: 115-176.

Deflandre, G., 1947. Braarudosphaera nov. gen., type d'une famille nouvelle de Coccolithophorides actuels a elements composites. *Comptes Rendus Hebdomadaires des Séances de l'Académie des Sciences. Paris*, 225: 439-441.

Deflandre, G., 1952. Classe des Coccolithophoridho. (Coccolithophoridae. Lohmann, 1902). *Traite de Zoologie.* Masson, Paris, 439-470.

Deflandre, G., 1959. Sur les nannofossiles calcaires et leur systtsysttst. *Revue de Micropaleontologie*, 2: 127-152.

De Vargas, C. et al., 2007. Origin and evolution of coccolithophores: from coastal hunters to oceanic farmers. *In: P.G. Falkowski and A.H. Knoll (Editors), Evolution of primary producers in the sea. Elsevier Academic Press, Amsterdam, Boston*, 251-287.

Diester-Haass, L. & Zahn, R., 1996. Eocene-Oligocene transition in the Southern Ocean: History of water mass curculation and biological productivity. *Geology*, 24: 163-166.

Dockery III, D.. et al., 1991. A continuous core through the undifferenti- ated Yazoo Clay (late Eocene, Jackson Group) of Central Mississippi. *Mississippi Geology*, 12: 23-27.

Dockery III, D., 1997. Windows into Mississippi's Geologic Past. *Mississippi Department of Environmental Quality Office of Geology, Circular 6*. 44-48.

Dunkley Jones, T. et al., 2008. Major shifts in calcareous phytoplankton assemblages through the Eocene-Oligocene transition of Tanzania and their implications for low-latitude primary production. *Paleoceanography*, 23: 1-14.

Dunkley Jones, T., Bown, P.R. & Pearson, P., 2009. Exceptionally well preserved upper Eocene to lower Oligocene calcareous nannofossils (Prymnesiophycidae) from the Pande Formation (Kilwa Group), Tanzania. *Journal of Systematic Palaeontology*, 7(4): 359-411.

Dunkley Jones, T. et al., 2013. Climate model and proxy data constraints on ocean warming across the Paleocene/Eocene Thermal Maximum. *Earth-Science Reviews*, 125: 123-145.

Dupont-Nivet, G. et al., 2007. Tibetan plateau aridification linked to global cooling at the Eocene-Oligocene transition. *Nature*, 445(February): 635–638.

Expedition 320/321 Scientists, 2010. Methods. *In: H. Pälike, M. Lyle, H. Nishi, I. Raffi, K. Gamage, A. Klaus and E. Scientists (Editors)*, *Proceedings of the Integrated Ocean Drilling Program, Tokyo*, 1-80.

Ezard, T.H.G. et al., 2011. Interplay between changing climate and species' ecology drives macroevolutionary dynamics. *Science,* 332: 349-351.

Falkowski, P.G. et al., 2004. The Evolution of Modern Eukaryotic Phytoplankton. *Science*, 305: 354-360.

Field, C.B., et al., 1998. Primary production of the biosphere: integrating terrestrial and oceanic components. *Science,* 281: 237-240.

Fioroni, C. et al., 2015. Middle Eocene-Lower Oligocene calcareous nannofossil biostratigraphy and paleoceanographic implications from Site 711 (equatorial Indian Ocean). *Marine Micropaleontology,* 118: 50–62.

Fluegeman, R.H., 1996. Preliminary paleontological report on the foraminifera of the Mossy Grove core, Hinds County, Mississippi. *Mississippi Geology,*17.

Fluegeman, R.H., 2003. Late Eocene–early Oligocene benthic foraminifera in the Gulf Coast Plain: regional vs global influence. *In D. R. Prothero, L. C. Ivany, & E. A. Nesbitt,*

eds. From Greenhouse to Icehouse: The Marine Eocene–Oligocene Transition. Columbia University Press, 283–293.

Fluegeman, R.H., Grigsby, J.D., Hurley, J.V., 2009. Eocene–Oligocene greenhouse to icehouse transition on a subtropical classic shelf: the Jacksonian–Vicksburg Groups of the eastern Gulf Coastal Plain of the United States, in: Koeberl, C., Montanari, A. (Eds.), The Late Eocene Earth: hothouse, icehouse, and impacts. *The Geological Society of America,* 261–277.

Fluegeman, R.H., 2009. Late Eocene and early Oligocene benthic foraminiferal paleoecology and sequence stratigraphy in the eastern Gulf Coastal Plain, U.S.A. *In: Thomas, D.D., Gary, A.C. (Eds.), Geologic Problem Solving with Microfossils: A volume in honor of Garry D. Jones*, 293–307.

Funakawa, S. et al., 2006. Radiolarian faunal turnover and paleoceanographic change around Eocene/Oligocene boundary in the central equatorial Pacific, ODP Leg 199, Holes 1218A, 1219A, and 1220A. *Palaeogeography, Palaeoclimatology, Palaeoecology*, 230, pp.183–203.

Gallagher, L.T., 1989. Reticulofenestra : A critical review of taxonomy, structure and evolution. *In: Crux, J.A. and Heck, S.E.v. (Editors), Nannofosils and their applications. Ellis Horwood, Chichester*, 41-75.

Gartner, S., 1969. Two new calcareous nannofossils from the Gulf Coast Eocene. *Micropaleontology*, 15: 31-34.

Gartner, S., 1971. Calcareous nannofossils from the JOIDES Blake Plateau cores and revision of the Paleogene nannofossil zonation. *Tulane Studies in Geology and Paleontology*, 8: 101-121.

Gibbs, S.J. et al., 2006. Nannoplankton Extinction and Origination across the Paleocene-Eocene Thermal Maximum. *Science,* 314: 1770-1773.

Gibbs, S., Shackleton, N.J. & Young, J.R., 2004. Identification of dissolution patterns in nannofossil assemblages: a high-resolution comparision of synchronous records from Ceara Rise, ODP Leg 154. *Paleoceanography*, 19 (1): 1-12.

Goldner, A., Herold, N. & Huber, M., 2014. Antarctic glaciation caused ocean circulation changes at the Eocene–Oligocene transition. *Nature,* 519: 574-577.

Gradstein, F.M., Ogg, J.G. & Hilgen, F.J., 2012. On The Geologic Time Scale. *Newsletters on Stratigraphy,* 45(2):171–188.

Gran, H.H. & Braarud, T., 1935. A quantitative study of the phytoplankton in the Bay of Fundy and the Gulf of Maine (including observations on hydrography, chemistry and turbidity). *Journal of the Biological Board of Canada*, 1: 279-467.

Haq, B.U. & Berggren, W.A., 1978. Late Neogene calcareous plankton biochronology of the Rio Grande Rise (South Atlantic Ocean). *Journal of Paleontology*, 52: 1167-1194.

Haq, B.U., 1968. Studies on upper Eocene calcareous nannoplankton from NW Germany. *Stockholm Contributions in Geology,* 18: 13-74.

Haq, B.U., 1966. Electron microscope studies on some upper Eocene calcareous nannoplankton from Syria. *Stockholm Contributions in Geology*, 15: 23-37.

Haq, B.U., 1971. Paleogene calcareous nannoflora. Parts I-IV. *Stockholm Contributions in Geology*, 25: 1-158.

Hay, W.W. & Mohler, H.P., 1967. Calcareous nannoplankton from early Tertiary rocks at Pont Labau, France, and Paleocene-Eocene correlations. *Journal of Paleontology*, 41: 1505-1541.

Hay, W.W. & Towe, K.M., 1962. Electron microscope examination of some coccoliths from Donzacq (France). *Eclogae Geologicae Helvetiae*, 55: 497-517.

Hay, W.W. et al., 1967. Calcareous nannoplankton zonation of the Cenozoic of the Gulf Coast and Caribbean-Antillean area, and transoceanic correlation. *Transactions of the Gulf Coast Association of Geological Societies*, 17: 428-480.

Hay, W.W., Mohler, H.P. & Wade, M.E., 1966. Calcareous nannofossils from Nal'chik (northwest Caucasus). *Eclogae Geologicae Helvetiae*, 59: 379-399.

Haywood, A.M. et al., 2005. Warmer tropics during the mid-Pliocene? Evidence from alkenone paleothermometry and a fully coupled ocean-atmosphere GCM. *Geochemistry Geophysics Geosystems*, 6(3):1-20.

Hemoso, M., Horner, T., Minoletti, F., and Rickaby, R., 2014, Constraints on the vital effect in coccolithophore and dinoflagellate calcite by oxygen isotopic modification of seawater: *Geochemica et Cosmochemica Acta,* 141: 612-627.

Jafar, S.A. & Martini, E., 1975. On the validity of the calcareous nannoplankton genus *Helicosphaera*. *Senckenbergiana lethaea*, 56: 381-397.

Jerkovic, L., 1970. *NoL., 1970. ,* nov. gen. type d'un nouvelle famille de Coccolithophoridor fossiles: NoNoiles: Noorid du MiocMio suppMioc: de Yugoslavie. *Comptes Rendus Hebdomadaires des Sadaires del'Acadadai des Sciences. Paris. SPari D - Sciences Naturelles*, 270: 468-470.

Kalb, A.L. & Bralower, T.J., 2012. Nannoplankton origination events and environmental changes in the late Paleocene and early Eocene. *Marine Micropaleontology*, 92–93: 1–15.

Kamptner, E., 1948. Coccolithen aus dem Torton des Inneralpinen Wiener Beckens. *Anzeiger. n aus dem ckens Akademie der Wissenschaften. Mathematische-Naturwissenschafliche Klasse. Wien*, 157: 1-16.

Kamptner, E., 1963. Coccolithineen-Skelettreste aus Tiefseeablagerungen des Pazifischen Ozeans. *Annalen des Naturhistorischen Museums in Wien*, 66: 139-204.

Katz, M., et al. 2008, Stepwise transition from the Eocene greenhouse to the Oligocene icehouse, *Nature Geoscience*, 1(5): 329-334.

Kennett, J.P., 1977. Cenozoic Evolution of Antarctic Glaciation, the Circum-Antarctic Ocean, and Their Impact on Global Paleoceanography. *Journal of Geophysical Research*, 82(27).

Kennett, J.P. et al., 1975. Cenozoic paleoceanograpy in the southwest Pacific Ocean, Antarctic Glaciation, and the development of the Circum-Antarctic Current. *DSDP Project* 1155–1169.

Kennett, J.P. & Stott, L.D., 1991. Abrupt deep-sea warming, palaeoceanographic changes and benthic extinctions at the end of the Palaeocene. *Nature*, 354: 225–229.

Kim, J.-H. et al., 2010, New indices and calibrations derived from the distribution of crenarchaeal isoprenoid tetraether lipids: Implications for past sea surface temperature reconstructions: *Geochimica et Cosmochimica Acta,* 74(16): 4639-4654.

Kim, J.-H. et al., 2008, Global sediment core-top calibration of the TEX86 paleothermometer in the ocean: *Geochemica et Cosmochemica Acta,* 72: 1154-1173.

Kim, S., and ONeil, J., 1997, Equilibrium and nonequilibrium oxygen isotope effects in synthetic carbonates: *Geochimica et Cosmochimica Acta*, 61(16): 3461-3475.

Klumpp, B., 1953. Beitrag zur Kenntnis der Mikrofossilien des Mittleren und Oberen Eozän. *Palaeontographica A,* 103: 377-406.

Lazarus, D. & Caulet, J.P., 1993. Cenozoic Southern Ocean Reconstructions. *The Antarctic Paleoenvironment: A Perspective on Global Change Antarctic Research Series*, 60:145–174.

Lear, C.H. et al., 2000. Cenozoic Deep-Sea Temperatures and Global Ice Volumes from

Mg/Ca in Benthic Foraminiferal Calcite. *Science,* 287: 269-287.
Lear, C., Rosenthal, Y., and Slowey, N., 2002, Benthic foraminiferal Mg/Ca-paleothermometry: A revised core-top calibration. *Geochimica et Cosmochimica Acta*, 66(19): 3375-3387.
Lear, C.H. et al., 2008. Cooling and ice growth across the Eocene-Oligocene transition. *Geology*, 36: 251–254.
Lemmermann, E., 1908. Flagellatae, Chlorophyceae, Coccosphaerales und Silicoflagellatae. *In: Brandt, K. and Apstein, C. (Editors), Nordisches Plankton. Botanischer Teil. Lipsius & Tischer, Kiel & Leipzig, 1-40.*
Levin, H.L. & Joerger, A.P., 1967. Calcareous nannoplankton from the Tertiary of Alabama. *Micropaleontology*, 13: 163-182.
Levin, H.L. 1965. Coccolithophoridae and related microfossils from the Yazoo Formation (Eocene) of Mississippi. *Journal of Micropaleontology*, 39: 265-272.
Liu, Z. et al., 2009. Global Cooling During the Eocene-Oligocene Climate Transition. *Science*, 323: 1187-1190.
Loeblich, A.R. & Tappan, H., (1978). The coccolithophorid genus Calcidiscus Kamptner and its synonyms. *Journal of Paleontology*, 52: 1390-1392.
Lohmann, H., 1902. Die Coccolithophoridae, eine Monographie der Coccolithen bildenden Flagellaten, zugleich ein Beitrag zur Kenntnis des Mittelmeerauftriebs. *Archiv für Protistenkunde*, 1: 89-165.
Loubere, P., Gary, A. & Lagoe, M., 1993. Sea-bed Biogeochemistry and Benthic Foraminiferal Bathymetric Zonation on the Slope of the Northwest Gulf of Mexico. *Palaios*, 8: 439–449.
Lourens, L. et al., 2005. Astronomical pacing of late Palaeocene to early Eocene global warming events. *Nature*, 435(7045), pp.1083–1087.
Lunt, D.J. et al., C., 2012. A model-data comparison for a multi-model ensemble of early Eocene atmosphere-ocean simulations: EoMIP. *Climates of the Past,* 8: 1229-1273.
Martini, E. & Ritzkowski, S., 1968. Was ist das 'Unter-OligozOl'? Eine Analyse der Beyrich'schen und v Koenen'schen Fassung der Stufe mit Hilfe des fossilen Nannoplanktons. *Nachr Akad Wiss Gottingen; II Mathematisch-Physikalische Klasse*, 13: 231-250.
Martini, E., 1958. Discoasteriden und verwandte Formen im NW-deutschen Eozän (Coccolithophorida). 1. Taxonomische Untersuchungen. *Senckenbergiana lethaea*, 39: 353-388.
Martini, E., 1959. Discoasteriden und verwandte Formen in NW-deutschen Eozzs (Coccolithophorida). 2. Stratigraphische Auswertung. *Senckenbergiana lethaea*, 40: 137-157.
Martini, E., 1965. Mid-Tertiary calcareous nannoplankton from Pacific deep-sea cores. *Colston Papers*, 17: 393-411.
Martini, E., 1971, Standard Tertiary and Quaternary calcareous nannoplankton zonation, in Farinacci, A., ed., *Proceedings of the Second International Conference on Planktonic Microfossils*, 2: 739.
Merico, A., Tyrrell, T., and Wilson, P. A., 2008, Eocene/Oligocene ocean de-acidification linked to Antarctic glaciation by sea-level fall: *Nature,* 452: 979-982.
Miller, K.G. et al., 1998. Cenozoic global sea level, sequences, and the New Jersey Transect: Results From coastal plain and continental slope drilling. *Reviews of Geophysics*, 36(98),: 569.

Miller, K. G., et al. 2008, Eocene-Oligocene global climate and sea-level changes: St Stephens Quarry, Alabama, *Geological Society of America Bulletin*, 120(1/2): 34-53.

Miller, K.G., Wright, J.D., Katz, M.E., Wade, B.S., Browning, J.V., Cramer, B.S., and Rosenthal, Y., 2009, Climate threshold at the Eocene-Oligocene transition: Antarctic ice sheet infl uence on ocean circulation, in Koeberl, C., and Montanari, A., eds., The Late Eocene Earth—Hothouse, Icehouse, and Impacts: *Geological Society of America Special Paper 452*, 169–178.

Müller, C., (1970). Nannoplankton aus dem Mittel-Oligozän von Norddeutschland und Belgien. *Neues Jahrbuch für Geologie und Paläontologie Abhandlungen*, 135: 82-101.

Noël, D., (1965). Sur les Coccolithes du Jurassique Européen et d'Afrique du Nord. *Éditions du Centre National de la Recherche Scientifique*, Paris.

Norris, R. D. et al., 2013, Marine Ecosystem Responses to Cenozoic Global Change: *Science*, 341: 492-498.

Pagani, M. et al., 2005. Marked decline in atmospheric carbon dioxide concentrations during the Paleogene. *Science (New York, N.Y.)*, 309: 600–603.

Pagani, M. et al., 2011. The Role of Carbon Dioxide During the Onset of Antarctic Glaciation. *Science,* 334: 1261-1264.

Pearson, P.N. et al., 2006. Overview of Eocene Planktonic Foraminiferal Taxonomy, Paleoecology, Phylogeny and Biostratigraphy. *In P. N. Pearson et al., eds. Atlas of Eocene Planktonic Foraminifera. Cushman Foundation for Foraminiferal Research Special Publication No. 41*, 11–28.

Pearson, P.N. et al., 2008. Extinction and environmental change across the Eocene-Oligocene boundary in Tanzania. *Geology*, 36(2):179–182.

Pearson, P.N., Foster, G.L. & Wade, B.S., 2009. Atmospheric carbon dioxide through the Eocene-Oligocene climate transition. *Nature*, 461(7267): 1110–1113.

Perch-Nielsen, K., 1971. Einige neue Coccolithen aus dem Paläozän der Bucht von Biskaya und dem Eozän der Labrador See. *Bulletin of the Geological Society of Denmark*, 21: 347-361.

Perch-Nielsen, K., 1971. Elektronenmikroskopische Untersuchungen an Coccolithen und vervandten Formen aus dem Eozän von Dänemark. *Det Kongelige Danske Videnskabernes Selskab Biologiske Skrifter,* 18: 1-76.

Perch-Nielsen, K., 1971. Neue Coccolithen aus dem Paläozän von Dänemark, der Bucht von Biskaya und dem Eozän der Labrador See. *Bulletin of the Geological Society of Denmark*, 21: 51-66.

Perch-Nielsen, K., 1977. Albian to Pleistocene calcareous nannofossils from the Western South Atlantic, DSDP Leg 39. *Initial Reports of the Deep Sea Drilling Project*, 39: 699-823.

Perch-Nielsen, K., 1984. Validation of new combinations. *Newsletter of the International Nannoplankton Association*, 6(1): 42-46.

Persico, D. & Villa, G., 2004. Eocene-Oligocene calcareous nannofossils from Maud Rise and Kerguelen Plateau (Antarctica): Paleoecological and paleoceanographic implications. *Marine Micropaleontology*, 52: 153–179.

Peters, S.E. et al., 2010. Large-scale glaciation and deglaciation of antarctica during the late Eocene. *Geology*, 38(8): 723–726.

Prins, B., 1979. Notes on nannology 1. Clausicoccus, a new genus of fossil Coccolithophorids. *INA Newsletter,* 1: N2-N4.

Prothero, D.R., 1994. The Late Eocene-Oligocene. *Annual Review Earth Planet Sciences*, (22):145–165.

Rabosky, D.L. and Sorhannus, U., 2009. Diversity dynamics of marine planktonic diatoms across the Cenozoic. *Nature,* 457(7226): 183-186.

Ravizza, G.E. and Peucker-Ehrenbrink, B., 2003. The marine 187Os/188Os record of the Eocene-Oligocene transition: the interplay of weathering and glaciation. *Earth and Planetary Science Letters,* 210: 151-165.

Romein, A.J.T., 1979. Lineages in Early Paleogene calcareous nannoplankton. *Utrecht Micropaleontological Bulletins*, 22: 231.

Roth, P.H. & Thierstein, H., 1972. Calcareous nannoplankton: Leg 14 of the Deep Sea Drilling Project. *Initial Reports of the Deep Sea Drilling Project*, 14: 421-485.

Roth, P.H., 1970. Oligocene calcareous nannoplankton biostratigraphy. *Eclogae Geologicae Helvetiae*, 63: 799-881.

Salamay, K. a & Zachos, J.C., 1999. Latest Eocene - early Oligocene climate change and southern Ocean fertility: inferences from sediment accumulation and stable isotope data. *Palaeogeogr. Palaeoclimatol. Palaeoecol.,* 145: 61–77.

Scher, H.D. and Martin, E.E., 2004. Circulation in the Southern Ocean during the Paleogene inferred from neodymium isotopes. *Earth and Planetary Science Letters*, 228: 391-405.

Scher, H.D. and Martin, E.E., 2006. Timing and Climatic Consequences of the Opening of Drake Passage. *Science*, 312: 428-430.

Scher, H. D., Bohaty, S. M., Zachos, J. C., and Delaney, M. L., 2011, Two-stepping into the icehouse: East Antarctic weathering during progressive ice-sheet expansion at the Eocene-Oligocene transition. *Geology*, 39(4): 383-386.

Scher, H.D. et al., 2014. Isotopic interrogation of a suspected late Eocene. *Paleoceanography*, 29: 628–644.

Schiller, J., 1930. Coccolithineae. *In: Rabenhorst, L. (Editor), Kryptogamen-Flora von Deutschland, gamen-Flora von Deutschine. Akademische Verlagsgesellschaft, Leipzig*, 89-267.

Shafik, S., 1989. Some new calcareous nannofossils from Upper Eocene and Lower Oligocene sediments in the Otway Basin, southeastern Australia. *Alcheringia*, 13: 69-83.

Siesser, W. G. 1983. Paleogene Calcareous Nannoplankton Biostratigraphy: Mississippi, Alabama and Tennessee. *Bulletin of the Mississippi Department of Natural Resources*, 125: 9-61.

Siesser, W.G., 1994. Historical background of coccolithophore studies. *In A. Winter & W. G. Siesser, eds. Coccolithophores. Cambridge University Press,* 1–11.

Sluijs, A. et al., 2009. Warm and wet conditions in the Arctic region during Eocene Thermal Maximum 2. *Nature Geoscience*, 2:777–780.

Steurbaut, E., 1990. Ypresian calcareous nannoplankton biostratigraphy and palaeogeography of the Belgian Basin. *Bulletin de la Societe Belge de Gde G de G*, 97(1988): 251-285.

Stickley, C.E. et al., 2004. Timing and nature of the deepening of the Tasmanian Gateway. *Paleoceanography*, 19(4), pp.1–18.

Stradner, H & Edwards, A.R. 1968. Electron microscope studies on Upper Eocene coccoliths from Oamaru Diatomite, New Zealand. *Jahrb. Geol. Bundesanst. (Wien), Special Volume,* 13: 1-66.

Stradner, H., 1959. Die fossilen Discoasteriden Osterreichs. *II. Teil. Erdoël-Zeitschrift*, 75: 472-488.

Stradner, H., 1962. 72-4,neue und wenig bekannte Nannofossilien aus Kreide und Alttertite. *Sonderabdruck aus den Verhandlungen der Geologischen Bundesanstalt*, 2: 363-377.

Sullivan, F.R., 1964. Lower Tertiary nannoplankton from the California Coast Ranges. I. Paleocene. *University of California Publications in Geological Sciences*, 44: 163-227.
Sullivan, F.R., 1965. Lower Tertiary nannoplankton from the California Coast Ranges. II. Eocene. *University of California Publications in Geological Sciences*, 53: 1-74.
Suto, I., 2007. Diversity explosion and extinction events of the fossil diatom resting spore assemblage across the E/O boundary. *In 2nd Neogene Polar Marine Diatom Workshop*.
Tamsin, L., 2007. Late Eocene nannofossils from the Mississippi coast, USA. *Master dissertation-unpublished.*
Tan, S.H., 1927. Discoasteridae incertae sedis. Proceedings of the Koninklijke Nederlandse Akademie van Wetenschappen, *Sect Sci,* 30: 411-419.
Tan, S.H., (1927). Over de samenstelling en het onstaan van krijt en mergelgesteenten van de Molukken. *Jaarboek van het Mijnwezen in Nederlandsch-Indie*, 55: 111-122.
Taylor, K. W. R., Huber, M., Hollis, C. J., and Hernandez-Sanchez, M. T., 2013, Re-evaluating modern and Palaeogene GDGT distributions: Implications for SST reconstructions. *Global and Planetary Change,* 108: 158-174.
Theodoridis, S., 1984. Calcareous nannofossil biostratigraphy of the Miocene and revision of the helicoliths and discoasters. *Utrecht Micropaleontological Bulletin*, 32: 1-271.
Tremolada, F. & Bralower, T.J., 2004. Nannofossil assemblage fluctuations during the Paleocene-Eocene Thermal Maximum at Sites 213 (Indian Ocean) and 401 (North Atlantic Ocean): Palaeoceanographic implications. *Marine Micropaleontology*, 52:107–116.
Varol, O., 1991. New Cretaceous and Tertiary Calcareous Nannofossils. *Neues Jahrbuch für Geologie und Paläontologie Abhandlungen*, 182: 211-237.
Villa, G. & Persico, D., 2006. Late Oligocene climatic changes: Evidence from calcareous nannofossils at Kerguelen Plateau Site 748 (Southern Ocean). *Palaeogeography, Palaeoclimatology, Palaeoecology*, 231: 110–119.
Villa, G. et al., 2008. Middle Eocene-late Oligocene climate variability: Calcareous nannofossil response at Kerguelen Plateau, Site 748. *Marine Micropaleontology*, 69: 173–192.
Villa, G. et al., 2014. Middle Eocene to Late Oligocene Antarctic glaciation/deglaciation and Southern Ocean productivity. *Paleoceanography*, 29: 223–237.
Wade, B.S. & Pearson, P.N., 2008. Planktonic foraminiferal turnover, diversity fluctuations and geochemical signals across the Eocene/Oligocene boundary in Tanzania. *Marine Micropaleontology*, 68: 244–255.
Wade, B.S. et.al., 2012. Multiproxy record of abrupt sea-surface cooling across the Eocene-Oligocene transition in the Gulf of Mexico. Geological Society of America. *Geology,* 40(2): 159-162.
Wade, B.S. & Bown, P.R., 2006. Calcareous nannofossils in extreme environments: The Messinian Salinity Crisis, Polemi Basin, Cyprus. *Palaeogeography, Palaeoclimatology, Palaeoecology*, 233: 271–286.
Wade, B.S. & Palike, H., 2004. Oligocene climate dynamics. *Paleoceanography*, 19(4): 1–16.
Wade, B.S. & Pearson, P.N., 2008. Planktonic foraminiferal turnover, diversity fluctuations and geochemical signals across the Eocene/Oligocene boundary in Tanzania. *Marine Micropaleontology*, 68: 244–255.
Wallich, G.C., 1877. Observations on the coccosphere. *Annals and Magazine of Natural History*, 19: 342-350.

Wise, S.W., 1973. Calcareous nannofossils from cores recovered during Leg 18, Deep Sea Drilling Project: biostratigraphy and observations on diagenesis. *Initial Reports of the DSDP*, 18: 569-615.

Wise, S.W., 1983. Mesozoic and Cenozoic calcareous nannofossils recovered by DSDP Leg 71 in the Falkland Plateau region, Southwest Atlantic Ocean. *Initial Reports of the DSDP*, 71: 481-550.

Wei, W. & Wise, S.W., 1990. Biogeographic gradients of middle Eocene-Oligocene calcareous nannoplankton in the South Atlantic Ocean. *Palaeogeography, Palaeoclimatology, Palaeoecology*, 79: 29–61.

Wei, W., Villa, G. & Wise, S.W.J., 1992. Paleoceanographic implications of eocene-oligocene calcareous nannofossils from sites 711 and 748 in the indian ocean. *Proceedings of the Ocean Drilling Program, Scientific Result*, 120.

Yamaguchi, T., Norris, R.D. and Dockery III, D.T., 2014. Shallow-marine ostracode turnover during the Eocene-Oligocene transition in Mississippi, the Gulf Coast Plain, USA. *Marine Micropaleontology*, 106: 10-21.

Young, J.R., 1987. Possible Functional Interpretations of Coccolith Morphology. *Abh. Geol. B.-A.*, (1968): 305–313.

Young, J.R., 1994. Functions of coccoliths. *In A. Winter & W. G. Siesser, eds. Coccolithophores. Cambridge University Press,* 68–82.

Young, J.R. & Bown, P.R., 1997. Cenozoic calcareous nannoplankton classification. *Journal of Nannoplankton Research*, 19(1): 36-47.

Young et al., 1999. Coccolith ultrastructure and biomineralisation, 215: 195–215.

Young, J.R. & Henriksen, K., 2003. Biomineralization Within Vesicles : The Calcite of Coccoliths. *Biomineralisaton. Reviews in Mineralogy and Geochemistry*,189–215.

Young, J.R., Geisen, M. and Probert, I., 2005. A review of selected aspects of coccolithophore biology with implications for paleodiversity estimation. *Micropaleontology*, 51(4): 267-288.

Young, J.R. & Bown, P. R., 2014. Some Emendments to Calcareous Nannoplankton Taxonomy. *Journal of Nannoplankton Research*, 33 (1): 39-46.

Zachos, J. et al., 2001. Trends, rhythms, and aberrations in global climate 65 Ma to present. *Science,* 292(5517): 686–693.

Zachos, J.C., Dickens, G.R. & Zeebe, R.E., 2008. An early Cenozoic perspective on greenhouse warming and carbon-cycle dynamics. *Nature*, 451(7176): 279–283.

Zachos, J. C., et al. (1995), The late Eocene/early Oligocene deep-sea sediment record of continental glaciation, ocean productivity, and deep water circulation and chemistry, *American Geophysical Union, Spring Meeting, Abstracts*, 187.

Zanazzi, A. et al., 2007. Large temperature drop across the Eocene-Oligocene transition in central North America. *Nature*, 445(7128): 639–642.

Zhang, Y.G. et al., 2013. A 40-million-year history of atmospheric CO2. Philosophical Transactions of the Royal Society A: Mathematical, Physical and Engineering Sciences, 371.

Ziveri, P. et al., 2004. Biogeography of selected Holocene coccoliths in the Atlantic Ocean. *In: J.R. Young and H.R. Thierstein (Editors), Coccolithophores: From molecular process to global impact. Springer, Berlin,* 403-428.